UNIVERSITY OF CALIFORNIA, SAN DIEGO

Spinal Glial Regulation of Nociceptive Processing During Inflammation

A dissertation submitted in partial satisfaction of the requirements for the degree

Doctor of Philosophy

in

Molecular Pathology

by

Christina Christianson

Committee in charge:

Professor Tony Yaksh, Chair
Professor Don Cleveland, Co-Chair
Professor Gary Firestein
Professor Veronica Shubayev
Professor Camilla Svensson
Professor Robert Terkeltaub

2011

The dissertation of Christina Christianson is approved, and it is acceptable in quality and form for publication in microfilm:

Chair

University of California, San Diego

2011

DEDICATION

Dedicated to the friends and family who have helped me on this journey.

TABLE OF CONTENTS

LIST OF ABBREVIATIONS

15d-PGJ_2	15-deoxy-$\Delta^{12,14}$-Prostaglandin J_2 (15d- PGJ_2)
ANOVA	analysis of variance
AP-1	activator protein 1
APMA	*p*-aminophenylmercuric acetate;
ATF3	activating transcription factor 3
AUC	area under the curve
BDNF	brain derived neurotrophic factor
BLT1	leukotriene B4 receptor
C3	complement 3
C3a	complement 3a
C5a	complement 5a
CCL2	chemokine (C-C motif) ligand 2
CCL5	chemokine (C-C motif) ligand 5
CCR7	chemokine (C-C motif) receptor 7
CGRP	Calcitonin gene related peptide
CIA	collagen induced arthritis
CNS	central nervous system
COX	cyclooxygenase
COX-2	cyclooxygenase-2
CSF	cerebrospinal fluid
CXCL1	chemokine (C-X-C motif) ligand 1

CXCL8	chemokine (C-X-C motif) ligand 8
CYP	cytochrome P450
DRG	dorsal root ganglia
DMSO	dimethyl sulfoxide
DTT	dithiothreitol
ECM	extra cellular matrix
EDTA	ethylenediaminetetraacetic acid
ELISA	enzyme-linked immunosorbent assay
GABA	gamma-aminobutyric acid
GFAP	glial fibrillary acidic protein
GM6001	N-[(2R)-2-(Hydroxamidocarbonylmethyl)-4-methylpentanoyl]-L tryptophanmethylamide
GPI	glucose 6 phosphate isomerase
H&E	hematoxylin and eosin
HIV-1 gp120	human immunodeficiency virus type 1 exterior envelope glycoprotein 120
HKLM	heat-killed preparation of Listeria monocytogenes
HMGB1	high-mobility group box 1
HPLC	High-performance liquid chromatography
HRP	horseradish peroxidase
HSP90	heat shock protein 90

Iba1	ionized calcium binding adaptor molecule 1
IκBα	nuclear factor of kappa light polypeptide gene enhancer in B-cells inhibitor, alpha
IL	interleukin
IT	intrathecal
LC/MS/MS	liquid chromatography tandem mass spectrometry
LDS	lithium dodecyl sulfate
LOX	lipoxygenase
LPS	lipopolysaccharide
LPS-RS	lipopolysaccharide rhodobacter sphaeroides
M1	classically activated macrophages
M2	alternatively activated macrophages
Mal	MyD88-adapter-like
MALDI-TOF	matrix-assisted laser desorption/ionisation-time of flight
MMP-3	matrix metalloproteinase-3
MyD88	myeloid differentiation primary response gene (88)
NaCl	sodium chloride
NFκB	nuclear factor kappa B
NFM	non fat milk
NK1	tachykinin receptor 1
NMDA	*N*-Methyl-D-aspartic acid
NNGH	N-Isobutyl-N-(4-methoxyphenylsulfonyl) glycyl hydroxamic acid

NOD	non-obese diabetic
NeuN	neuronal nuceli
Ox-42	complement receptor type 3
PAMPs	pathogen-associated molecular patterns
PARs	proteinase activate receptors
PBS	phosphate buffered saline
PE	polyethylene
PFA	paraformaldehyde
PI3K/AKT	phosphoinositide 3-kinase/ protein kinase B
PLA2	phospholipase A2
PolyI:C	polyinosinic:polycytidylic acid
PPARγ	peroxisome proliferator activated receptor gamma
RA	rheumatoid arthritis
RIPA	radioimmunoprecipitation assay
ROS	reactive oxygen species
RT-PCR	reverse transcriptase polymerase chain reaction
S.E.M	standard error of the mean
sMRM	scheduled multiple reaction monitoring
TACE	TNFalpha cleaving enzyme
TAK1	Transforming Growth Factor-β-Activated Kinase-1
Th1	T helper cell 1
Th2	T helper cell 2

TIMPs	Tissue inhibitors of metalloproteinases
TNF	tumor necrosis factor
TLR	toll-like receptor
TRIF	toll-IL-1 receptor-domain-containing adapter-inducing interferon-β
TRPA1	transient receptor potential cation channel, member A1
WT	wild type

LIST OF FIGURES AND TABLES

ACKNOWLEDGEMENTS

Chapter 1, in part is a reprint of material as it appears in Christianson CA, Corr M, Yaksh TL, Svensson CI. "K/BxN serum transfer arthritis as a model of inflammatory joint pain**."** In: Pain Research: Methods and Protocols (Ed. ZD Luo). Methods in Molecular Medicine series. Ed. John M. Walker. The Humana Press. (2011). The dissertation author was the primary author of this material.

Chapter 2, in full, is a reprint of material as it appears in Christianson CA, Corr M, Firestein GS, Mobargha A, Yaksh TL, Svensson CI . "Characterization of the acute and persistent pain state present in K/BxN serum transfer arthritis." Pain, Vol. 151 2010. The dissertation author was the primary investigator and author of this material.

Chapter 3, in part, has been submitted for publication to appear in *Pain* as "Role of toll-like receptor 4 in 15d-PGJ_2 mediated mechanical hypersensitivity following K/BxN serum transfer arthritis" by Christianson CA, Dumlao DS, Corr M, Stokes JA, Dennis E, Svensson CI, Yaksh TL. The dissertation author was the primary investigator and author of this material.

Chapter 4, in full, has been submitted for publication to appear in *Neuroscience* as " Spinal matrix metalloproteinase 3 mediates inflammatory hyperalgesia via a TNF dependent mechanism" by Christianson CA, Fitzsimmons BF, Shim JH, Agrawal A,

Cohen S, Hua XY, Yaksh TL. The dissertation author was the primary investigator and author of this material.

VITA

Education:

2006- 2011	University of California San Diego, San Diego, CA PhD in Molecular Pathology
2002-2006	University of Rochester, Rochester, New York B.S. in Biochemistry

Fellowships/ Awards:

2010	European League Against Rheumatism Travel Award
2008, 2010	International Association for the Study of Pain (IASP) Travel Award
2009-2010	IASP Collaborative Research Grant (contributing member) "Toll-like receptor 4 and spinal glial activation during inflammatory arthritis (K/BxN)"
2009-2011	F31 NIH (NINDS) "Spinal Matrix Metalloproteinases in Hyperalgesia and Allodynia"
2008-2009	Pharmacology Training Grant Award, UCSD Pharmacology Department

Publications:

1. Christianson CA, Stokes JA, Corr M, Svensson CI, Yaksh TL. "Toll-Like Receptor 4 is Required During the Inflammatory Stage for Persistent Pain Post-Inflammation in K/BxN Serum Transfer Mediated Arthritis." *In preparation.*

2. Christianson CA, Shim JH, Agrawal A, Cohen S, Hua XY, Yaksh TL. "Role of toll-like receptor 4 in 15d-PGJ_2 mediated mechanical hypersensitivity following K/BxN serum transfer arthritis." *In revision to J. Neurochemistry.*

3. Christianson CA, Corr MP, Yaksh TL, Svensson CI. "K/BxN serum transfer arthritis as a model of inflammatory joint pain**."** In: Pain Research: Methods and

Protocols (Ed. ZD Luo). Methods in Molecular Medicine series. Ed. John M. Walker. The Humana Press. (2011).*In Press.*

4. Christianson CA, Corr MP, Firestein GS, Mobargha A, Yaksh TL, Svensson CI. "Characterization of the acute and persistent pain state present in K/BxN serum transfer arthritis: evidence for persistent neuropathic pain triggered by inflammatory arthritis. *Pain* 2010 Nov;151(2):394-403.

5. Nazarian A, Christianson C, Hua XY, and Yaksh TL. "Dexmedetomidine and ST-91 Analgesia in the Formalin Model is Mediated by α_{2A}-adrenoceptors: Mechanism of Action Distinct from Morphine." *British Journal of Pharmacology*. 2008 Dec;155(7):1117-26

6. Weber JM, Forsythe SR, Christianson CA, Frisch BJ, Gigliotti BJ, Jordan CT, Milner LA, Guzman ML, Calvi LM. "Parathyroid hormone stimulates expression of the Notch ligand Jagged1 in osteoblastic cells." *Bone.* 2006 Sep;39 (3):485-93

Invited Oral Presentations:

1. CA Christianson, M Corr, TL Yaksh, CI Svensson. "Toll-like receptor 4: role in evolution of a persistent pain state." Abstract presentation. *Frontiers of Clinical Investigation Symposium. Pain 2010: from Bench to Bedside.* La Jolla, CA. 2010.

2. LM Calvi, BJ Frisch, BJ Gigliotti, CA Christianson, JM. Weber, CT Jordan, and RJ O'Keefe. "Prostaglandin E_2 (PGE2) Regulates Osteoblastic Jagged1 and Expands Primitive Hematopoietic Cells In Vivo." Blood (American Society of Hematology Annual Meeting Abstracts), Nov 2006; 108: 89.

Abstracts at Scientific Meetings

1. C.A. Christianson, J.A. Stokes, M.Corr, C.I. Svensson, T.L. Yaksh. "Toll-like Receptor 4 Contributes to Mechanical Hypersensitivity During K/BxN Serum Transfer Arthritis". Program No. 81.20. *Society for Neuroscience.* San Diego, CA: 2010.

2. K. Sándor, D. Balkisbas, J. Petterson, J. Gregory, C. Christianson, S. Codeluppi, R. Holmdahl, K. Nandakumar, C. Svensson. "Collagen Antibody Induced Arthritis (CAIA) Evokes Persistent Allodynia and Spinal Astrocyte Activation." Program No. 80.19. *Society for Neuroscience.* San Diego, CA: 2010.

3. C.A. Christianson, J.A. Stokes, M. Corr, C.I. Svensson, T. L. Yaksh. "Toll-like receptor 4 is required for continued mechanical hypersensitivity during K/BxN serum

transfer arthritis." *International Association for the Study of Pain.* Montreal, Canada: 2010.

4. D. B. Baş, J. Petterson, K. S. Nandakumar, S. Codeluppi, J. Gregory, C. Christianson, R. Holmdahl, Y. Kesim, C. I. Svensson. "Collagen Antibody Induced arthritis (CAIA) and Pain" *International Association for the Study of Pain.* Montreal, Canada: 2010.

5. J. A. Stokes, C. Christianson, M. Corr, T. L. Yaksh. "Spinal Toll-Like Receptors; Initiation Of Tactile Allodynia And Glial Activation". *International Association for the Study of Pain.* Montreal, Canada: 2010.

6. C.A. Christianson, M. Corr, G.S. Firestein, A. Mobargha, T.L. Yaksh, C.I. Svensson. "Persistent tactile allodynia and spinal non-neuronal cell activation in K/BxN serum induced arthritis". *European League Against Rheumatism.* Rome, Italy: 2010.

7. C.A. Christianson, M. Corr, T.L. Yaksh, C.I. Svensson. "Persistent Tactile Allodynia in Serum Induced Arthritis". Program No. 76.16. *Society for Neuroscience.* Chicago, IL 2009.

8. C.A. Christianson, J.-H. Shim, X.-Y. Hua, T. Yaksh. "Spinal Matrix Metalloproteinase 3 Contributes to Inflammatory Pain." Program No. 669.3. *Society for Neuroscience*. Washington, DC, 2008.

9. C.A. Christianson, C.I. Svensson, X.Y.-Hua, T. Yaksh. "Inhibition of Matrix Metalloproteinases Regulates Onset of Hyperalgesia in a Carrageenan Model of Inflammation." *International Association for the Study of Pain.* Glasgow, Scotland 2008.

10. J. M. Weber, S. R. Forsythe, C.A. Christianson, L. M. Calvi. "Parathyroid Hormone Increases Osteoblastic Jagged1 through Protein Kinase A (PKA) Activation". *American Society for Bone and Mineral Research* Nashville, TN 2005

ABSTRACT OF THE DISSERTATION

Spinal Glial Regulation of Nociceptive Processing During Inflammation

by

Christina Christianson

Doctor of Philosophy in Molecular Pathology

University of California, San Diego, 2011

Professor Tony Yaksh, Chair

Chronic pain is a major health issue affecting 20% of the population and reducing quality of life measures and incurring a large health care related cost for society. In this thesis we investigate the role of non-neuronal cells of the spinal cord in regulating both the onset of acute inflammatory pain and the maintenance of chronic inflammatory pain.

We demonstrate that a two-week peripheral inflammation as produced by the K/BxN serum transfer arthritis model results in chronic mechanical hypersensitivity as

measured by von Frey hairs with changes in the ATF3 transcription factor of the dorsal root ganglia, a characteristic of neuropathic pain, in addition to spinal non-neuronal cell activation. The transition to a chronic mechanical hypersensitivity is further demonstrated by knockout and antagonist treatments to be spinal toll-like receptor 4 dependent. By LC/MS/MS lipid spinal cord analysis this is shown to be critical in production of the anti-inflammatory/ anti-nociceptive arachidonic acid metabolite 15d-PGJ_2 which is lost during K/BxN serum transfer arthritis. Additional studies utilizing the carrageenan model, wherein an inflammatory stimulant is injected into the hindpaw resulting in inflammation concurrent with thermal hyperalgesia and tactile allodynia, were conducted to investigate endogenous compounds released from non-neuronal cells during initiation of pain-like behavior. Here we demonstrate that the catalytically active form of matrix metalloproteinase 3 is released spinally and will induce an enzymatically mediated, microglia specific, release of tumor necrosis factor. Intrathecal antagonist blockade of MMP activity attenuates the onset of thermal and tactile hypersensitivity suggesting a role for these enzymes in the initial stages of peripheral inflammation induced pain-like behavior. This thesis reveals the crucial role of non-neuronal cells related factors in mediating both acute peripheral inflammation and chronic inflammation induced pain-like behavior utilizing multiple animal inflammation models and converging biochemical and molecular biological techniques.

Chapter 1.

General Introduction

1.1 Scope of the Problem

Following acute tissue injury, such as a surgical interventions including hernia repair, arthroscopy, and joint replacement, the individual typically reports pain with a time course that parallels the resolution of the inflammatory phase and the " healing of the wound" which occurs over intervals of days to at most weeks. A significant population of patients, however, report pain that fails to resolve over extended intervals [1-3]. When such intervals exceed three to six months, patients are said to reflect a transition of the pain phenotype from acute to chronic. Researchers have proposed that a prolonged acute pain state informs persistent changes within the peripheral and central nervous systems [4]. This however, does not explain why a percentage of people develop chronic pain, whereas others do not.

Chronic pain is a major health problem affecting approximately 20 percent of the population resulting in markedly reduced quality of life for the individual as well as extensive costs for society [5]. While chronic or persistent pain states are often secondary to a peripheral nerve injury (diabetic neuropathy or surgical trauma) or a persistent inflammation (rheumatoid arthritis or pancreatitis); we will make the argument in this thesis that persistent pain behavior resulting from a long lasting inflammation can evolve biological markers and pharmacological properties that display a phenotype typically assigned to events which characterize a neuropathic pain state. We believe that this transition in phenotype may provide insight into the

problems faced in the use of traditional therapeutics, such as NSAIDs and opiates in the management of such pain states.

Research regarding the mechanism underlying the inflammation in many disorders, particularly the chronic arthridices, has targeted the modification of the disease through the inflammatory cascade, with biologicals such as the TNF and interleukin blockers. Importantly, many of these treatments can, to some degree, ameliorate the associated disability arising from the pain state [6]. Classically, this improvement in pain has been specifically attributed to the peripheral effects upon the disease [7]. As will be seen in the present studies, such effects likely go well beyond a simple effect upon disease modification and joint morphology.

Despite the efficacy of new therapeutics (e.g. TNF and interleukin blockers) and treatment strategies (e.g. combination therapies), pain is still a significant problem. In a recent survey, more than 85% of RA patients described their RA as somewhat/ completely controlled, yet greater than 75% of them reported moderate to severe pain within the previous two months **[8]**. Drug development in the area of truly chronic inflammatory pain has hitherto been circumscribed and frequently limited to the perspective changes in joint markers and pathology and not pain. Importantly, a recurrent theme in this thesis is that while peripheral inflammation is an important component of the pain phenotype (reflecting the sensitization of the peripheral sensory afferent terminal), the persistent peripheral inflammatory state leads to prominent changes in the structure and function of the primary afferent, dorsal root ganglion and the dorsal horn of the spinal cord where the encoding of the pain

state is enabled. Thus, it is critical to increase our understanding of the events which transpire during both the acute peripheral inflammation and during the post-inflammation phase to understand the events leading to the emergence of a chronic pain state. Here we seek to investigate signaling components critical in this process, with a particular emphasis upon the contribution of non-neuronal cells.

1.2 Chronic Inflammatory Arthritis

Approximately one percent of the population is diagnosed with rheumatoid arthritis (RA), a systemic autoimmune mediated disease comprising synovial inflammation and matrix destruction. Swelling is particularly prominent in the small joints of the hands and feet. Pain is frequently the most egregious symptom reported and can persist after resolution of joint swelling with anti-inflammatory treatment. The inflammatory processes that result in rheumatoid arthritis are complex, with interactions among the cytokine network, autoantibodies, and the complement cascade. While the peripheral inflammation is an important component in generating pain in RA, the peripheral pathology cannot fully explain the amount of pain the arthritis patient experiences and facilitation of pain processing at the level of the spinal cord has been implicated [5]. Collagen-induced arthritis (CIA) is the gold-standard in the rheumatology field for understanding the pathogenesis and investigating new pharmacological treatments for chronic inflammatory arthritis[9]. CIA is induced by immunization with type II collagen in CFA, producing an automimmune reaction against the cartilage in the joints with a concurrent increase in ATF-3 DRG expression

[10]. Although recently characterized as a pain model, CIA is limited by the need for a specific genetic background in the recipient animals [11, 12] thus reducing the usefulness in asking questions using a genetically altered subject. For this reason we sought to characterize and utilize an alternative model of chronic inflammation.

1.3 Modeling rheumatoid arthritis and pain-like behavior

An important element in the investigation of acute and chronic pain transitions is the development of appropriate preclinical surrogate models which permit systematic interventions and analyses. Classically, rodent models such as those based on the intra-plantar injection of irritants such as carrageenan and formalin have great popularity for the study of pain mechanisms and pharmacology. Such models lead to prominent changes in pain sensitivity and behavior, however, many of these models do not mirror the changes in peripheral morphology that model the human condition and more critically have a limited time frame (hours to days)[13] . Thus, changes in pain related processes during chronic diseases, such as RA, may not be revealed. An important element of this thesis is the characterization of the behavior and pharmacology of a model of joint inflammation which persists for approximately 2 weeks. While widely characterized as model of rheumatotid disease [14], its pain profile had surprisingly not been considered yet.

The KRN mice are transgenic for a T cell receptor that is cognate for a peptide derived from bovine pancreatic RNAse [14]. Crossing KRN mice on the C57Bl/6 background with non-obese diabetic (NOD) mice generates K/BxN mice. These mice

develop severe destructive arthritis that resembles human rheumatoid arthritis in many respects. Serum transfer from the K/BxN mice will reliably induce transient inflammatory arthritis in the joints of a wide range of mouse strains [14] utilizing autoantibodies against glucose-6-phosphate isomerase [15].

The use of preclinical models as predictive of human biology depends upon the characterization of its functional phenotype. Peripheral tissue injury and inflammation typically yields a reduction in the magnitude of the stimulus required to produce escape behavior in humans and in preclinical animal models. This event has been interpreted as indicating that the injury/inflammation has resulted in a change in processing wherein a somatic (thermal or mechanical) stimulus of moderate intensity with little or no initial aversive characteristics now constitutes an aversive event. The stimulus leads to a verbal report of pain (in humans) or an escape response (in the rat). This transition represents the onset of a "hyperalgesic" state" [16] . The extreme is where a somatic stimulus of such an intensity that has no escape evoking properties, a normally innocuous stimulus, becomes aversive, thus representing an "allodynic" state [17]. Considerable evidence has developed emphasizing that an important component of this hyperalgesic state results from a sensitization of not only the peripheral nerve terminal innervating the site of injury but a profound change in the encoding process in the spinal dorsal horn at the level of the first and second order synapse [18].

1.4 Neuronal nociceptive mechanisms.

Tissue injury initiates an inflammatory response which is intended to protect the organism from lasting damage. Peripheral nociceptors, located on the distal terminals of primary sensory neurons detect high intensity, potentially tissue injuring stimuli and evoke activity in spinal systems which activate spinal and supraspinal circuits mediating the withdrawal of the related body part from the stimulus to prevent tissue damage. Here, pain and the physiological reactions following the acute peripheral stimulus are transient and beneficial to the function of the organism to prevent damage [18].

The first link in the pathway signaling nociception are the primary afferents, originating in the periphery and terminating in the spinal cord. Afferents which are activated by high intensity thermal, mechanical or chemical stimuli are referred to as nociceptors. Some nociceptors are located on thinly mylinated medium (2-6μM) diameter Aδ fibers, however the majority are on thin (0.4-1.2μM) diameter unmyelinated C fibers (reviewed in ([19, 20]). Large diameter (>10μM) myelinated fibers are typically low threshold, rapidly adapting, mechanorecptors (light touch) which do not typically transmit nociceptive information. However, after nerve injury, it is believed that there are organizational changes at the level of the DRG and spinal cord wherein this population of afferents serves to evoke allodynia and that their selective blockade suppresses allodynia [21, 22]. Nociceptive primary afferent fibers terminate in the superficial dorsal horn (lamina I,II) of the spinal cord driving synaptic input to second order neurons. Large afferents typically terminate deeper than these superficial lamina.

It can be seen that the superifical neurons tend to be “nociceptive specific” while the deeper neurons respond to both high and low threshold stimuli and are therefore referred to as wide dynamic range neurons. An important property of this system is that it normally responds in a frequency dependent fashion where increasing stimulus intensity (nociception) is encoded by the cells which are activated and results in a proportional discharge.

1.5 Spinal sensitization

In the face of peripheral injury, there is the generation of a high frequency repetitive input from small high threshold primary afferents. Dating from the early descriptions of Mendell and Wall (1965) it has been appreciated that this repetitive C fiber input will lead to an enhanced discharge of the second order. This phenomenon is called wind-up. It is considered to be the primary example of the phenomena of spinal sensitization. In spinal sensitization, the response from the second order neuron is no longer proportional to the input. This enhanced response can persist for brief intervals after offset of the stimulus [23]. This sensitization of spinal nociceptive neurons is well established and is believed to underlie in part the enhanced response (hyperalgesia and allodynia) shown by the organism after tissue injury. This spinal sensitization is achieved by numerous mechanisms: local circuits, bulbospinal pathways and glial cell activation.

i) Local circuits include cascades leading to increased intracellular calcium secondary to persistent activation of glutamatergic NMDA and AMPA receptors

(reviewed in [24, 25])and tachykinin NK1 receptor activation (reviewed in [25]). Enhanced intracellular calcium can activate kinases which serve to phosphorylate membrane voltage sensitive sodium and calcium channels to decrease their thresholds for activation and enhance their opening times and receptors to increase their functionality[26].

ii) Spino-bulbo-spinal pathways consist of spinofugal projections from marginal cells to caudal midline medullary cells which give rise to bulbospinal serotonergic projections back to the dorsal horn which act though a variety of serotonergic receptors to enhance dorsal horn excitability[27].

iii) Spinal microglia and astrocyte are activated by periepheral tissue and nerve injury (reviewed in [28],[29]) and are believed to play an important role in the central sensitization and hyperalgesia reported in variety of nociceptive states including peripheral inflammation [30], osteosarcoma [31], HIV-1 gp120 induced pain [32], and spinal nerve ligation induced neuropathic pain [33, 34]. The role of microglia and astrocytes in central sensitization has attracted significant interest as interventions directed at blocking the action of these cells are anti-nociceptive in many pain models (reviewed in [28, 35, 36]).

1.6 Non-Neuronal Cells

The role of glia in maintaining chronic pain has been emphasized by pretreatment and reversal of pain-like behavior in animal models utilizing glia-inhibitory compounds including minocycline [37, 38] and propentofylline [39, 40]. It

has been shown that after persistent tissue or nerve injury that non-neuronal cells may show morphological changes and increased expression of markers such as OX-42 or Iba-1 in microglia and GFAP in astrocytes[41]. Given the ability of these cells to secrete pro-excitatory products including lipid mediators, cytokines, and superoxides and furthermore to regulate the extracellular concentrations of neurotransmitters such as glutamate, these cells have been held to potentially regulate the excitability of local circuits [42]. Further, the probable role of the microglia, a brain resident macrophage, suggests the importance of elements that are closely allied with cascades of events normally associated with the innate immune response. The role of microglia in initiation of a pain state was underscored in work by Tsuda et al where it was demonstrated that intrathecal administration of stimulated microglia, via the $P2X_4$ receptor, is sufficient to produced tactile allodynia in naïve rats [29]. Further, in the face of peripheral inflammation, it is possible to detect a marked increase in the presence of phosphorylated p38 MAPK prior to morphological changes in the microglia. Blockade of spinal p38 function has a potent anti-hyperalgesic action [37]. Importantly, the time course of the effects of microglia contributions are measured in minutes to hours and not days, emphasizing that though the cells may not show prominent changes in morphology or the expression of cell surface signs of activation (e.g OX-42), they are playing a major role in the local events that transpire early in the development of the post tissue injury hyperalgesic state.

1.7 Tissue Injury, inflammation and the innate immune response.

Early stages of peripheral inflammation are marked by the activation and/or influx of the complement system, release of mast cell components, neutrophil migration, and macrophage influx. In contrast to earlier theories, resolution of inflammation is now considered to be an active process. Here we briefly review the coordinated actions of the innate immune system following peripheral inflammation as would arise following tissue injury. Two points should be emphasized. First, that the inflammatory cascades represent both an initial response that leads to the cardinal signs of inflammation followed by a resolution phase in which there is not only a loss of the proinflammatory components, but an active series of events which leads to resolution of the inflammation. Second, as will be seen during portions of this cascade, events associated with the peripheral injury site are recapitulated in the spinal dorsal horn.

1.7.1 Complement

The complement system consists of 30 associated proteins. The activation of this cascade results in the production of other inflammatory mediators. When considering the pro-inflammatory actions of the complement system one normally describes the functions of C3a and C5a. These signaling molecules are chemotactic for phagocytic cells and induce pro-inflammatory cytokine release (CITATION [43]). When soluble complement receptor 1, which prevents C3a and C5a from functioning, is injected directly into the intrathecal space it prevents or reverses peripheral nerve inflammation, partial sciatic nerve injury, and IT HIV gp120 induced neuropathic pain

[44] . Based on strain modeling it was determined that K/BxN serum transfer arthritis is dependent upon the alternative pathway of complement activation in order to induce clinical signs of arthritis [45]. Recent studies have further demonstrated that circulating C3 is both necessary and sufficient to confer susceptibility in this model, thus demonstrating the critical role for complement during the induction of peripheral inflammation in this arthritis model [45].

1.7.2 Mast cells

Mast cells, normally present in tissue, will respond to signals including neuropepetides released by tissue injury, bacteria and their patterning, as well as complement products by releasing histamine, pre-formed TNF, leukotrienes, tryptases, synthesizing cytokines and chemokines. Histamine is the major cause for vasodilation and extravasation of fluid following tissue injury [46]. Products released by mast cells directly recruit and/or activate neutrophils and lymphocytes to continue the inflammation program. The requirement of functional mast cells for K/BxN serum transfer arthritis has been has clearly demonstrated by utilizing mast cell deficient mice. Clinical signs of joint inflammation were restored by mast cell engraftment [47].

1.7.3 Neutrophils

Neutrophils are not identified in healthy tissue, but are located proximal to the site of injury in both nerve injury [48]and experimental inflammatory arthritis animal models [49]. Thus, neutrophils must be signaled to the sites of injury. Mice lacking the

receptor for leukotriene B4 (BLT1) or treated peripherally with the antagonist for BLT1 do not display neutrophil chemotaxis into the joints or clinical indications of disease. Recruitment is influenced by the presence of chemoattractants including nerve growth factor β, CXCL1, monocyte chemoattractant protein-1 [50], and leukotriene-B4 at the site of injury [49]. Neutrophils affect the inflammatory response by three major mechanisms. Neutrophils will release a superoxide burst [51] which is essential for phagocytosis[52] . Secondly, activated neutrophils can release pro-inflammatory cytokines including TNF and IL-1β which will directly activate neurons [53, 54] in addition to their modulatory immune-glial cell activity function [55]. Thirdly, neutrophils secrete mediators that are chemotactic for macrophages [56] which include macrophage inflammatory protein-1α and -1β, IL-1β, and the defensins [57].

1.7.4 Macrophages

Peripheral macrophages are derived from circulating monocyctes. Macrophages eliminate apoptotic cells, debris, viruses, and bacteria in addition to participating in the inflammatory response following injury or infection [58]. To this end, macrophages secrete mediators that regulate all aspects of host defense, inflammation, and homeostasis most of which are directly implicated in chronic pain including ROS, bioactive lipids, and pro-inflammatory cytokines (reviewed in [59]).

Macrophages are recruited to the site of tissue injury within hours and will be increased locally for days to weeks depending upon the injury stimulus. Macrophages will undego local proliferation and maturation to maintain this. Classically activated

macrophages (M1) express pro-inflammatory cytokines TNF, IL-6, IL-12. IL-1β, interferon gamma, chemokines CCL2, CCl5, CXCL8, CCR7, and ROS while alternatively activated macrophages (M2) may actually contribute to resolution of inflammation [60]. This description of polarization of M1 vs M2 is simplistic, however, given the rapid plasticity [61] that these cells have demonstrated in both pro-inflammation and pro-resolution roles dependent upon local signals [62]. A characteristic M1 pro-inflammatory response is necessary for tissue injury and infectious diseases clearance. Mice lacking interferon gamma or TNF, key M1products, die from infections such as *L. monocytogenes* [63].

1.7.5 Resolution of Inflammation

Resolution of inflammation is now considered to be an active process which utilizes both arachonic acid derived metabolites and a number of omega-3 poly-unsaturated fatty acid products. There is a still a great deal of information regarding the coordination and regulation of these products that remains to elucidated. The same eicosanoid machinery that produces pro-inflammatory leukotriene mediators will produce pro-resolution lipid mediators such as the lipoxins dependent upon signals from cells within the immediate vicinity [64]. The presence of lipoxins impede the entry of new neutrophils to a site of inflammation [65], reduce permeability of the vasculature [66], increase nonphlogistic monocytes[67], and stimulate macrophage clearance of apoptotic neutrophils [68]. The other major pro-resolution lipid mediators are the resolvins E-series compounds produced from eicosapentaenoic acid and the

resolvins D-series compounds produced from docosahexaenoic acid. Resolvin E1 is the most studied in the E-series and has been demonstrated at nanomolar levels to reduce neutrophil migration, clinical signs of tissue injury, and attenuates IL-12, TNF, and iNOS during a model of colitis [69]. Resolvin D1 further regulates leukocyte migration and microglial pro-inflammatory cell production [69, 70]. When delivered i.p. to adjuvant –induce arthritic mice resolvin D1 reduces peripheral TNF and IL-1β levels in addition to blocking NFκB and COX-2 within the spinal cord and DRG and increasing mechanical thresholds [71]. Recent work pharmacological data further indicates that resolvins E1 and D1 are both involved in peripheral and centrally mediated inflammatory and neuropathic pain. Intraplantar or intrathecal administration of resolvin E1 or resolvin D1will reduce inflammatory pain behaviors induced by formalin, carrageenan, or complete Freund's adjuvant [72]. It is important therefore to bear in mind that the regulation of onset and resolution of inflammation and (potentially pain-like behavior arising from the inflammation) are part of a regulated system.

1.7.6 Adaptive Immune System

All these are components of the innate immune system, and while we do not discuss the role of the adaptive immune system in this thesis there is considerable evidence accumulating regarding the involvement of T lymphocytes. The Th1 subpopulation directly contributes to pro-inflammatory responses wherease the Th2

cells contribute to the release of anti-inflammatory cytokines including IL-4, IL-5, IL-10 and IL-13 [73].

1.8 TLR function

In the course of work performed in the early phases of this thesis, a fortuitous observation performed in mice with a point mutation in toll-like receptor 4 (TLR4) led to a concerted focus on the role of this receptor in the pain phenotype occurring after persistent inflammation. This work has provided insight into the evolution of a chronic pain state from a persistent, but reversible inflammatory conditions. As such we believe that this work has illuminating significance for our understanding the potential mechanisms underlying the clinical phenomena of the acute to chronic pain transition.

The survival of all organisms requires the ability to identify and defend against invading pathogens. Conserved pathogen associated molecular patterns (PAMPS) expressed on microorganisms are identified by components of the innate immune system and subsequently initiate a broad cascade of pro-inflammatory mediators, antimicrobial effectors and activate the adaptive immune system in order to eliminate the foreign attack [74]. As early as three years after the identification of the first human homologue of the toll-like receptor protein it was hypothesized that these pattern recognition receptors may also interact with endogenous protein ligands to assist in homeostasis [75] . In this thesis we explore the role toll-like receptors (TLRs),

with an emphasis upon TLR4, within the central nervous system to better understand the interplay between the innate immune system and inflammatory pain.

TLRs 1-9 are conserved between humans and mice while mouse TLR10 is not functional and TLR11, 12, and 13 are not identified in the human genome[76]. TLR4 is a cell surface expression protein whose stimulation recruits adaptor proteins to the cytoplasmic tails of the membrane spanning receptor. TLR4 can signal through two distinct pathways a MyD88 dependent and a MyD88 independent pathway, which are described in Figure 1.1. Adaptor protein Mal is required for MyD88 recruitment which eventually leads to the recruitment and phosphorylation of the NFκB inhibitor IκBα by TAK1 thus permitting NFκB translocation to the nucleus and transcription of a variety of pro-inflammatory genes (reviewed in [77, 78]). Of interest TAK1 can also phosphorylate upstream mediators of p38 and Jnk signaling via MKK3/6 and MKK4, respectively, while phosphorylation of ERK signaling can be accomplished via the intermediary TPL2 and MKK1/2[79]. A MyD88 independent activation of TLR4 utilizes the adaptor protein TRIF to produce interferon α/β. In addition, TRIF signaling activates TAK1 in a distinct mechanism allowing for MyD88 independent MAPK and NFκB activity.

1.9 TLRs in the CNS as modulators of persistent inflammatory pain

In the central nervous system TLR4 was initially reported to be primarily present on microglia [80], but recent evidence suggests their detection critical function on astrocytes [81, 82] and neurons [83] as well. TLR function has been investigated

regarding clinical signs of inflammation during inflammatory arthritis models and regarding pain-like behavior in nerve injury models. TLR function has not, to this point, been investigated for a role in the pain-like behavior resulting from inflammatory arthritis. The first direct evidence of TLR function in RA came from the crossing of *Tlr4-/-*mice with *IL1rn-/-* (which develop spontaneously an autoimmune T cell-mediatted arthritis). The lack of TLR4 protected the mice from more severe histopathologically evaluated arthritis signs [84]. Unexpectedly, *Tlr2-/-* mice when crossed with *IL1rn-/-* mice developed more severe arthritis in combination with reduced Treg formation and increased IFN-γ suggesting a highly complicated TLR regulation of inflammatory arthritis. More recently, the CIA mouse was treated post arthritis induction i.p. with a TLR4 antagonist, thus preventing joint inflammation and cartilage and bone damage [85]. Further studies suggest TLR4 as a potential mediator in the transition from an acute to chronic response in inflammatory arthritis, using the streptococcal wall arthritis model [86].

In addition to a function in mediating inflammation in RA models, TLR4 also contributes significantly to maintenance of neuropathic pain. Initial studies utilized *Tlr4-/-* and TLR4 point mutant mice, and IT TLR4 antisense treated rats to demonstrate reduced tactile and thermal hypersensitivity following L5 spinal nerve injury. This behavioral data is in combination with reduced microglia activation and a concurrent reduction in the pro inflammatory cytokines IFN-γ, IL-1β, and TNF [87]. Later work by other groups confirmed the role of spinal TLR4 by delivery of an IT TLR4 antagonist to rats following sciatic nerve chronic constriction injury animals

[88]. Finally, work from our group suggests PGE_2 release following spinal TLR4 stimulation may regulate this activity [89]. Thus, the combination of TLR specificity for inflammatory transitions in RA models and the direct contribution of TLR4 to nerve injury mediated pain-like behavior suggests this as a novel and exciting area for investigation.

1.10 MMPs as a modulator of acute inflammatory pain

Our final area of investigation in this thesis concerns the potential function and regulation of microglia and astrocytes during inflammation by matrix metalloproteinases. Key observations regarding the role of microglia and astrocytes during peripheral inflammation induced pain were made using the drug minocycline. Minocycline is a second generation tetracycline derivative without antibacterial properties. Intrathecal delivery of tetracycline derivatives such as minocycline and doxycycline will block microglial activation, the phosphorylation of spinal microglial P38 MAPK [37], and at comparable doses will dose-dependently reduce injury/inflammation evoked hyperalgesia [90]. The mechanism of the minocycline inhibition of microglial function is unclear, however, one proposed mechanisms suggests their effect upon pain processing may be mediated though the regulation of matrix metalloproteinases (MMPs) [91]. As such we are investigating the role of matrix metalloproteinases as modulators of acute inflammatory associated pain-like behavior.

MMPs are part of a family of zinc-dependent metalloproteinases that are numbered and categorized according to their substrates. There are four basic regulatory mechanisms for these enzymes. 1) Transcriptional: most MMPs are not expressed in high levels but are upregulated following cell activation, though it should be noted that transcriptional level does not always equate with levels of active protein. 2) Post translational modification: all MMPs are translated with a pro-domain that is requires cleavage to activate. 3) Endogenous inhibitors: tissue inhibitors of metalloproteinases (TIMPs) bind to the catalytic site and prevent activity, although in rare circumstances they can aid in the activation of MMPs by bringing enzymes into correct conformations. 5) SIBLING binding proteins: the inhibition produced by TIMP binding to MMP-2, MMP-3, and MMP-9 can be reversed with the binding of members of the SIBLING family of integrin-binding phosphoglycoproteins (bone sialoprotein, osteopontin, and dentin matrix protein-1 respectively)[92-94].

Using qPCR techniques, a variety of MMPs can be identified at low mRNA levels in the spinal cord under normal conditions. Following injury and in several neurological pathologies, sets of MMPs and/or their endogenous TIMP inhibitors are upregulated. For example, following LPS administration, microglial mRNA levels of MMP 1, 3, 8, 19, and 21 are reported to become significantly elevated. This increase correlates with higher protein secretion of the active forms of TNF, IL-1β, and IL-10 [95]. Of particular interest is a regulatory role for MMP-3 in neuronal /glial circuitry signaling. The basic structure of MMP-3 is shown in Figure 1.2. n 2005, Kim et al. demonstrated through 2-D electrophoresis and MALDI-TOF mass spectrometry that

serum deprived neuronal PC12 cells release MMP-3 into the media, and *in vitro* the catalytic form of MMP-3 can activate primary microglial cell cultures yielding increased TNF [96]. An unexplored area of the pain field involves the role of MMP-3 in initiation and maintenance of nociceptive behaviors.

The identification of inducers, activators, and substrates within the central nervous system has begun, but much remains to be elucidated. Previous *in vitro* assays describe MMP-3 as being able to increase activation of MMP-2 and MMP-9[97, 98]. Activation of MMP-2 and MMP-9 by MMP-3 is of particular interest given recent work by Kawasaki et al that demonstrates time and cell type dependent fluctuations in MMP-2 and MMP-9 following sciatic nerve injury and data showing IT administration of MMP-9 will produce a four day tactile allodynia [99].

MMP-3 can also cleave numerous known substrates to form, for example; brain derived neurotrophic factor, IL-1β, monocyte chemotactic proteins, and transforming growth factor β which could themselves be released to initiate and sustain acute or chronic pain sensations[100]. Activation of BDNF is another likely intermediary substrate given its appearance in primary afferent terminals and release following electrical stimulation or capsaicin treatment[101]. Given the number and identity of substrates and cytokine products evoked by MMP-3 we have pharmacologically investigated the spinal activity of MMP-3 during peripheral inflammation evoked mechanical and thermal hypersensitivity.

1.11 Objectives of the Dissertation

The purpose of this project is to characterize and determine spinal mediators contributing to nociceptive processing during peripheral inflammation. For this, a rheumatoid arthritis model has been characterized for nociceptive behaviors and investigated for the function of toll like receptors during the dynamic progression of this inflammatory disease with a particular emphasis upon the eicosanoid profile changes. In addition, a second inflammatory model has been utilized to test the role of MMPs as spinal mediators of nociception during the onset of peripheral inflammatory. We will examine the following specific aims:

Aim 1: Characterize the behavior, analgesic pharmacology and spinal glial activation in a model of inflammatory arthritis (K/BxN).

Hypothesis 1. Long term inflammation initiates the development of persistent pain states.

Using the K/BxN serum transfer model of inflammatory arthritis we propose to assess pain-like behavior changes and to asses molecular and pharmacological determinants of this arthritis progression process. We will quantify the temporal profile of mechanical and thermal hypersensitivity during the initiation of inflammation and through the post-inflammation stages. To understand the relationship with spinal nociceptive processing we will determine spinal microglia and atstrocyte activation in addition to investigating markers of persistent pain states in the dorsal root ganglia. The understanding of the temporal development of a persistent pain state following peripheral inflammation will be further clarified by the delivery of

analgesics known to have different actions during inflammation and post-inflammation.

Aim 2: Define the role of TLR4 receptors and downstream mediators in the initiation and maintenance of K/BxN serum transfer arthritis mechanical hypersensitivity.

Hypothesis 2: Spinal toll-like receptor 4is activated during peripheral inflammation and mediates the transition from an acute to a persistent pain state

Using the K/BxN serum transfer model of arthritis we propose to investigate components required for the transition from an acute to a persistent pain state. Preliminary studies suggested TLR4 as a necessary signaling component during this process. We will quantify the temporal profile of mechanical and thermal hypersensitivity in WT and *Tlr4-/-* mice, from both constitutive deletion mutants and from those with point mutations, during K/BxN serum transfer arthritis. To better understand the spinal nociceptive processing role of TLR4 during arthritis progression we will analyze activation of spinal astrocytes and microglia, measure persistent pain markers in the DRG, and measure levels of endogenous TLR4 ligands. Further behavioral studies will identify the peripheral versus central signaling requirements for TLR4 by delivery of an antagonist, and the mechanism of any activity will be investigated by western blotting for MAPK activity and by mass spectrometry for eicosanoid changes.

Aim 3: Characterize role of spinal MMP activity in hyperalgesic states initiated by peripheral inflammation.

Hypothesis 3: Matrix metalloproteinases (MMPs) are essential mediators for spinal nociceptive processing during peripheral inflammation via TNF release.

Using the carrageenan model of peripheral inflammation we propose to assess the function of MMPs (focusing on MMP-3) in during spinal nociceptive processing of the inflammatory insult. We will assess the anti-nociceptive efficacy, mechanical and thermal hypersensitivity, of pre-treatment and post-treatment with broad spectrum MMP and MMP-3 specific inhibitors prior to carrageenan induced peripheral inflammation. Furthermore, we will determine the nociceptive behavioral effects of spinal MMP-3 delivery and investigate a TNF specific pathway using direct spinal measurements and pharmacological interventions.

1.12 Acknowledgments

Chapter 1, in part is a reprint of material as it appears in Christianson CA, Corr M, Yaksh TL, Svensson CI. "K/BxN serum transfer arthritis as a model of inflammatory joint pain**."** In: Pain Research: Methods and Protocols (Ed. ZD Luo). Methods in Molecular Medicine series. Ed. John M. Walker. The Humana Press. (2011). The dissertation author was the primary author of this material.

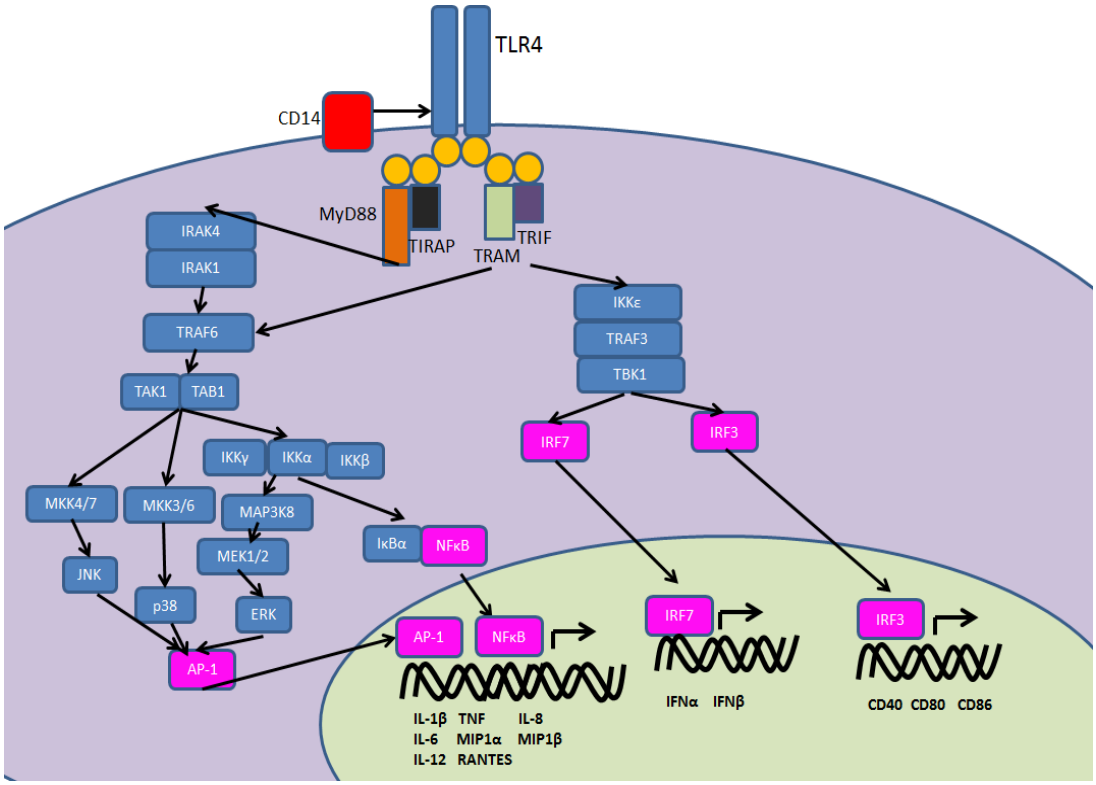

Figure 1.1 Toll like receptor 4 downstream activation pathways. Activation of TLR4 can induce signaling via both a MyD88 dependent and an independent pathway to stimulate transcription factor movement to the nucleus. Key features of the MyD88 dependent pathway include production of AP-1 through MAPK activation and NFκB production to yield proinflammatory cytokine production. The MyD88 independent pathways can also traffick through TRAF6, but more rapidly induces interferons and T cell stimulatory components.

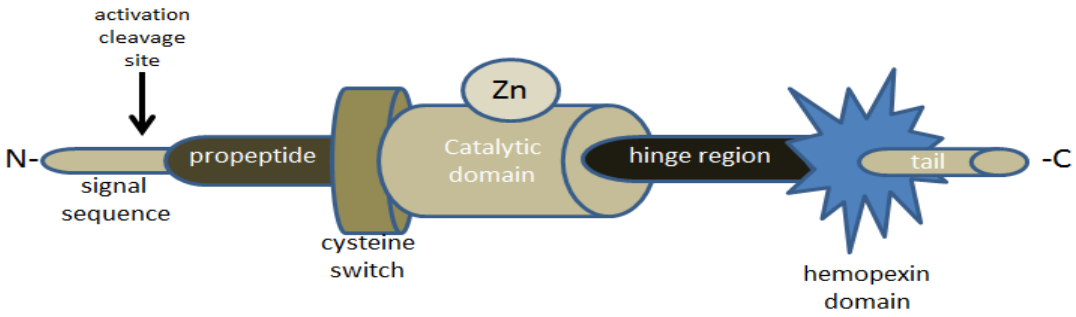

Figure 1.2 Matrix metalloproteinase 3 structural components. MMP-3 consists of a signal sequence domain that directs the protein to the secretory pathway, a prodomain which interacts with the catalytic domain when the enzyme is inactive, and a hinge linker region connected to the hemopexin domain. Activation requires a conformational change resulting in delocalization of the prodomain and cleavage to produce an enzyme of reduced molecular size. This is frequently accomplished via the "cysteine switch" wherein the conserved cysteine residue is no longer bound to the Zn atom in the catalytic domain which blocks it from functioning as an active site. The concept of the hemopexin domain is conserved between the majority of MMPs, but the specifics differentially affect activity, substrate specificity, and further localization signals.

Chapter 2

Characterization of the acute and persistent pain state present in K/BxN serum transfer arthritis

2.1. Introduction:

Rheumatoid arthritis (RA) is an autoimmune disease hallmarked by synovial inflammation and matrix destruction. Therapy reduces clinical signs of arthritis, yet joint pain often persists [5]. Common rodent models used to study inflammation-induced pain include intra-plantar and intra-articular injections of inflammatory agents. Although useful, these models often do not fully address the impact of autoimmune mechanisms, such as B and T cell responses, nor do they allow assessment of chronic inflammation. From this aspect, the K/BxN serum transfer model may be useful as a model of arthritis-induced pain.

K/BxN mice spontaneously produce autoantibodies against the ubiquitous protein glucose-6-phosphate isomerase (GPI), which is present in the joints, with resultant immune complex-mediated development of inflammatory arthritis [14, 15]. Serum from these mice can be used to induce transient inflammatory arthritis in a wide range of mouse strains [102]. This broad transfer applicability distinguishes the K/BxN serum transfer model from many other common models of RA, such as collagen induced arthritis (CIA) which requires a specific genetic background [11, 12]. The K/BxN serum transfer model has a predictable onset of clinical signs of arthritis as recipient mice receive the same quantity of autoantibodies at the time of injection, and this model is not dependent upon breaking T cell tolerance. The clinical profile

has a severe inflammatory phase that reliably resolves as the autoantibodies are cleared and not replenished by autologous B cells.

While well established in the RA field, the K/BxN serum transfer arthritis model has not been characterized as an experimental model of inflammatory pain. In humans and animal models, persistent inflammation in the joint is associated with ongoing pain and a hypersensitivity to innocuous stimuli [103, 104]. As ligaments, fibrous capsule, meniscus, periosteum and the synovial layer are innervated by sensory Aβ, Aδ- and C-fibers noxious sensation can be evoked from these structures [103]. The increased pain sensitivity is thought to reflect changes in the innervated joint, peripheral nerve, dorsal root ganglia (DRG) as well as in the spinal cord neurons, leading to altered processing of nociceptive transduction [10, 103, 105]. Noteworthy, an increased expression of activating transcription factor 3 (ATF3) [106] has been reported in DRGs following chronic joint inflammation, indicating that long-term inflammation may lead to changes resembling a nerve injury state [10, 107, 108]. In addition, activation of microglia and astrocytes has been implicated in spinal nociceptive processing, both in models of inflammation and nerve injury-induced pain (reviewed in [28]). Pharmacologic interventions reducing glia activation reduce pain behavior, supporting a role for these cells in pain signaling [37, 40, 109-111].

The aim of this study was to characterize the K/BxN serum transfer model as a model of arthritis-induced pain. Hence we examined i) the temporal profile of pain behaviors, ii) the anti-nociceptive effect of three conventional analgesics, iii) spinal

microglia and astrocyte activation as well as iv) expression of the nerve-injury marker ATF3 protein in the DRG.

2.2. Materials and methods:

2.2.1 Animals

All animal experiments were carried out according to protocols approved by the Institutional Animal Care and Use Committee of the University of California, San Diego (under the Guide for Care and Use of Laboratory Animals, National Institutes of Health publication 85-23, Bethesda, MD, USA) and the local Ethical Committee for animal experiments in Sweden (Stockholms Norra Djurförsöksetiska Nämnd).

Mice were housed up to four per standard cage at room temperature, maintained on a 12-h light/dark cycle (light on at 07:00 h). Testing was performed during the light cycle. Food and water were available *ad libitum*. C57BL/6 mice (male, 25-30 g) were purchased from Harlan (Indianapolis, IN). KRN T cell receptor (TCR) transgenic mice were a gift from Drs. D. Mathis and C. Benoist (Harvard Medical School, Boston, Massachusetts, USA) and Institut de Génénetique et de Biologie Moléculaire et Cellulaire (Strasbourg, France), and were maintained on a C57BL/6 background (K/B). Arthritic mice were obtained by crossing K/B with NOD/Lt (N) animals (K/BxN). NOD/Lt mice were purchased from The Jackson Laboratory (Bar Harbor, Maine, USA).

2.2.2 Serum transfer and arthritis scoring

Blood from arthritic adult K/BxN mice was collected, centrifuged at 10,000 rpm for 10 min and the sera pooled. Groups of six to nine recipient C57BL/6 mice received 100 μl sera by intraperitoneal (i.p.) injection on days 0 and 2 (total volume 200 μl). Control animals were injected with pooled sera from naïve C57BL/6 mice. Clinical arthritis scores were evaluated using a scale of 0–4 as described previously [112]. Briefly, one point was given if swelling was observed for i) any or all of the digits ii) the knuckles, iii) the dorsal aspect of the paw and/or iv) the ankle. Hence, a higher number represents a greater disease progression, with a maximum score per paw of 4 and 16 per mouse. Ankle thickness was measured with a caliper in mm and compared to baseline thickness.

2.2.3 Drugs and drug delivery

Groups of K/BxN serum treated arthritic mice (n=6) received a single i.p. injection of gabapentin (100mg/kg; Pfizer), ketorolac (7.5mg/kg; Sigma), or etanercept (5 mg/kg; Amgen) during the period of acute inflammatory arthritis (day 4-10) or during the period of persistent allodynia (day 19-23) and were measured for changes in tactile allodynia for four hours following treatment. Gabapentin, ketorolac, or vehicle were delivered randomized to the mice on day 4 and tactile allodynia monitored for four hours; subsequently drugs were allowed to wash out for 48 hours before the same procedure was repeated on day 6. Following a second drug washout period of 3 days, etanercept or vehicle were injected on day 10. A second cohort of arthritic mice was used to test the drugs at the post-inflammation stage following a

similar protocol of testing on days 19, 21, and 23. All drugs were dissolved in normal saline, which was used as vehicle control. Etanercept [10], gabapentin [113, 114], and ketorolac [115] dosages were based on previous studies.

2.2.4 Behavioral tests

Animals were subjected to two behavioral tests, the thermal paw threshold test and the von Frey mechanical threshold test. To assess the thermally evoked paw withdrawal response, a Hargreaves-type testing device was used [116] (UARDG, Department of Anesthesiology, University of California, San Diego, 92103-0818). The device consists of a glass surface (maintained at 30 °C) on which the mice are placed individually in Plexiglas cubicles. The thermal nociceptive stimulus originates from a focused projection bulb positioned below the glass surface. A timer is activated by the light source, and latency was defined as the time required for the paw to show a brisk withdrawal as detected by photodiode motion sensors that stopped the timer and terminated the stimulus.

Mechanical sensitivity was assessed using von Frey hairs with hair values ranging from 2.44 to 4.31 (0.03g to 2.00g) and the up–down method [17] was applied as previously described. The 50% probability withdrawal threshold (force of the von Frey hair to which an animal reacts to 50% of the presentations) was recorded. Given the systemic nature of this model mechanical and thermal sensitivity values for both paws were measured and averaged in order to attain a single data point per day of measurement.

The data were also presented as the hyperalgesic index, which represents the area under the time-effect curve after drug delivery in which the percentage change from baseline (e.g .arthritic state) threshold is plotted against time. The resulting value has the units percentage change × time. The formula for calculating the percentage change is 100 × (baseline threshold − post-drug threshold)/(baseline threshold), where threshold was expressed in grams. Decreasing values indicate analgesic efficacy. The experimenter was blinded to drug treatments during all behavioral testing.

2.2.5 Histology

Whole knee joint sections were stained with hematoxylin and eosin (H&E) (HistoTox, Boulder, Colorado, USA). Histopathological evaluation was performed as previously described for inflammation and erosion [112].

2.2.6 Immunohistochemistry

At specified time points, mice were deeply anesthetized with euthasol and perfused intracardially with 0.9% saline followed by 4% paraformaldehyde. The lumbar spinal cord and L4–6 DRGs were removed, post-fixed and cryoprotected in sucrose. The DRGs were cut in transverse sections (10 μm) and mounted on glass slides. Lumbar sections (L4-L6) of the spinal cord were cut as free floating sections (30 μm). Tissue sections were incubated with anti-GFAP antibody (1:1000, Sigma), anti-Iba1 antibody (1:500, Abcam), anti-NeuN:biotinylated (1:1000, Chemicon) or anti-ATF3 (1:1000, Santa Cruz). Binding sites were visualized with secondary

antibodies conjugated with fluoro-Alexa-488 and Alexa-555 or streptavadin conjugated fluoro-Alexa-555 where appropriate (1:5000, Molecular Probes, Eugene, OR). An avidin/ biotin blocking kit (Vector Labs) was utilized as appropriate before biotinylated NeuN. Images were captured by Leica TCS SP5 confocal imaging system and quantified using Image-Pro Plus v.5.1 software.

Reactivity of glia is characterized by both an increase in the number of cells, and in the conformational extension of these cells (rounding of the cell bodies and thickening of processes) leading to an increase in labeling with increasing glia reactivity. Microglia (Iba1) and astrocyte (GFAP) staining was quantified by measuring the total integrated intensity of pixels divided by the total number of pixels in a standardized area of the dorsal horn. The investigator was blinded to experimental conditions during the quantification. Staining intensity was examined in lamina I-II of the superficial dorsal horn or of a standardized box in lamina V of the deeper dorsal horn region with 3 slices (separated by at least 180 μm) examined per animal and 3 animals per experimental condition. Only pixels above a preset background threshold were included. An increase in the integrated intensity / pixels for Iba1 and GFAP staining was interpreted to signify microglia and astrocyte reactivity, respectively. All data is presented as % change from the corresponding control group. Statistics were performed on raw data values.

ATF3 staining was assessed by counting the number of cells with ATF3 positive nuclei over the total number of NeuN positive cells with visible nuclei. L4 and L5 DRGs were group mounted for individual animals onto slides. Each slide

contained 2-4 DRGs (L4-L5). All slides were separated by at least 60 μm. Three to five slides per animal (n=3-4) were counted.

2.2.7 Quantitative Real-time PCR (RT-PCR)

The mRNA from flash frozen lumbar spinal cord lumbar was extracted using Trizol (Invitrogen) according to the manufacturer's protocol. Complementary DNA was prepared and quantitative real-time PCR performed with TaqMan Gene Expression Assays (both according to the manufacturer's instructions, Applied Biosystems) to determine relative mRNA levels, using the GeneAmp 7500 Fast Sequence Detection system (Applied Biosystems). Pre-developed specific primers were used to detect glial fibrillary acidic protein (GFAP) (Assay ID Mm00546086_m1), CD11b (Assay ID Mm00434455_m1), and HPRT1 (Assay ID Mm00446968_m1) (Applied Biosystems). Relative abundance was calculated by comparing delta-CT values [117] and the data were then normalized to HPRT1 gene expression to obtain relative concentration and presented as relative gene expression.

2.2.8 Statistics

Data are given as mean ± standard error. For comparison of change of pain behavior, a two-way ANOVA for repeated measures with Bonferroni *post hoc* tests was used. For comparison of microglia, and astrocyte changes a one-way ANOVA with Bonferroni *post hoc* test was used. ATF3 and mRNA changes were analyzed by a student's t-test compared to control values. Drug treatment data were also presented

as a hyperalgesic index, a derived value that defines the magnitude of arthritis induced sensitization by quantifying the area under the curve compared to baseline values.

2.3. Results

2.3.1 Characterization of arthritic pain behavior and clinical signs

Mice were injected on days 0 and 2 with 100µl pooled K/BxN sera. As previously reported, within 24 hours following serum transfer, mice developed significant clinical signs of arthritis [14].These signs, including redness and swelling, were significantly increased over days 1-12, peaking at day 6, $p<0.05$-0.001 (Figure 2.1A). Ankle joints diameter was also significantly increased compared to baseline levels on days 3-9, $p<0.05$-0.001 (Figure 2.1B). Significant tactile allodynia was present in arthritic animals on days 2-28, excluding day 12, compared to control sera treated animals, $p<0.01$-0.001 (Figure 2.1C). Animals reached maximum severity of tactile allodynia at day 4, which surprisingly remained robustly stable excluding day 12 through the end of the study at day 28. A mild thermal hypoalgesia was initially present in these arthritic mice compared to control sera treated mice from days 4-6, $p<0.001$, before returning to baseline. Arthritic animals showed no other signs of thermal sensitivity after day 6 (Figure 2.1D).

Histopathologic changes in the knee joints were examined using H&E staining. Joint sections from mice injected with control sera harvested day 6 (Figure 2.2A) and day 28 (Figure 2.2B) showed no evidence of infiltrating inflammatory cells or alterations in the bone or cartilage architecture. In comparison, knee joint sections

from K/BxN sera treated arthritic mice showed inflammatory cell infiltration (Figure 2.2C; as indicated by the arrow) at day 6, which paralleled visible ankle joint swelling measurements. Although the clinical swelling in the paw and ankle and accompanying microscopic inflammatory cell infiltrate visualized in the knee joint were resolved by day 28, joint sections from the mice that received K/BxN sera displayed persistent bony erosions (Figure 2.2D) at this time point.

2.3.2 Characterization of microglia and astrocyte spinal cord changes in acute and chronic phases

Persistent allodynia, especially during chronic pain can be linked to changes in the spinal cord [34, 118]. To investigate this, lumbar spinal cord gene and protein expression levels of markers for activated astrocytes (GFAP) and microglia (Cd11b or Iba1) were measured during peak inflammation (day 6) and during the persistent allodynia, without inflammation, late phase (day 28). Changes in mRNA transcription levels of CD11b and GFAP were quantified by real time RT-PCR. CD11b mRNA levels were increased in day 6 arthritic mice (6.67 +/- 0.7 vs. 3.04 +/-0.54 relative expression units (REU) in arthritic vs. control mice, respectively, $p<0.01$) and in day 28 arthritic mice (7.93 +/- 1.6 vs. 3.55 +/- 0.8 REU in control mice, $p<0.05$), Figure 2.3A. GFAP mRNA levels were increased in day 6 arthritic mice (6.87 +/- 0.7 vs. 2.9 +/- 0.4 REU in control mice, $p<0.001$) and day 28 arthritic mice (9.75 +/- 2.0 vs. 3.58 +/- 0.9 REU in control mice, $p<0.05$), Figure 2.3B.

GFAP and Iba1 protein expression levels were assessed using immunoreactivity. The average of control scores for each day of interest were set to 100% and changes in staining were reported as percent change compared to control values for the day of interest. Immunostaining of sections from L4-L6 with antibodies targeting microglia (Iba1) showed an increase in microglia staining in the superficial region of the dorsal horn (lamina 1 and 2) and in deeper dorsal horn areas (sample from lamina 5) at day 6 compared to control (Figure 2.4A and 2.4C). On day 6 superficial microglia dorsal horn staining is 539±114% ($p<0.001$) of control levels. Deeper dorsal staining is 381±28% ($p<0.05$) of control levels. On day 28 staining of microglia was still significantly elevated in the superficial dorsal horn region as compared to control animals (Figure 2.4A and 2.4D). On day 28, superficial microglia dorsal horn staining is 201±34% ($p<0.05$) of day 28 control levels. Microglia staining in the deeper dorsal horn region on day 28 is 142±26% ($p>0.05$) of control staining values.

The same spinal cord sections were also stained for the astrocyte marker (GFAP) and evaluated according to the same protocol as used for microglia staining. The integrated intensity of superficial dorsal horn staining was markedly enhanced on day 6 (Figure 2.4B and 2.4E) but did not remain elevated by day 28 as compared to control mice (Figure 2.4B and 2.4F). On day 6 superficial astrocyte dorsal horn staining is 170±16% ($p<0.05$) of control staining. No significant changes in deep dorsal horn staining were seen at either time point measured.

2.3.3 Mechanical hypersensitivity induced by arthritis during the peak inflammation phase is attenuated by anti-inflammatory and analgesic agents

To further characterize pain behavior in the K/BxN serum transfer model of arthritis we assessed reversal of allodynia during peak inflammation following injection of different classes of analgesic compounds. The average C57BL/6 control mechanical threshold is presented on these graphs as a dotted line at 1.52g (Figure 2.5). All drugs were given i.p. with saline as vehicle and the mice tested by application of von Frey filaments, using the up-down method, for four hours following drug delivery. Gabapentin, ketorolac, or vehicle were delivered randomized to the mice on day 4 and tactile allodynia monitored; subsequently drugs were allowed to wash out for 48 hours before the same procedure was repeated on day 6. Following a second drug washout period of 3 days, etanercept or vehicle were injected on day 10. To begin with, we assessed the anti-allodynic effect of ketorolac, a mixed cyclooxygenase (COX) inhibitor. Ketoroloac treated animals (7.5mg/kg) had significantly increased tactile thresholds at 60, 120, and 180 minutes ($p<0.01$, 0.01 and 0.05) after treatment (Figure 2.5A). The second drug investigated was gabapentin, originally approved for seizures, but also currently prescribed for neuropathic pain. Gabapentin treated animals (100mg/kg) had significantly increased tactile thresholds at 30, 60, and 120 minutes ($p<0.05$, 0.001 and 0.001) after treatment (Figure 2.5B). Lastly, we tested the anti-allodynic effect of etanercept, a TNF decoy receptor fusion protein, which significantly reduced swelling, clinical signs, and tactile allodynia in CIA [10]. Etanercept treated animals (5mg/kg) had significantly increased tactile thresholds at

120 and 180 minutes ($p<0.01$ and 0.001) after injection. Drug efficacy was also quantified by comparing the hyperalgesic index for animals receiving and not receiving treatment. Etanercept ($p<0.05$), gabapentin ($p<0.001$), and ketorolac ($p<0.01$) all display significant analgesic activity in comparison to their respective saline treated vehicle control arthritic animals according to this measure (Figure 2.5D).

2.3.4 Post inflammation arthritis induced mechanical hypersensitivity is attenuated by gabapentin but not by etanercept or ketorolac

Given the changes in joint inflammation, clinical signs, and spinal cord glial staining in mice between day 6 and day 28 we decided to investigate changes in analgesic responsiveness during this second time period. The average C57BL/6 control threshold is also presented on these graphs as a dotted line at 1.52g (Figure 2.6). All drugs were given i.p. in saline at identical dosages to day 6 and tested in the same fashion as during day 6. Etanercept treated animals (5mg/kg) had a very modest but significant increase in tactile threshold at 60 minutes ($p<0.01$) after injection (Figure 2.6A). Gabapentin treated animals (100mg/kg) had significantly increased tactile thresholds at 30, 60, and 120 minutes ($p<0.05$, 0.001 and 0.01) after treatment (Figure 2.6B). Ketorolac treated animals (7.5mg/kg) displayed no significant difference in tactile thresholds during the four hours following treatment (Figure 2.6C). Drug efficacy was also quantified by comparing the hyperalgesic index for animals receiving drug treatment and those receiving vehicle treatments. Only

gabapentin ($p<0.05$) displayed a significant analgesic activity in comparison to saline treated vehicle controls according to this measure (Figure 2.6D).

2.3.5 Changes in ATF3 in the DRG during inflammation and post inflammation

Given the efficacy of gabapentin on pain behavior in the K/BxN serum transfer arthritis, DRGs from 6 and 28 day control and arthritic mice were immunostained for ATF3, a marker of nerve injury, and NeuN. DRGs were scored such that values represent the number of ATF3 positive stained cells out of the total number of neuronal cells containing a visible nucleus. Control animals from day 6 and day 28 had a mean ATF3/NeuN ratio of 0.004 ±0.0005 and 0.05 ±0.03, respectively (Figure 2.7A, D). Day 6 arthritic animals (Figure 2.7B, C) had a mean ATF3/NeuN ratio of 0.14 ±0.09 ($p>0.05$ vs control) and day 28 arthritic animals (Figure 2.7E) had a mean ATF3 staining ratio of 0.23 ± 0.06 ($p<0.05$ vs control). ATF3 expression in DRGs from day 6 arthritis animals was variable. Hence, representative images from low ATF3 (Figure 2.7B) and high ATF3 expressing mice are depicted in Figure 2.7C. The staining is quantified in Figure 2.7F.

2.4. Discussion

Several monoarticular arthritis models are commonly used as pain models of "inflammatory arthritis" including intra-articular injection of inflammatory agents such as carrageenan or CFA [119, 120]. These models are very useful in studies of local acute inflammation and the short-term impact of such inflammation on the

nervous system. Given the chronic inflammation present in RA we sought to define the effects of a longer-lasting inflammation, using the K/BxN serum transfer arthritis model, upon nociceptive processing. The current report is the first to examine this model as a tool for evaluating pain behavior and understanding changes in nociceptive processing during arthritic disease progression. Mice injected with K/BxN serum display robust mechanical allodynia. The onset correlates with an increase in paw and ankle swelling and the number of affected joints. Surprisingly, the mechanical hypersensitivity did not return to baseline even two weeks after loss of visible and histologic signs of synovitis. An increase in spinal microglia (Iba1) and astrocyte (GFAP) staining was observed, with the most prominent increase at day 6, during peak inflammation. During this stage of K/BxN serum transfer mediated arthritis, i.p. bolus injection of etanercept, ketorolac, and gabapentin had anti-allodynic effects. At day 28, microglia staining remained elevated, while astrocyte staining was not significantly different from control. Interestingly, arthritic mice at the post inflammation stage showed no response to the previously effective dose of etanercept or ketorolac, but an anti-allodynic effect was observed following bolus injection of gabapentin.

Recently, the CIA model, the most widely used model of chronic murine arthritis, was validated as a pain model [10]. CIA mice display maximal clinical scores 7-10 days post arthritis induction, with correlating tactile allodynia. A robust tactile allodynia is characteristic of both models, however the thermal hypersensitivity reported in the CIA model was not detected in the K/BxN serum transfer model.

Rather, a transient mild hypoalgesia was observed corresponding to the period of peak inflammation. There is a clear correlation between development of arthritis and mechanical hypersensitivity in animal models and RA patients [121, 122]. However, thermal hypersensitivity in RA patients is unclear. Leffler and colleagues reported no differences in thermal sensitivity over the affected joint in RA patients of short (< 1year) duration, longer duration (>5 years) or in control groups [104]. In contrast, Edwards et al. reported that RA patients have reduced thermal thresholds [123]. Differential control of thermal and mechanical hypersensitivity have been observed in other animal models of pain [124-129]. Further studies are warranted to expand our understanding of the mechanisms that lead to differential sensory processing.

Consistent mechanical allodynia occurs following induction of K/BxN serum transfer arthritis. Based on our observations that i) etanercept, a TNF blocker not crossing the blood-brain barrier, diminishes allodynia, ii) ATF3 expression is induced in the DRGs and iii) spinal glia are activated, hypersensitivity is likely driven by both peripheral sensitization of the joint innervating nerves and central sensitization. During joint inflammation low threshold Aδ fibers have increased output in response to noxious and non-noxious stimuli while high threshold Aδ and C fibers have reduced mechanical thresholds (reviewed in [103]). ATF3, a member of the ATF/CREB transcription factors family, is induced in a variety of tissues exposed to stress [130]. Although its function is not clearly elucidated, ATF3 is commonly used as a marker of nerve injury [106, 131, 132]. This study reports clinical signs of inflammation lasting approximately 2 weeks which appears to be sufficient to induce signs of nerve

damage. In the CIA model, ATF3 was induced in DRGs 14 days after arthritis onset [10]. Of note, ATF3-induction has been observed in DRGs of horses with laminitis in hoof [108] and in rats with monosodium iodoacetate-induced osteoarthritis [133], indicating that other long-term painful conditions, which are not directly associated with nerve injury but rather chronic inflammation and joint damage, respectively, may also transition to a painful state with a neuropathic trait. Hence, it is possible that long-term inflammation or joint damage leads to a state that exhibits some features in common with neuropathic pain. However, further studies to examine the underlying mechanisms for such transition are necessary, and at current state we cannot exclude the possibility that the persistent pain is driven by continuous nociceptive input from the damaged joint.

Spinal sensitization is a complex event linked to diverse mechanisms including repeated activation of glutamate NMDA receptors (reviewed in [24, 25]), tachykinin NK1 receptor activation (reviewed in [25]), spino-bulbo-spinal loop activity [27] and glial activation (reviewed in [28]),[29]. Spinal microglia and astrocyte activation during central sensitization has been reported in variety of nociceptive states including peripheral inflammation [30], osteosarcoma [31], HIV-1 gp120 induced pain [32], and spinal nerve ligation induced neuropathic pain [33, 34]. The role of microglia and astrocytes in central sensitization has attracted significant interest as interventions directed at blocking the action of these cells are anti-nociceptive in many pain models (reviewed in [28, 35, 36]). K/BxN serum transfer arthritis increased spinal astrocyte and microglia associated mRNA levels and immunoreactivity, which we interpreted to

indicate activation. However, we did not functionally assess the consequences of glia blockade. Common between other chronic pain models such as the paw incision and L5 nerve transection model and our investigation are early microglia reactivity. Increases in astrocyte immunoreactivity are present in all models, but they display varying temporal patterns [109, 134].

Spinal glial changes are presumed to be an effect of the peripheral inflammation and resulting nociceptive input. Serum transfer could, however, have a direct effect upon the spinal cord. This is unlikely, given unaltered tactile thresholds in control mice following injection of naïve mouse serum. Furthermore, the GPI autoantibody has been identified as the pathogenic factor during K/BxN serum transfer arthritis. Positron emission tomography has tracked anti-GPI antibodies following serum transfer, and describes preferential localization to the paws, ankles and knees but not to the vertebral joints [135]. Though a direct spinal action of the serum cannot be completely eliminated, spinal glial activation is more likely the result of sustained peripheral inflammation and associated nociceptive input.

The clinical signs of arthritis during K/BxN transfer arthritis are reduced by COX and IL-1β inhibitors [112, 136, 137]. Here, we assessed the anti-allodynic effect as opposed to reduction of clinical signs for three classes of drugs. We tested a non-selective COX-1/COX-2 inhibitor (ketorolac), a TNF receptor fusion protein (etanercept), and synthetic gabapentin. All three compounds reduced mechanical hypersensitivity during the inflammatory phase. Surprisingly, only i.p. gabapentin robustly reversed the post inflammation mechanical hypersensitivity. Gabapentin and

pregabalin are approved for neuropathic pain treatment with efficacy against diabetic neuropathy [138] and post herpetic neuralgia [139]. These compounds bind to the α2δ subunit of voltage sensitive calcium channels and *in vitro* acutely alter neurotransmitter release including glutamate, noradrenaline, GABA, substance P and CGRP [140, 141]. Though not commonly prescribed for pain indications besides neuropathic pain, gabapentin also attenuates inflammation-induced pain in rats [142]. Hence, the observation that only gabapentin was effective in the post-inflammatory phase strongly suggests that the mechanisms that drive the allodynia in the two phases are different, it does not prove that the post-inflammatory allodynia has a neuropathic trait.

TNF-blockers such as etanercept improve clinical signs and slow disease progression in RA. Beyond being an important inflammatory factor, TNF has a direct neuronal action [143, 144]. Boettger et al demonstrated that intra-articular etanercept injection reduced joint afferents' responses to rotation of the inflamed joint within 30 minutes after injection, without gross changes in inflammation or alteration of the normal joint response to rotation [145]. Accordingly, we observed an anti-allodynic effect during the inflammation phase within 1 hour following bolus i.p. injection of etanercept, indicating a peripheral anti-nociceptive effect of TNF-neutralization. Current data suggests that COX and TNF play a minor role in pain processing during the post-inflammation phase, or that a single injection is not sufficient to reverse established allodynia. The anti-allodynic effect of a single dose of gabapentin has potential therapeutic implications given that the most common agents for RA therapy

include TNF blockers and NSAIDs, which address different mechanisms. Further investigation of gabapentin and pain relief in RA patients would be of great interest.

In summary, K/BxN serum transfer arthritis induces tactile allodynia during the inflammatory phase with an expected sensitivity to systemic NSAIDs and etanercept. Of interest, however, is the extension of the allodynic state beyond the period of clinical inflammatory arthritis, with a time dependent shift towards characteristics indicative of a neuropathic state, including loss of sensitivity to NSAIDs, a continued sensitivity to gabapentin, and the appearance of ATF3. At the spinal level this model demonstrated continued microglial activity, but not astrocytic activation. We believe that the K/BxN serum transfer arthritis model will be of importance in pain studies as it can be applied to different strains of mice. Characterization of this model describes a pain state transition, which is recapitulated in this model unlike other models, and might also occur in RA despite adequate therapy. In conclusion, the K/BxN serum transfer model represents a multifaceted model for studies exploring pain mechanisms in conditions of joint inflammation and may serve as a platform for exploring novel treatment strategies for pain in human arthritic conditions.

2.5 Acknowledgements

Chapter 2, in full, is a reprint of material as it appears in Christianson CA, Corr M, Firestein GS, Mobargha A, Yaksh TL, Svensson CI . “Characterization of the acute

and persistent pain state present in K/BxN serum transfer arthritis.” Pain, Vol. 151 2010. The dissertation author was the primary investigator and author of this material.

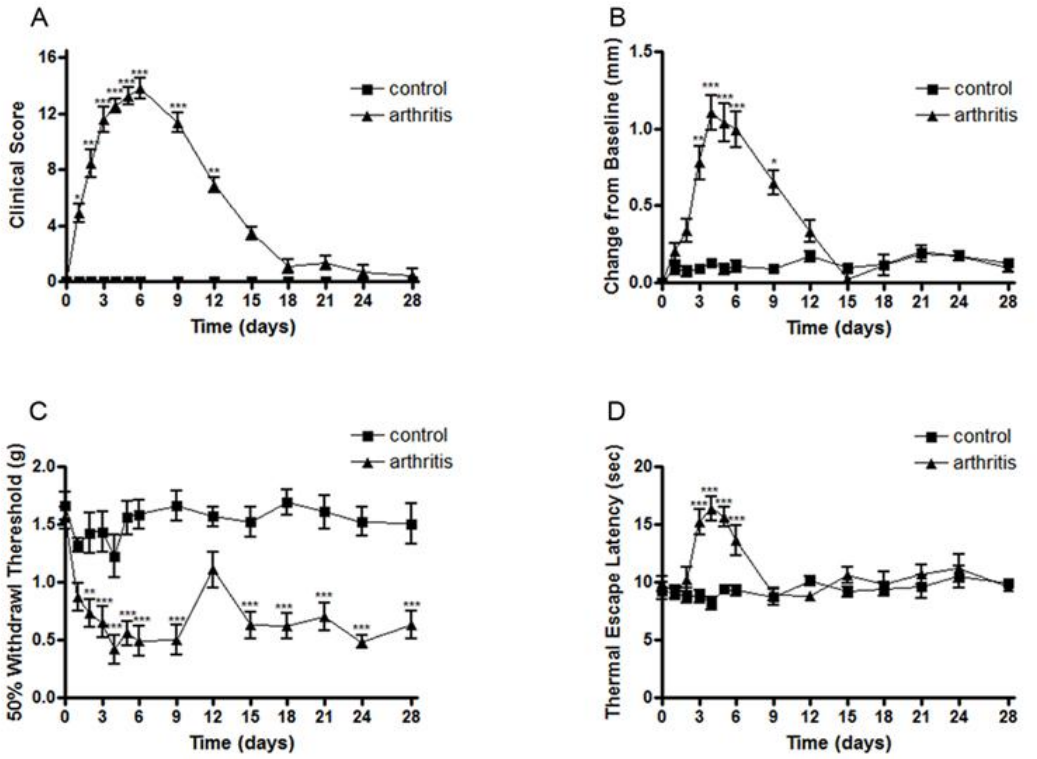

Figure 2.1. Characterization of K/BxN arthritis pain behavior. Graphs display (A**)** arthritis clinical scores assessed for 28 days, demonstrating an increase in clinical signs of arthritis day 1-12, (B) ankle thickness measured with calipers showing a significant ankle swelling in arthritic animals day 3-9, (C) tactile thresholds (g) showing tactile allodynia day 2-28 (excluding d12) and (D) thermal thresholds (sec) demonstrating that arthritic animals displayed significant thermal hypoalgesia day 3-6, with no changes from baseline at any other time point. Each time point represents mean ± SEM (n=9 mice/group), *= $p<0.05$, **= $p<0.01$, and ***= $p<0.001$ by Bonferroni post test.

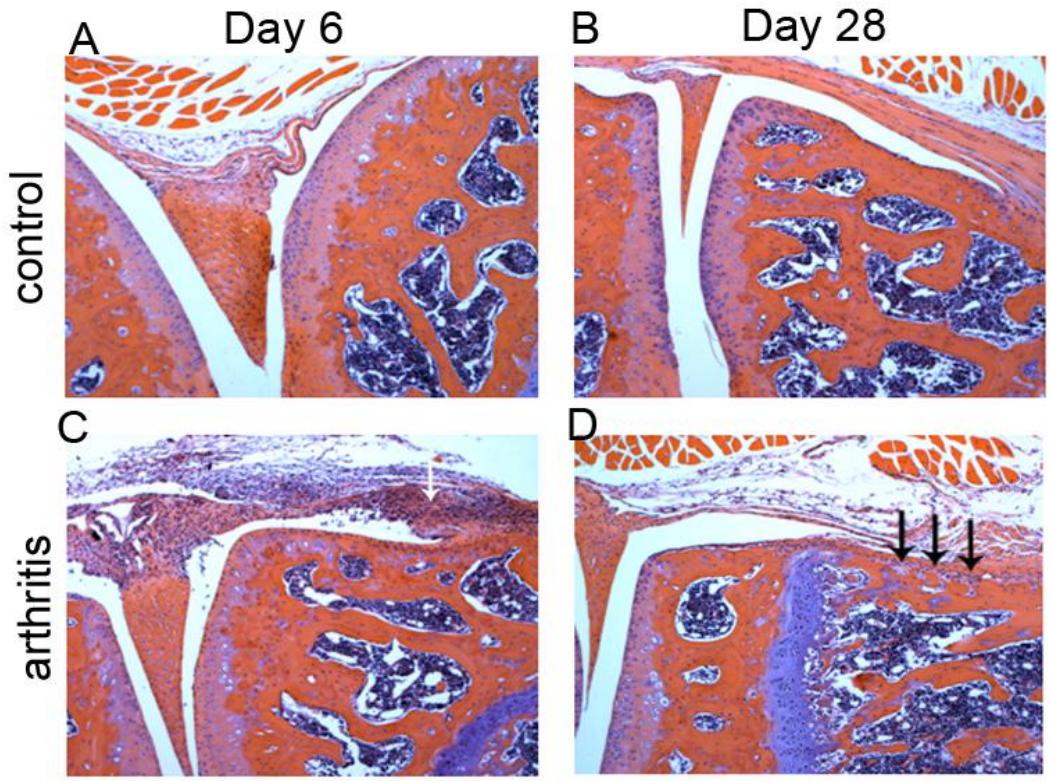

Figure 2.2. K/BxN serum transfer induced joint destruction. Mice were sacrificed on days 6 and 28 and the knee joints removed and prepared for histology, sectioned and stained with Hematoxylin and Eosin. Representative images are shown. There was a prominent inflammatory infiltrate on Day 6 in the mice that received K/BxN sera (white arrow) and residual bony erosions on Day 28 (black arrowheads). Original x50 magnification.

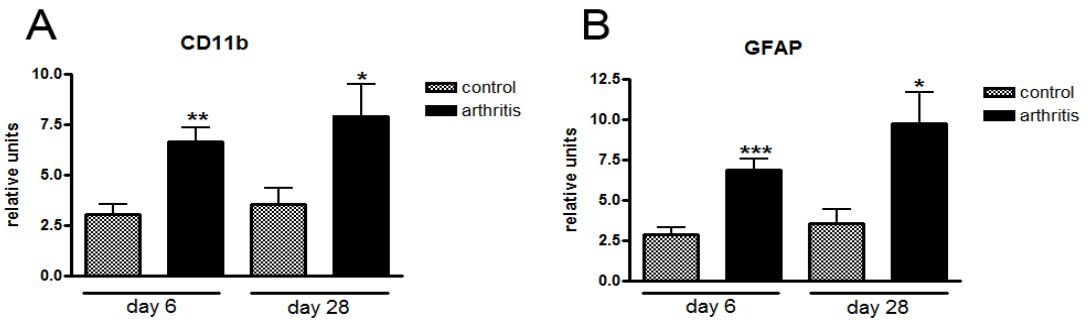

Figure 2.3. Microglia (CD11b) and astrocyte (GFAP) mRNA levels are elevated in the spinal cords of arthritic animals compared to control mice. Graphs show (A) CD11b and (B) GFAP mRNA relative expression units (REU) in the spinal cords of day 6 and day 28 arthritic compared to control serum treated animals. Each time point represents mean ± SEM (n=5-6 mice/group), *=$p<0.05$, **= $p<0.01$, and ***=$p<0.001$ by student's t-test.

Figure 2.4. Microglia and astrocyte immunoreactivity are elevated in the lumbar regions of spinal cord following induction of serum transfer mediated arthritis. (A) Representative images for Iba1 immunoreactivity in arthritic and control mice on days 6 and 28 post induction of arthritis. Increased staining for Iba1 is present in the superficial dorsal horn (lamina I-II) and deep dorsal horn (lamina V) 6 days in the superficial dorsal horn day 28. (C, D) Graphs showing quantification of Iba1 signal intensity. (B) Representative images of GFAP immunoreactivity days 6 and 28 post serum injection. Increased GFAP staining was observed in the superficial dorsal horn (lamina I-II) day 6, but not day 28 or in the deep dorsal horn, after induction of arthritis. (E,F) Graph depicting quantification of GFAP signal intensity. Each time point represents mean ± SEM (n=3 mice per group, 3-5 sections per mouse), *= $p<0.05$, and ***=$p<0.001$ by Bonferroni post test. Scale bars represent 50μm.

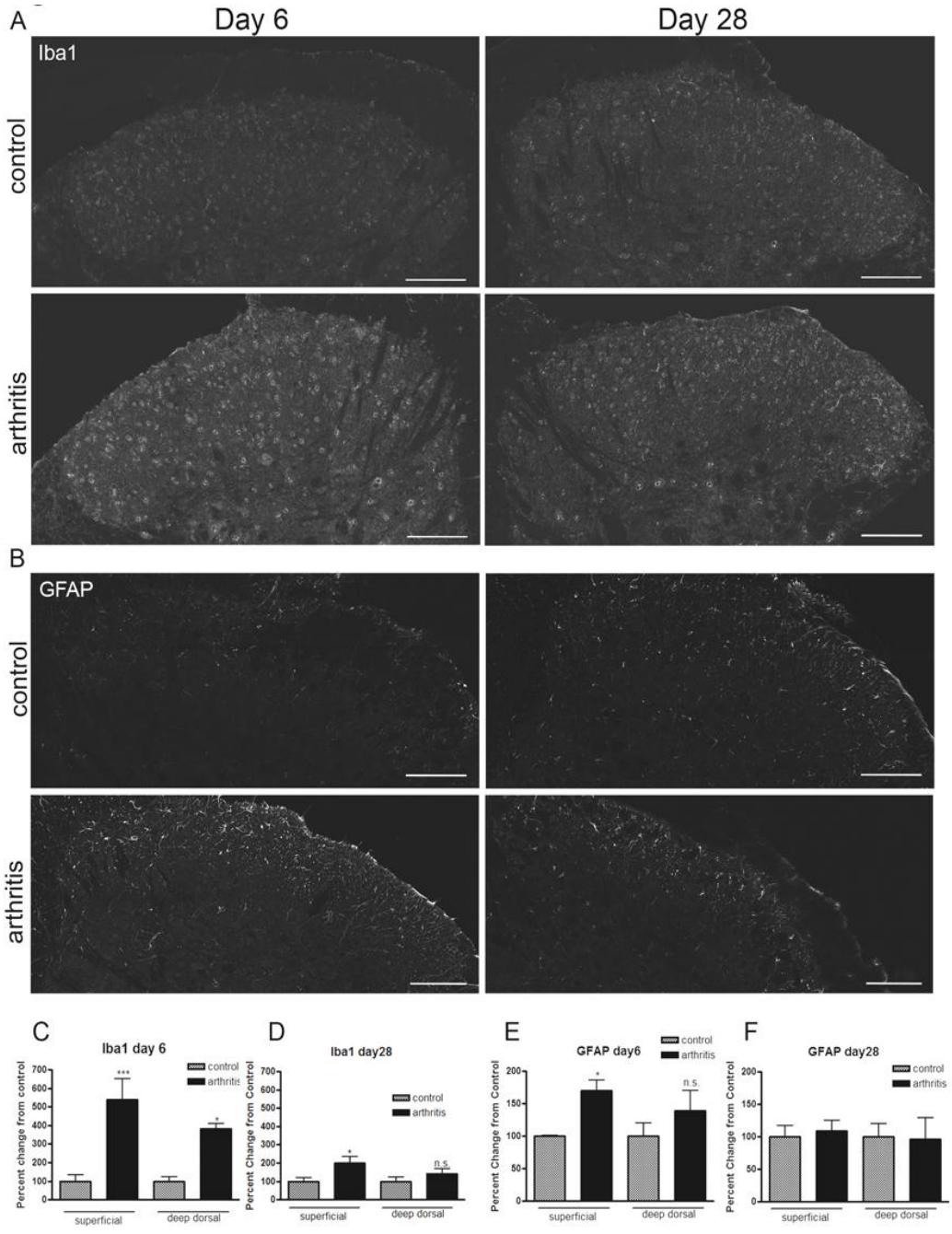
A
Day 6
Day 28
Iba1
control
arthritis
B
GFAP
control
arthritis
C
Iba1 day 6
D
Iba1 day28
E
GFAP day6
F
GFAP day28
control
arthritis
Percent change from control
Percent Change from Control
superficial
deep dorsal
n.s.

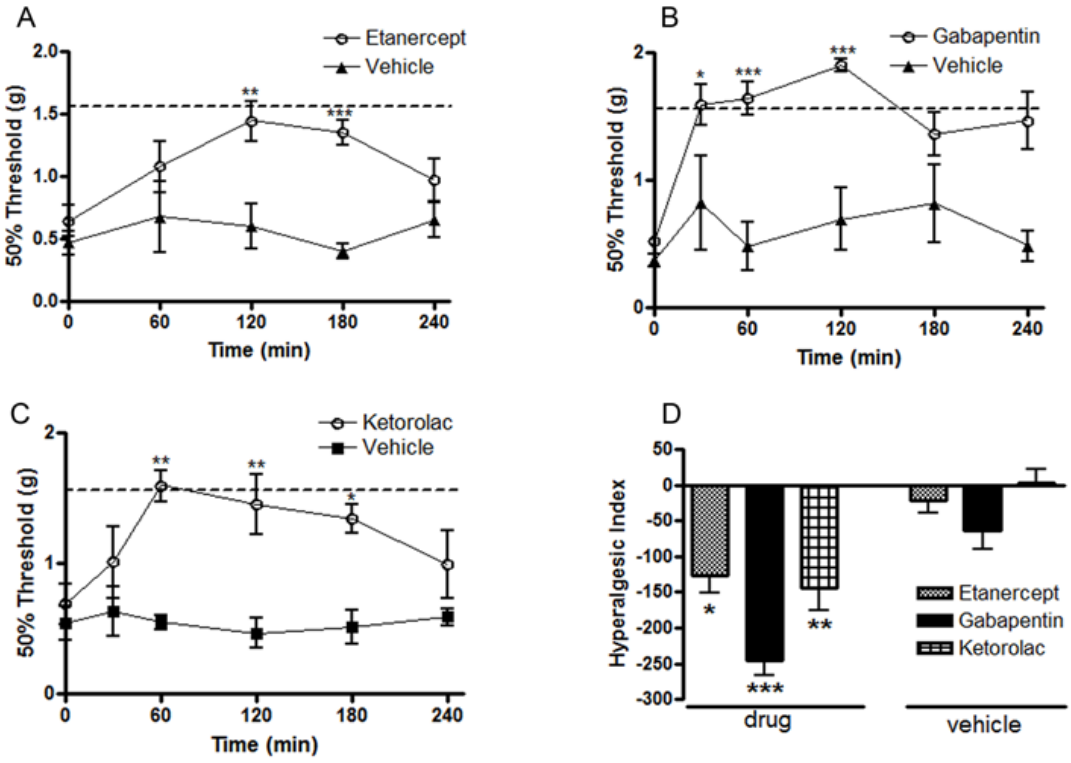

Figure 2.5. Intraperitoneal injection of etanercept, gabapentin and ketorolac reverses tactile allodynia in the K/BxN serum transfer arthritis model. Graphs showing anti-allodynic effect of i.p. injection of (A) etanercept (5mg/kg), (B) gabapentin (100mg/kg) and (C) ketorolac (7.5mg/kg) at the peak of paw swelling when tested for changes in mechanical thresholds every 30 minutes for four hours. Saline was used as vehicle for all drugs. (D) Hyperalgesic index indicates a significant decrease in pain behavior for etanercept, gabapentin, and ketorolac. Dotted line indicates average control tactile threshold (1.52g). Each time point and bar represents mean ± SEM (n=6-7 mice/group for all groups), *= $p<0.05$, **=$P<0.01$, and ***=$p<0.001$ by Bonferroni post-test.

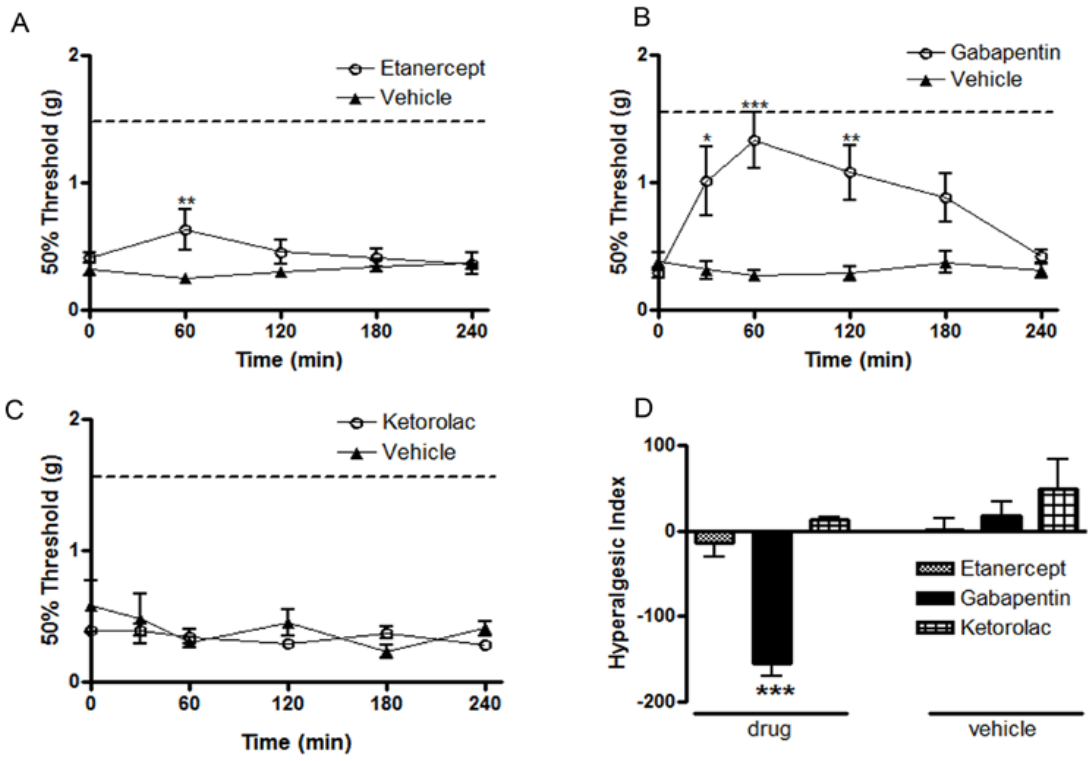

Figure 2.6. K/BxN serum transfer arthritis induced day 28 tactile allodynia is reduced by intraperitoneal injection of gabapentin, but not etanercept or ketorolac. Graphs depicting effect of i.p injection of vehicle and (A) etanercept (5mg/kg), (B) gabapentin (100mg/kg i.p.) and (c) ketorolac at one hour intervals for four hours. (D) Hyperalgesic index indicates a significant decrease in pain behavior for gabapentin, but not for etanercept or for ketorolac as compared to vehicle. Dotted line indicates average control tactile threshold (1.52g). Each time point represents mean ± SEM (n=6 mice/group), *= $p<0.05$, **=$P<0.01$, and ***=$p<0.001$ by Bonferroni post test.

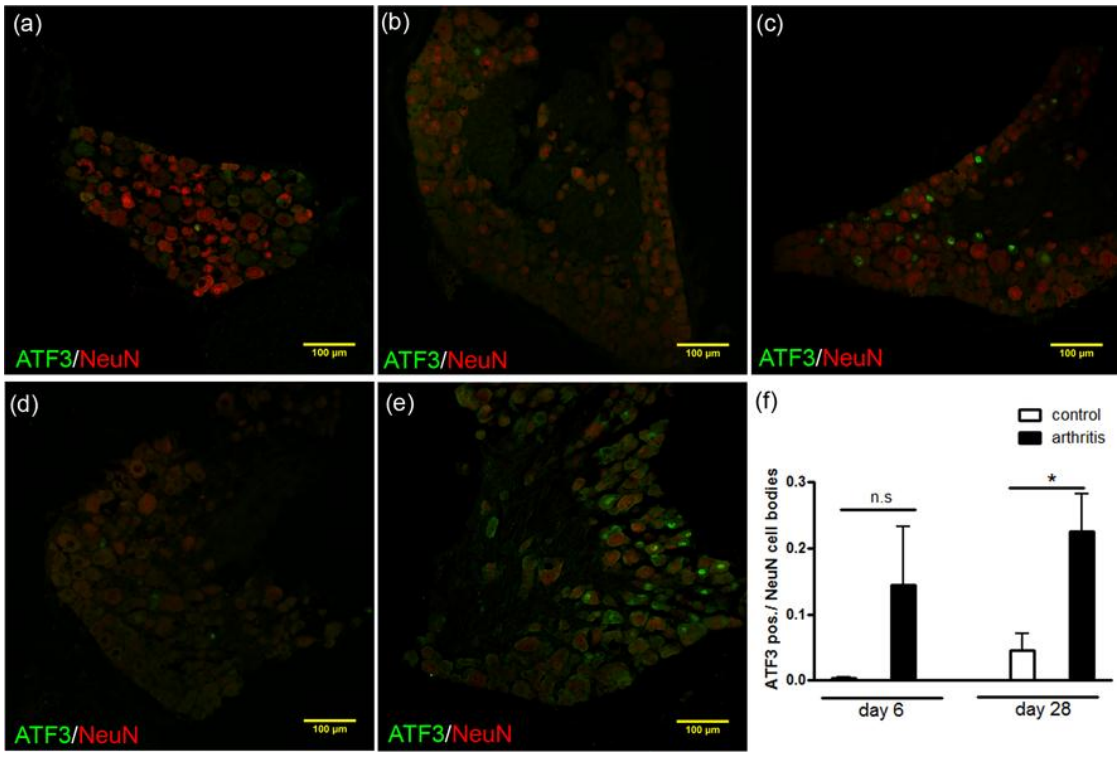

Figure 2.7. The number of ATF3 positive cells is increased in dorsal root ganglia following induction of K/BxN serum transfer arthritis. Representative images of (A) day 6 control mice and day 6 arthritis mice with (B) low and (C) high ATF3 immunoreactivity. ATF3 staining in 28 days (D) control and (E) arthritic mice showed that injection of K/BxN serum lead to a significant increase in number of ATF3 positive neurons day 28. (F) Graph showing the number of cells positive for ATF3 divided by the total number of NeuN positive nuclear cell bodies in the different groups. Each bar represents mean ± SEM (n=3-4/group, 3-5 sections per mouse) and *=$p<0.05$ by student's T-test. Scale bars represent 100µm.

Chapter 3

Role of toll-like receptor 4 in 15d-PGJ_2 mediated mechanical hypersensitivity following K/BxN serum transfer arthritis

3.1. Introduction:

Approximately one percent of the population is diagnosed with rheumatoid arthritis (RA), a systemic autoimmune mediated disease comprising synovial inflammation and matrix destruction. Despite the efficacy of new therapeutics and treatment strategies (e.g. combination therapies), pain is still a significant problem, which can persist after resolution of joint swelling. In a recent survey, more than 85% of RA patients described their physical RA symptoms as somewhat/ completely controlled, yet greater than 75% of them reported moderate to severe pain within the previous two months [8]. Thus, while peripheral inflammation is an important component of RA, it cannot fully explain the magnitude of pain the arthritis patient reports. This may represent the initiation of a facilitated state of nociceptive processing at the level of the spinal dorsal horn [5].

Toll-like receptors (TLRs), notably TLR4, present on peripheral inflammatory cells (lymphocytes, macrophages, and mast cells) recognize both microbial and endogenous ligands. The synovial tissue of moderately inflamed RA patients contains increased TLR4 protein as compared to osteoarthritic or normal tissue [146, 147]. Using animal models, studies have postulated a role for TLR4 in maintaining

inflammation during inflammatory arthritis. *Tlr4-/-* mice subjected to streptococcal cell wall (SCW) induced arthritis have normal acute joint swelling but a suppressed persistent inflammation phase including reduced levels of IL-1β, TNF, IL-6 and reduced cartilage destruction [86]. Similarly, lack of the endogenous TLR4 ligand tenascin-C protects mice from joint destruction during antigen-induced arthritis. While these mice mount an acute inflammatory response to the antigen, synovial inflammation resolves with little or no synovitis, pannus formation and destruction of the articular cartilage or bone erosion [148].

Activation of the TLR4 complex can initiate two distinct pathways; 1) resulting in NFκB activation including pro-inflammatory cytokines and TH1 responses and 2) resulting in interferon-β production (reviewed in [149]). In addition to a peripheral distribution, TLR4 is extensively expressed on spinal microglia [150], astrocytes [81], and certain small primary afferent neurons [151]. These non-neuronal cells are critical in the development of facilitated pain states following inflammation and nerve injury (reviewed in [28, 41, 152, 153]). Nerve injury induced hypersensitivity is attenuated in *Tlr4-/-* mice and in mice in which spinal TLR4 has been knocked-down using antisense oligonucleotides [87, 88].

We have previously demonstrated that K/BxN serum transfer arthritis induces mechanical hypersensitivity concurrent with the onset of inflammation, which remains reduced despite resolution of the clinical arthritis signs. In the present studies, we thus sought to investigate the role of TLR4 in the transition to a persistent pain-like behavior resulting from chronic inflammatory arthritis. Using *Tlr4-/-* mice and IT

delivery of LPS-RS, a TLR4 antagonist, we demonstrate that the transition to persistent mechanical hypersensitivity is dependent upon spinal TLR4 during the inflammation phase. This TLR4 blockade returns spinal cord 15-deoxy-$\Delta^{12,14}$-Prostaglandin J_2 (15d- PGJ_2) to pre-arthritic levels.

3.2. Materials and Methods:

3.2.1 Animals

Animal experiments were all conducted according to protocols approved by the Institutional Animal Care and Use Committee of the University of California San Diego.

Mice were housed up to five per standard cage at room temperature and maintained on a 12 hour light/ dark cycle. All behavioral testing was performed during the light cycle period. Both food and water were available *ad libitum.* Wild type C57Bl/6 (WT) mice (male 25-30g), C3H/Hej mice (male 25-30g), and C3H/HeOuJ mice (male 25-30g) were purchased from Harlan (Indianapolis, IN). KRN T cell receptor (TCR) transgenic mice were a gift from Drs. D. Mathis and C. Benoist (Harvard Medical School, Boston, Massachusetts, USA) and Institut de Génénetique et de Biologie Moléculaire et Cellulaire (Strasbourg, France). These mice were maintained on a C57Bl/6 background (K/B). Arthritic mice were obtained by crossing K/B with NOD/Lt (N) animals (K/BxN). NOD/Lt mice were purchased from The Jackson Laboratory (Bar Harbor, Maine, USA). Toll-like receptor 4 knockout (*Tlr4-/-*)

mice were provided by S. Akira (Osaka University, Osaka, Japan) and maintained on a C57Bl/6 background.

3.2.2 Serum transfer and arthritis scoring

Groups of adult arthritic K/BxN arthritic mice were bled and centrifuged at 10,000 rpm for 10 min and the sera pooled. In all experiments where arthritis was introduced 4-6 mice per arthritic group received 100µl pooled sera from arthritic K/BxN mice by intraperitoneal (i.p.) injection on days 0 and 2 (total volume 200µl). Animals in individual experiments were injected from a single pool of sera, however, different experiments utilized different pooled collections. Due to the variable amount of auto-antibodies present in each pooled collection of sera a variable duration of arthritis is possible. Clinical arthritis scores were evaluated, as described previously (Choe 2003), using a scale of 0-4 for each paw with a higher number representing a greater disease progression with a total possible score of 16. Ankle thickness was measured with calipers in mm and compared to baseline thickness.

3.2.3 Drugs and drug delivery

Twelve WT naïve mice received a single IT injection of LPS (n=6; 0.1µg Invivogen) or control saline (n=6). Co-administration studies were performed on WT naïve mice where mice were co-injected with LPS+ saline (n=6; 0.1µg Invivogen), LPS + LPS-RS (n=6; 0.1µg +10µg Invivogen), saline + LPS-RS (n=6 10µg Invivogen), HKLM + saline (n=6; 10^6 cells, Invivogen), HKLM + LPS-RS (n=6; 10^6

cells + 10μg Invivogen), Poly I:C + saline (n=6; 0.5μg Invivogen), or Poly I:C + LPS-RS (n=6; 0.5μg + 10μg Invivogen). Twelve WT arthritic mice received IT injections of LPS-RS (n=6; 10μg Invivogen) or control saline (n=6) on day 6, 9, and 12. Twelve WT arthritic mice received IT injections of LPS-RS (n=6; 10μg Invivogen) or control saline (n=6) on day 18, 21, and 24.Twelve arthritic *Tlr4-/-* mice received IT injections of LPS-RS (n=6; 10μg Invivogen) or control saline (n=6) on day 6, 9, and 12. Twelve WT mice received IT injections of cMMP-3 (n=6; 1pmol EMD Biosciences) or control saline (n=6). Twelve *Tlr4-/-* received IT injections of cMMP-3 (n=6; 1 pmol EMD Biosciences) or control saline (n=6).

For mass spectrometry experiments 8 non-arthritics received IT injections of saline, 8 arthritic mice received IT injections of saline, and 8 arthritic mice received IT injections of LPS-RS (10μg; Invivogen). Confirmation of mass spectrometry findings were confirmed by IT delivery on day 6 of a) 15d-PGJ_2 (n=5; 0.5μg Cayman) to non-arthritic mice, of b) 15d-PGJ_2 (n=5; 0.5μg Cayman) to arthritic mice and c) saline vehicle to arthritic mice (n=5). 15d-PGJ_2 was prepared by in saline after methyl acetate solvent was evaporated using a gentle argon stream.

All IT injections were done under brief isoflourane anesthesia (2.5%) by lumbar puncture with a 30g needle attached to a Hamilton syringe. LPS-RS, LPS, and 15d-PGJ_2 were dissolved in normal saline and delivered in a 5μl volume followed by a 5μl saline flush. The LPS-RS, LPS, and 15d-PGJ_2 dosages were based upon previous studies [88, 154, 155] and preliminary dose ranging studies.

3.2.4 Behavioral tests

Animals were subjected to two behavioral tests, the thermal paw threshold test and the von Frey mechanical threshold test. Thermally evoked paw withdrawal responses were assessed using a Hargreaves-type testing device [116] (UARDG, Department of Anesthesiology, University of California, San Diego.) This device consists of a glass surface (maintained at 30℃) on which the mice rest in individual plexiglass cubicles. A thermal nociceptive stimulus originates from a focused projection bulb positioned below the glass surface. Latency was defined as the amount of time required for the mouse to produce a brisk withdrawal of the paw as detected by photodiode motion sensors that stop the timer and terminate the thermal stimulus.

Von Frey hairs ranging from 2.44 to 4.31 (0.03g to 2.00g) and the up-down method [17] were applied as described previously. The 50% probability withdrawal threshold (the force of the von Frey hair to which an animal reacts to 50% of the presentations) was record. The experimenter was blinded to drug treatments during all behavioral testing.

3.2.5 Histology

Whole ankle joint sections were stained with hematoxylin and eosin (H&E) (HistoTox, Boulder, Colorado, USA). Histopathological evaluation was performed as previously described for inflammation, erosion and cartilage destruction [112].

3.2.6 Immunohistochemistry

At indicated time points, mice were deeply anesthetized with euthasol and perfused intracardially with 0.9% saline followed by 4% paraformaldehyde. The spinal cords were removed, post fixed, and cryoprotected in sucrose. Lumbar sections (L4-L6) of the spinal cord were cut on a microtome (30μm) as free floating sections. Tissue sections were incubated with anti-GFAP antibody (1:1000 Sigma) or anti-Iba1 antibody (1:1000 Wako). Binding sites were visualized with secondary antibodies conjugated with fluoro-Alexa-488 and Alexa-555 (1:500, Molecular Probes, Eugene, OR). Images were captured by Leica TCS SP5 confocal imaging system and quantified using Image-Pro Plus v.5.1 software.

The reactive state of glia is characterized by both an increase in the number of cells, and in the conformational changes of these cells (rounding of the cell bodies and thickening of processes) leading to an increase in antibody labeling with glia reactivity increases. Microglia (Iba1) and astrocyte (GFAP) staining was quantified by measuring the total integrated intensity of pixels divided by the total number of pixels in a standardized area of the dorsal horn. The investigator was blinded to experimental conditions during the quantification. Staining intensity was examined in lamina I-II of the superficial dorsal horn or of a standardized box in lamina V of the deeper dorsal horn region with 3 slices (separated by at least 180 μm) examined per animal and 3-6 animals per experimental condition. Only pixels above a preset background threshold were included. An increase in the integrated intensity / pixels for Iba1 and GFAP staining was interpreted to signify microglia and astrocyte reactivity, respectively. All

data is presented as % change from the corresponding control group. Statistics were performed on raw data values.

3.2.7 Quantitative Real-time PCR (RT-PCR)

The mRNA from flash frozen lumbar spinal cord lumbar was extracted using Trizol (Invitrogen) according to the manufacturer's protocol. Complementary DNA was prepared and quantitative real-time PCR performed with TaqMan Gene Expression Assays (both according to the manufacturer's instructions, Applied Biosystems) to determine relative mRNA levels, using the GeneAmp 7500 Fast Sequence Detection system (Applied Biosystems). Pre-developed specific primers were used to detect tenascin-C(Assay ID: Mm00495662_m1), heat shock protein 90 (HSP90) (Assay ID: Mm00658568_gH), and HPRT1 (Assay ID Mm00446968_m1). Relative abundance was calculated by comparing delta-CT values [117] and the data were then normalized to HPRT1 gene expression to obtain relative concentration and presented as relative gene expression.

3.2.8 Western blotting

Mice were anesthetized in 4% isoflurane, decapitated, and spinal cords hydroextruded. 0.8 cm of the spinal cord lumbar enlargement was collected in 3% SDS lysis buffer (50mM Tris, 150mM NaCl, 1 mM EDTA, 0.5% Triton X-100, 3% SDS pH 7.4) containing protease and phosphatase inhibitors and homogenized by sonication. 30μg of protein were loaded with 0.1M DTT and 1xLDS loading buffer

(Invitrogen) and separated on a 4-12% Bis-Tris gel (Invitrogen). Proteins were transferred to a 0.45μm nitrocellulose membrane (Invitrogen), and blocked with 5% non-fat milk. Blots were incubated in anti-p-p38 (Sigma; 1:1000), anti-total p38 (Sigma; 1:1000), anti-p-pJnk (Sigma 1:1000), anti-Jnk (Sigma; 1:1000), anti-p-ERK (Sigma; 1:1000), anti- total-ERK (Sigma; 1:1000) or β-actin (Sigma; 1:100,000) followed by anti-rabbit/ anti-mouse secondary HRP conjugated antibody (Cell Signaling), for 1 hour at room temperature in 5% NFM. All blots were developed using femto or except anti-β-actin, which was developed in pico sensitive enhanced chemiluminescent detection system (SuperSignal Pierce). Western blots were scanned and quantified by densitometry using ImageQuant (Molecular Dynamics).

3.2.9 Liquid Chromatography and Mass Spectrometry

Isolated spinal cord samples were resuspended in 1 ml of 10% methanol and 50 μl of a 50 pg/μl solution of deuterated eicosanoid internal standards. The internal standard solution contained 50 pg/μL (2.5 ng total) of the following deuterated eicosanoids: (d_4) 6k $PGF_{1\alpha}$, (d_4) TXB_2, (d_4) $PGF_{2\alpha}$, (d_4) PGE_2, (d_4) PGD_2, (d_4) 15d PGJ_2, (d_{11}) 5-iso $PGF_{2\alpha}$ VI, (d_4) dhk $PGF_{2\alpha}$, (d_4) dhk PGE_2, (d_4) dhk PGD_2, (d_4) LTB_4, (d_8) 5-HETE, (d_8) 15-HETE, (d_6) 20-HETE, (d_4) 9-HODE, (d_4) 13-HODE, (d_7) 5-oxoETE, (d_8) 5,6-EET, (d_8) 8,9-EET, (d_8) 11,12-EET, (d_8) 14,15-EET, (d_4) 9,10-diHOME, and (d_4) 12,13-diHOME, (d_5) LTC_4, (d_4) LTE_4, and (d_4) AA. Cords were disrupted using a hand held sonicating probe for 6 s. Eicosanoids were extracted into 1 ml of methanol using solid-phase extraction columns (Phemononex, CA) as previously

described [156]. Samples were then stored at -80ºC until analyzed by the mass spectrometer. Samples were lyophilized to dryness using vacuum centrifugation, then resuspended in 100 µl of buffer A (30% acetonitrile, 70% water, 0.02% acetic acid; v/v/v). A 40 µl aliquot of sample was separated on a reverse-phase column (phenomenex, cat #) with a 25 min HPLC gradient at 0.3 ml/min that consisted of: 1 min (0% B), 3 min (25% B), 11 min (45% B), 13 min (60% B), 18 min (75% B), 18.5 min (90% B), 20 min (90% B), 21 min (0% B), and 25 min (0% B). Buffer A consisted of 30% acetonitrile, 70% water, 0.02% acetic acid and buffer B consisted of 50% acetonitrile and 50% isopropanol; v/v/v. Eicosanoids were subsequently detected using a tandem quadrupole mass spectrometer (ABI 4000 Q-TrapR, Analyst 1.5 software, Applied Biosystems) via scheduled multiple reaction monitoring (sMRM) in negative-ion mode. The electrospray voltage was -4.5 kV, the turbo ion spray source temperature was 525ºC. Collisional activation of eicosanoid precursor ions used nitrogen as a collision gas. Eicosanoids were identified in samples by matching their MRM signal and LC retention time with those of a pure standard. Quantitation: Eicosanoids were quantitated using ABI's Multiquant 1.1 software. Quantitated values were determined from a stable isotope dilution method using pure eicosanoid standards [157]. All data was filtered using the Grubb's test to remove outliers. Quantitated averages were determined from treatment groups whose N ranged from 6 – 8 animals. Quantitated amounts are reported as pg/mg of tissue ± S.E.M. Significant metabolites changes (p value < 0.05) were determined using a two-

tailed student's t-test. Table 1 details the average pg/mg of tissue for each eicosanoid investigated.

3.2.10 Statistics

Data are given as mean +/- standard error. For comparison of changes in pain behavior (thermal and mechanical hypersensitivity) a two-way ANOVA for repeated measures with a Bonferroni *post hoc* test was used. For comparison of microglia and astrocyte changes and western blotting changes a one-way ANOVA with a Bonferroni *post hoc* test was used.

3.3 Results

3.3.1 Toll-like receptor 4 is required to maintain mechanical hypersensitivity in the post inflammatory phase of K/BxN serum transfer arthritis

We sought to investigate the pain-like behavioral consequences of TLR4activity during K/BxN serum transfer arthritis. Wild type C57Bl/6 (WT) and *Tlr4-/-* C57Bl/6 (*Tlr4-/-*) mice were injected on days 0 and 2 with 100µl pooled K/BxN sera. As previously described [158], within 24 hours of serum transfer WT mice developed significant clinical signs of arthritis including redness and swelling of the paw and mechanical hypersensitivity. *Tlr4-/-*mice also developed significant clinical signs of arthritis and mechanical hypersensitivity compared to pre-serum injection thresholds. At no time were the clinical signs (Figure 3.1A) nor the measured ankle widths (Figure 3.1B) significantly different between the WT and *Tlr4-*

/-. WT and *Tlr4-/-* mice display equivalent mechanical hypersensitivity concurrent with clinical arthritis symptoms. The mechanical hypersensitivity of *Tlr4-/-* mice was reduced compared to WT mice from days 25-42 (Figure 3.1C, $p<0.001$), the time period where clinical signs were no longer present. Consistent with previous studies, WT mice displayed a modest thermal hypoalgesia (Figure 3.1D, $p<0.01$) during maximal inflammation.

Here we demonstrate using a TLR4 point mutant mouse, that the dependence of functional TLR4 binding behavior during the transition to persistent pain post-inflammation in the K/BxN serum transfer arthritis model is preserved in a second strain. C3H/HeOuJ (TLR4 competent) and C3H/Hej (TLR4 incompetent) mice were injected on days 0 and 2 with 100µl pooled K/BxN serum. A second group of C3H/Hej mice were injected with control serum. As previously reported, within 24 hours following K/BxN serum transfer, mice developed significant clinical signs of arthritis [14]. These signs, including redness and swelling, were significantly increased over days 1-28 in both C3H/Hej and C3H/HeOuJ mice, peaking at day 6, $p<0.05$-0.001 (Figure 3.2A). Ankle joint diameters of C3H/Hej mice were significantly increased compared to naïve serum injections on days 1-12, $p<0.05$-0.001 (Figure 3.2B). Ankle joint diameters of C3H/HeOuJ were also significantly increased compared to baseline levels on days 3-28, $p<0.05$-0.001 (Figure 3.2B). Significant mechanical hypersensitivity was present in C3H/HeOuJ (TLR4 competent) arthritic animals on days 1-28, compared to control sera treated animals, $p<0.01$-0.001 (Figure 3.2C). Tactile allodynia remained robustly stable through the end of the study at day

28. C3H/Hej (TLR4 incompetent) mice displayed significant mechanical hypersensitivity on days 2-15, $p<0.05$-0.001 vs control animals. C3H/Hej arthritic mice, however recovered tactile baselines compared to CH/HeOuj mice days 24 and 28, $p<0.05$ (Figure 3.2C). C3H/Hej displayed mild thermal hypoalgesia on day 3, $p<0.05$ vs control animals (Figure 3.2D). There were no significant differences in thermal thresholds between C3H/Hej and C3H/HeOuJ mice (Figure 3.2D).

3.3.2 K/BxN serum transfer arthritis does not differentially affect C57Bl/6 WT and Tlr4-/- mouse ankle joint histopathology.

Previous reports indicate that TLR4 may contribute to the shift in persistent mechanical hypersensitivity by affecting clinical signs of arthritis [86]. To determine if the difference in mechanical hypersensitivity could be attributed to differences in peripheral changes secondary to the K/BxN serum transfer arthritis inflammation, ankle joints were examined for histopathologic changes using H&E staining. Joints were scored according to previous methods [112] for signs of inflammation, erosion, and cartilage destruction. At no time point (naïve, day 6 post-arthritis induction, or day 42 post-arthritis induction) were there significant differences in scores between WT and *Tlr4-/-* arthritic mice (Figure 3.3).

3.3.3 Spinal cord microglia and astrocyte activation is reduced in *Tlr4-/-* mice compared to WT mice during inflammation and post-inflammation stages of K/BxN serum transfer arthritis

Acute and chronic pain is often accompanied by spinal cord changes including robust and persistent activation of microglia and astrocytes, reviewed by [159]. Here we examined activation of astrocytes (GFAP) and microglia (Iba1) during the inflammation period (day 6) and during the post-inflammation period where *Tlr4-/-* arthritic mice have significantly improved mechanical hypersensitivity scores using lumbar spinal cord gene and protein immunoreactivity.

Protein expression levels for microglia (Iba1) and astrocytes (GFAP) were assessed using immunoreactivity. The average of WT naïve densitometry scores were set to 100% and changes in densitometry scoring of staining were expressed as a percent change from WT naïve values. Immunostaining of sections from L4-L6 of the superficial dorsal horn and deeper dorsal horn against microglia (Iba-1) showed an increase at day 6 during the inflammation period in WT mice that was absent in *Tlr4-/-* mice (Figure 3.4A and 3.4C). On day 6 WT superficial microglia dorsal horn staining is 138 +/-18% and *Tlr4-/-* staining is 80 +/- 10% of naïve levels ($p<0.05$% WT vs *Tlr4-/-*). Day 42 post-inflammation WT superficial microglia staining is 84 +/- 15% and *Tlr4-/-* staining is 43% +/- 2% of naïve levels ($p>0.05$).

The same spinal cord sections were also immunostained for the astrocyte marker (GFAP) and evaluated for changes in the superficial dorsal horn using the same protocol as microglia (Figure 3.4B and 3.4D). On day 6 WT superficial astrocyte dorsal horn staining is 335 +/-22% and *Tlr4-/-* staining is 278 +/-34% ($p>0.05$% WT vs *Tlr4-/-*). Day 42 post-inflammation WT superficial astrocyte staining is 257 +/- 14% and *Tlr4-/-* staining is 189 +/-11% ($p<0.05$% WT vs *Tlr4-/-*).

3.3.4 Intrathecal activation of toll-like receptor 4 induces acute and chronic mechanical hypersensitivity with activation of microglia and astrocytes

The behavioral mechanical hypersensitivity differences observed between WT and *Tlr4-/-* mice following K/BxN serum transfer arthritis is suggestive of a mechanism wherein TLR4 activation would induce mechanical hypersensitivity. To determine pain-like behavior resulting from spinal TLR4 activation, mice were injected IT with 0.1μg of lipopolysaccharide (LPS), which specifically signals via I [160]. LPS induced mechanical hypersensitivity in WT but not *Tlr4-/-* mice from 30 minutes to 7 days following injection, $p<0.05$- 0.001 (Figure 3.5A). Baseline values dropped in WT mice from 1.62g (+/- 0.16g) to between 0.19g (+/- 0.03) and 0.36g (+/- 0.08g) following LPS delivery. Changes are presented according to the hyperalgesic index for 0-24 hours in Figure 3.5B and indicates a significant increase in pain-like behavior only in WT mice following IT LPS delivery, $p<0.01$ vs IT saline (WT) and $p<0.001$ vs IT LPS (*Tlr4-/-).*

We next determined if intrathecal TLR4 activation by LPS (0.1μg) induced spinal dorsal horn (L4-L6) microglia (Iba1) and astrocyte (GFAP) activation via changes in immunoreactivity. The average densitometry score (integrated intensity) of IT saline for each time point of interest (4 hours or 7 days) was established as 100% and changes in densitometry staining were reported as a percent change compared to IT saline control values. Astrocyte (GFAP) and microglia (Iba1) immunoreactivty in the superficial dorsal horn showed a significant increase 4 hours post IT LPS, but not

7days post IT LPS, compared to control ($p<0.05$; Figure 3.5C and 3.5D respectively). Densitometry indicated that Immunostaining of microglia and astrocytes were not significantly increased at day 7. Representative images for astrocytes (Figure 3.5E) and microglia (Figure 3.5F) 4 hours and 7 days following IT saline and IT LPS are shown.

3.3.5 TLR4 ligand mRNA levels are elevated in arthritic spinal cords during the post-inflammation phase

To understand the role of TLR4 in the transition to persistent pain during the post inflammation stage we investigated the levels of TLR4 associated proteins and ligands (HSP90 and Tenascin-C) in the spinal cord by real time mRNA transcript levels. All expression levels were measured in the lumbar spinal cord on day 42 during the post-inflammation period when WT arthritic mice no longer display clinical signs but persistent mechanical hypersensitivity is present. Endogenous TLR4 activating ligands induced during arthritis could explain the role of this receptor during persistent pain-like state.

Tenascin-C has recently been demonstrated to be a TLR4 ligand that is upregulated in the joints during rheumatoid arthritis [148]. Here we show an increase of tenascin-C in the spinal cords of mice 2.57 +/- 0.1 vs 3.88 +/- 0.3 REU in control vs arthritic mice respectively, $p<0.05$ (Figure 3.6A). Heat shock protein 90 (HSP90) has been demonstrated to contribute to TLR4 mediated mechanical hypersensitivity [161]. Here we show an increase of HSP90 of 16.08+/- 3.3 vs. 32.98 +/- 6.1 REU in control

vs. arthritic mice respectively, $p<0.05$ (Figure 3.6B). Chronic spinal cord increases in TLR4 ligands are suggestive of a mechanism including persistent stimulation by endogenous factors.

3.3.6 IT TLR4 antagonist LPS-RS during the inflammatory period prevents post-inflammation stage persistent mechanical hypersensitivity

The mechanical hypersensitivity present following IT TLR4 activation suggests the reverse may be plausible; that blockade of TLR4 may improve the mechanical hypersensitivity during K/BxN serum transfer arthritis. To determine the spinal involvement of TLR4 during the inflammation to post-inflammation transition WT arthritic mice were given either three IT injections of the TLR4 antagonist LPS-RS (10μg) or three IT injections of saline. IT LPS-RS delivered on days 6, 9, and 12 during the inflammation period significantly reduced the mechanical hypersensitivity on day 6 at 2 hours post injection, day 7, 8, on day 9 at 2 hours post injection, and day 15, 18, 21, 24 and 28; $p<0.05$- 0.001 (Figure 7A) as compared to IT saline injections. Clinical scores (Figure 7B) and changes in ankle widths (Figure 7C) were not affected by LPS-RS delivery on day 6, 9, and 12. IT LPS-RS delivered on days 18, 21, and 24 during the post-inflammation period at no point significantly reduced the persistent mechanical hypersensitivity present (Figure 7D) or altered clinical scores (Figure 7E) or ankle widths (Figure 7F) as compared to IT saline treatments.

3.3.6 Determining the specificity of LPS-RS

To have the greatest confidence in the results obtained utilizing LPS-RS we conducted several control experiments. The TLR4 antagonist LPS-RS (10μg) was delivered intrathecally in a co-administration paradigm with a TLR2 agonist (HKLM; 10^6 cells), a TLR3 agonist (Poly I:C; 0.5μg), and a TLR4 agonist (LPS; 0.1μg). These agonists were chosen because HKLM signals exclusively through a MyD88 dependent downstream pathway whereas Poly I:C signals exclusively through a TRIF dependent downstream pathway. IT co-administration of LPS + LPS-RS significantly prevented an LPS induced mechanical hypersensitivity for 180 minutes ($p<0.05$-0.001; Figure 3.8A). IT administration of HKLM and Poly I:C induced a significant mechanical hypersensitivity within 30 minutes of agonist delivery. The co-administration of LPS-RS with either HKLM (Figure 3.8B) or Poly I:C (Figure 3.8C) had no significant effect upon the induction of mechanical hypersensitivity by these agonist agents.

To further define the specificity of LPS-R, LPS-RS (10μg) or saline was delivered IT to arthritic *Tlr4-/-* mice. IT LPS-RS or saline was delivered in three separate injections; one on day 6,one on day 9, and one on day 12 during the inflammation period to *Tlr4-/-* mice to confirm that the anti-nociceptive behavioral effects seen following delivery of IT LPS-RS is a specific TLR4 mediated effect. IT LPS-RS does not significantly improve mechanical hypersensitivity (Figure 3.9A), ankle widths (Figure 3.9B), or clinical scores (Figure 3.9C) in Tlr4-/- mice as compared to IT saline delivery. This data confirms the specificity of LPS-RS and suggests that all the behavioral and biochemical effects observed following IT delivery are due to a TLR4 specific effect in the spinal cord.

3.3.7 IT LPS-RS mediated effects on spinal MAPKs during K/BxN serum transfer arthritis

One of the major pathways downstream of TLR4 signaling includes phosphorylation and activation of the MAPKs including p38, ERK, and Jnk, which have all been implicated in the regulation of persistent pain states [162, 163]. Protein levels were measured by western blotting for the phosphorylated form, for the total protein, and β-actin as a loading control in samples collected from the lumbar spinal cord (L4-L6) in non-arthritic IT saline treated mice, arthritic IT saline treated mice, and arthritic IT LPS-RS (10μ) treated mice on specified days following K/BxN serum transfer arthritis initiation. Mice were treated according to the previous behavioral paradigm; IT saline or LPS-RS was delivered on days 6, 9, and 12. Day 6 spinal cords were removed 2 hours following LPS-RS treatment. Data is reported as a percent change of non-arthritic mice which are set at 100%, where phosphorylated values have been normalized to the β-actin loading control.

No significant differences were revealed 6 days following K/BxN serum transfer arthritis between non-arthritic and arthritic mice or between LPS-RS and saline treated arthritic mice (Figure 3.10; $p>0.05$). Unexpectedly, we observed a significant increase in phosphorylated p-38 levels in the spinal cord on day 14 after initiation of K/BxN serum transfer arthritis and 2 hours following IT LPS-RS (10μg; 200.5 +/- 25% of non-arthritic control) treatment as compared to IT saline treatment (94.0 +/- 12.5% of non-arthritic control) as shown in Figure 3.10A; $p<0.05$. In comparison, p-p38 levels during the persistent pain stage at d28 of IT LPS-RS treated

arthritic mice are significantly reduced (-35 +/- 14.4% of non-arthritic controls) compared to IT saline treated arthritic mice (36.3 +/- 9.3% of non-arthritic controls) as shown in Figure 3.10A; $p<0.05$. Levels of p-ERK are significantly increased in the spinal cords of arthritic mice on day 14 during the transition phase, irrespective of saline (608.2 +/- 103%) or LPS-RS treatment (737.1 +/- 184%) as compared to non-arthritic controls (Figure 3.10B; $p<0.01$ and $p<0.001$ respectively). At no time point measured was p-Jnk significantly altered in the spinal cord by either K/BxN serum transfer arthritis or the LPS-RS treatment paradigm. This data suggests that regulation of the MAPK pathways may not be the predominant effect of IT LPS-RS delivery. An alternative pathway, the metabolites produced by arachidonic acid including the prostaglandins which were previously shown to be increased in the spinal cord following TLR4 activation [89] are considered below.

3.3.8 Peripheral inflammation from K/BxN serum transfer arthritis induces central changes to the spinal eicosanoid profile which intrathecal delivery of the TLR4 antagonist LPS-RS during the inflammation period replenishes 15d-PGJ_2, reduced by arthritis

We were interested in understanding how K/BxN serum transfer arthritis inflammation would affect the central eicosanoid profile. These species have been previously characterized to play an important role in regulating the sensitivity of sensory neurons both peripherally and in the spinal cord during peripheral inflammation [6]. The lumbar enlargement of the spinal cord was removed and

analyzed from three experimental groups; A) non-arthritic mice 2 hours after an IT saline injection, B) arthritic mice 2 hours after an IT saline injection and C) arthritic mice 2 hours after an IT TLR4 antagonist injection (10μg LPS-RS) on day 6 post-arthritis induction for eicosanoid levels.

Eicosanoids were measured and quantified using a stable isotope dilution technique coupled with a liquid chromatography tandem mass spectrometry (LC/MS/MS) method operating in selected multiple reaction monitoring (sMRM) mode (Dumlao *et al*., 2011 or Blaho *et al*., 2009). We detected and quantified 60 lipid metabolites out of 139 total metabolites monitored using individually optimized sMRM pairs, which are summarized in supplementary table 1. Significant differences ($p < 0.5$) between the eicosanoids produced were determined using the student's t-test. 26 of the 60 detected eicosanoids were significantly different when non-arthritic (IT saline injected) control mice were compared to K/BxN induced arthritic (IT saline injected) mice. Only 11 significantly different eicosanoids were detected between arthritic IT saline treated mice and arthritic IT LPS-RS treated mice.

The data are shown in a heat map in order to view the global changes to the eicosanoid profile between non-arthritic and arthritic IT saline treated groups (Figure 3.11A). K/BxN serum transfer arthritis induced the production of eicosanoids from the 5-,12-,15-lipoxygenase (LOX), cytochrome P450 (CYP), and non-enzymatic pathways. Central COX metabolites remained largely unaffected, although K/BxN arthritic mice had reduced levels of 15d-PGJ_2, a dehydration product of PGD_2.

Few changes in the eicosanoid profile were detected when comparing arthritic + IT saline and arthritic + IT LPS-RS treated mice (Figure 3.11B). Intrathecal LPS-RS treatment rapidly improved mechanical hypersensitivity and caused reduced amounts of LOX degradation (HEDH) and CYP metabolites. Interestingly, PGD_2 dehydration products (15d- PGD_2, PGJ_2, and 15d-PGJ_2) increased with LPS-RS treatment. These results suggest that blocking TLR4 activation with LPS-RS treatment causes 15-deoxy PGJ_2 levels to return to normal.

On day 6 the spinal cords of non-arthritic IT saline injected mice had PGE_2 values of 70.1 (+/- 8.6 S.E.M.) pg/mg of tissue. In comparison, day 6 arthritic mice two hours after intrathecal treatment of saline had PGE_2 values of 82.7 (+/- 7.4) pg/mg of tissue and those after 10μg of LPS-RS had value of 102.9 (+/- 5.0) pg/mg of tissue ($p<0.05$ vs arthritic saline treated; Figure 3.12A). The levels of 15k- PGE_2, the PGE_2 enzymatic breakdown product were not significantly difference (Figure 3.12C). This indicates that PGE_2 may not be the predominant factor in TLR4 mediated mechanical hypersensitivity.

While PGD_2 levels were not significantly different between the three treatment groups (Figure 3.12B), a significant change was detected for the non-enzymatic breakdown product of PGD_2, 15-deoxy-PGJ_2. Non-arthritic saline treated mice had values of 0.95 (+/- 0.2) pg/mg of tissue which dropped significantly in the spinal cords of IT saline treated arthritic mice to 0.57 (+/-0.1) pg/mg of tissue ($p<0.05$) and recovered to 1.69 (+/- 0.2) pg/mg of tissue, higher than baseline values following IT LPS-RS treated ($p<0.05$; Figure 3.12D). These findings are in accordance with the

known role for 15-deoxy-PGJ_2 as an anti-inflammatory mediator [15,16] required for pro-resolution function following activation of the cyclooxygenase pathway.

To determine if 15d-PGJ_2 will attenuate the nociception prominent during the inflammation period of K/BxN serum transfer arthritis we delivered 0.5µg intrathecally on day 6. Arthritic mice with an average baseline of 0.23g +/- 0.08 displayed a transient recovery of mechanical hypersensitivity to 1.05g+/- 0.2 15 minutes after intrathecal delivery of 0.5µg of 15d-PGJ_2 as compared to saline vehicle treated mice (Figure 3.12E; $p<0.05$). Evidence indicates that 15d-PGJ_2 can directly activate the TRPA1 receptor [25], therefore non-arthritic mice were also injected as a control. At the given dose, these mice displayed no significant changes as compared to pre-injection baselines over the two hour time course. Drug efficacy is also quantified according to the hyperalgesic index where IT 15d-PGJ_2 displays a significant analgesic activity ($p<0.05$) in comparison to saline treated vehicle controls according to this measure (Figure 3.12F).

3.3.9 Toll like receptor 4 is required for ATF3 generation in the DRG during the post-inflammation phase of K/BxN serum transfer arthritis

Here we sought to determine the role of TLR4 in ATF3 generation, a marker for nerve injury, in the dorsal root ganglia (DRG) during K/BxN serum transfer arthritis. WT and *Tlr4-/-* mice were injected with 100µL pooled serum on day 0 and day 2 to initiate arthritis. DRGs from L4-L6 were collected on day 28, during the post-inflammation phase from WT non-arthritic mice, WT arthritic mice, and *Tlr4-/-*

arthritic mice. DRGs were scored such that values represent the number of ATF3 positive stained cells out of the total number of neuronal cells (NeuN stained) containing a visible nucleus. Control animals from day 42 had a mean ATF3/NeuN ratio of 0.004 ±0.0005 (Figure 3.13A). Day 42 WT arthritic animals (Figure 3.13B) had a mean ATF3/NeuN ratio of 0.14 ±0.09 ($p>0.05$ vs control) and day 42 *Tlr4-/-* arthritic animals (Figure 3.13C) had a mean ATF3 staining ratio of 0.23 ± 0.06 ($p<0.05$ vs control). The staining is quantified in Figure 3.13D. This data demonstrates that K/BxN serum transfer arthritis induced ATF3 activation in the dorsal horn during the post-inflammation phase is blocked in *Tlr4-/-* mice. This corresponds with the loss of persistent pain during the post-inflammation phase in *Tlr4-/-* mice.

3.3.10 Matrix metalloproteinase 3 induced mechanical hypersensitivity is attenuated in the absence of TLR4.

Here we sought to determine if TLR4 regulates another nociceptive processing component, matrix metalloproteinases, during acute mechanical hypersensitivity. Intrathecal delivery of the catalytically active form of MMP-3 (1pmol) to WT mice will significantly reduce mechanical thresholds from 1.95g +/-0.03 to 0.49g +/-0.2 by 120 minutes ($p<0.001$ vs IT saline); to 0.36g +/- 0.1 ($p<0.01$ vs IT saline) by 180 minutes; and to 0.35g +/- 0.1 ($p<0.01$ vs IT saline) by 240 minutes. In comparison, mechanical thresholds following IT cMMP-3 delivered to *Tlr4-/-* mice are not significantly different from IT saline delivery (Figure 3.14).

3.3.11 TLR4 mechanical hypersensitivity and TNF release is MMP-3 dependent

In accordance with previously published reports [164] IT LPS (10μg) induced a significant decrease in tactile threshold from 13.9 ±0.9g to 4.8 ±0.9g ($p<0.001$ at 30 minutes) (Figure 3.15A). This decrease in tactile threshold at 30 minutes was prevented by pretreatment with 1μg GM6001 (10±1.4g; $p<0.001$) or 7.5μg NNGH (11.9±0.9g; $p<0.01$). These values are graphed by hyperalgesic index (Figure 3.15B) indicating that rats pretreated with NNGH have a significantly ($p<0.05$) reduced hyperalgesic index and that although rats pretreated with GM6001 also showed a trend towards reduction the difference does not reach statistical significance ($p >0.05$).

In cultured spinal microglia, application of LPS (100ng/mL) produced a time-dependent and progressive increase in TNF released into the media over 24 hours. A 30 minute pretreatment of microglia with GM6001 (7.5μg/mL) or NNGH (7.5μg/mL) significantly attenuated LPS-induced TNF release 1, 4, and 24 hours ($p<0.001$, Figure 3.15C) post treatment.

3.4 Discussion

K/BxN serum transfer arthritis has revealed that similar to clinical arthritis, even with resolution of the peripheral inflammation a persistent pain condition exists [158]. Using the K/BxN model, we have previously shown that the persistent mechanical hypersensitivity outlasting the clinical signs of arthritis is associated with ATF-3 activation in the DRG and a pharmacology suggestive of a transition from an inflammatory to a neuropathic pain state [158]. Here we demonstrate for the first time

that activation of spinal TLR4 is critical for the continuation of mechanical hypersensitivity during the transition from the inflammation to the post-inflammation phase of K/BxN serum transfer inflammatory arthritis.

Current evidence supports a role for the innate immune system, in particular toll-like receptors during glial activation in the central nervous system following peripheral insult [165]. Genetic and pharmacological interventions that block glial activation attenuate nociceptive behavior in a variety of pain models (reviewed in [35, 36]). TLR4 is expressed in both microglia and astrocytes [166] and is part of the receptor complex that recognizes lipopolysaccharide from invading gram negative bacteria. Importantly, TLR4, is also activated by endogenous ligands (reviewed in [167-169]). TLR4 activation couples to NF-κB through two distinct pathways. It can induce a MyD88 dependent cascade leading to early NF-κB activation and subsequent upregulation or activation of cytokines including TNF, IL-18 and enzymes such as cyclooxygenase-2 and p38, and JNK mitogen activated protein kinase, or a TRIF dependent cascade leading to delayed NF-κB activation which results in interferon-β production (reviewed in [78]). Many of the cytokines produced in response to TLR4 activation are also known to be pro-nociceptive and contribute to spinal sensitization [28, 42, 103]. Earlier work has shown that spinal NF-κB is important in both inflammatory and nerve injury-induced pain [170, 171] and of particular interest, direct blockade of NFκB activity in astrocytes attenuates mechanical hypersensitivity and release of chemokines including CCL2 and CXCL10 following chronic constriction injury of the sciatic nerve [172]. Consistent with a role for TLR4 and

downstream products in glial activation and pain-like behavior in the present study we demonstrated that during K/BxN serum transfer arthritis progression, a constitutive TLR4 deletion attenuated increased spinal astrocyte and microglia immunoreactivity; which we interpret as a reduced activation of these cells.

Constitutive disruption of TLR4 reduced the severity and histopathology in the IL-1 receptor antagonist knockout mouse model of spontaneous arthritis [84] and in previous reports of K/BxN serum transfer arthritis [112]. We, however, did not detect a significant difference in clinical scores or peripheral pathology between WT and *Tlr4-/-* mice. We believe this reflects a combination of strain differences and the high number of auto-antibodies transferred during serum transfer. During the inflammation period, maximal inflammation scores were achieved by both genotypes making differences in clinical scores difficult to ascertain.

Spinal cord mRNA changes clearly indicate a role for intrinsic TLR4 ligands released during chronic arthritis. Researchers have identified a diverse groups of endogenous TLR4 ligands including heat shock proteins 60 [173],70 [174], and 90 [175], fibrinogen [176], fibronectin [177, 178], hyaluronic acid [179], HMGB1 [180], and tenascin-C [148]. Many of these ligands have been identified as contributing to the inflammation and cartilage destruction in the joint during inflammatory arthritis, thus supporting a role for TLR4 during this disease. While human and animal models suggest a peripheral function, this is the first study examining TLR4 expression and endogenous activation during inflammatory arthritis in the central nervous system.

A role for endogenous TLR4 ligands is further supported by the utilization of IT LPS-RS, a TLR4 antagonist. A single dose of IT LPS-RS when delivered during the inflammation period will reverse mechanical hypersensitivity within two hours. Three doses delivered during the inflammation period will prevent the transition to persistent hypersensitivity. It is interesting to note that intrathecal LPS-RS during the post-inflammation phase was ineffective, in contrast to a previous report in which a single dose of IT LPS-RS in rats rapidly and effectively reversed neuropathic pain for three hours resulting from a chronic constriction injury [88]. This may reflect some element distinguishing the events secondary to chronic inflammation as compared to a frank mechanical nerve injury. LPS-RS was carefully examined to eliminate potential off-target effects. LPS-RS appears to be a TLR4 specific tool given its inability to moderateTLR2 or TLR3IT ligand mediated mechanical hypersensitivity and its lack of effect in a *Tlr4-/-* K/BxN serum transfer arthritic mouse when directly compared to WT activity. Thus, here we have clearly demonstrated the role of TLR4 during the transition to the post-inflammation stage. Of great interest would be the possibility of evoking a new bout of inflammation and determining if one can uncouple or stimulate the necessary pathways with IT LPS-RS to initiate resolution of the pain-like behavior as was accomplished by treatment during the initial inflammation phase.

TLR4 signaling is linked to MAPK activity [77, 78] for which there is evidence that pharmacological intervention improves persistent pain-like behavior (reviewed in [163]). To determine if LPS-RS is improving mechanical hypersensitivity by altering MAPK levels lumbar spinal cords were assed for p-p38, p-ERK, and p-Jnk

activity in three treatment groups A) non-arthritic mice with IT saline injections (controls), B) arthritic mice with IT saline injections (arthritic vehicles) and C) arthritic mice with IT TLR4 antagonist injection (arthritic drug treated) at three distinct times(day 6- two hours after IT treatment, day 14, and day 28) to create a temporal profile. Since no changes were identified on day 6 when the behavioral improvements are first noticed it is suggestive of an alternative mechanisms of regulation.

A likely alternative mechanism of regulation is informed by evidence suggesting the lipid mediator prostaglandin E_2 (PGE_2) is elevated in the CSF following persistent inflammation [181-183] and is thought to an important factor in spinal sensitization. While PGE_2 is the most highly studied lipid mediator, recent work has demonstrated significant changes in spinal cord levels of lipid mediators in the cyclooxygenase, 12-lipoxygenase, 15-lipoxygenase, and cytochrome P450 pathways following peripheral inflammation [156]. The lipid metabolite profiles were recently investigated in the joints of mice subjected to Lyme disease and it was found that the lipid mediator profiles temporally co-varied with inflammation. Of note, different patterns were observed in C3H/Hej (TLR4 point mutant mice) as compared to DAB (arthritis resistant) mice [184]. Given these findings we investigated the lipidomic profiles in spinal cords of K/BxN mice as compared to control mice, and the effect of IT LPS-RS treatment. While we found an increase of lipid mediators including 9-HETE, 13-HODE, 5,6 EET and 8,9 EET in the spinal cords from K/BxN, the most striking finding was a prominent decrease in 15d-PGJ_2, which was completely

reversed by the IT LPS-RS injections. Of importance, IT delivery of 15d-PGJ_2 during the inflammation phase attenuated tactile allodynia, suggesting that 15d-PGJ_2 has anti-nociceptive actions in the spinal cord. Consistent with the present results, intrathecal 15d-PGJ_2 [185] attenuated the decreased mechanical thresholds in spared nerve injured rats.15d-PGJ_2 is a potent PPARγ ligand [186, 187] and noteworthy, PPARγ gene and protein expression have been confirmed in the spinal cord [188] [185]. Intra peritoneal administration of 15d-PGJ_2 reduced peripheral inflammation and joint destruction in antigen induced arthritis in rat [189] and oral dosing of rosiglitazone (a PPARγ agonist) reduced the levels of pro-inflammatory mediators iNOS, TNF, and COX-2 during adjuvant-induced rheumatoid arthritis in mice[190]. In macrophages reduction in production of proinflammatory cytokines such as TNF, IL-1, and IL-6 [191, 192] are suggested to be mediated via activation of PPARγ and the transrepression of gene expression requiring NFκB or AP-1 as transcription factors [191, 193]. Thus it is possible that TLR activation downregulates PPARγ expression in the spinal cord and that IT injection of LPS-RS allows for reestablishment of 15d-PGJ2 levels that are sufficient to activate of PPARγ and drive suppression of pro-inflammatory/pronociceptive TLR4 target genes.

We believe increased 15d-PGJ_2 levels represent a significant biological event that can alter spinal nociceptive processing. Endogenous 15d-PGJ_2 interacts with molecular targets that result in both acute and chronic effects. Rapid interactions with the TRPA1 receptor lead to acute (10 min) activation and desensitization of DRG neurons in mice [155]; Nevertheless, we do not believe that TRPA1 activation is the

main mechanism for the 15d-PGJ_2 mediated antinociception in the current study as intrathecal delivery of exogenous 15d-PGJ_2 at a level that relieves mechanical hypersensitivity in arthritic mice does not induce significant mechanical hypersensitivity in naïve mice. Hence, the acute anti-nociceptive behavioral effects of IT 15d-PGJ_2 suggest an additional short-term role for this molecule. In our study a long-lasting anti-nociceptive effect was observed following IT LPS-RS and it is possible that this caused a sustained production of 15d-PGJ_2 thus inducing long-term phenotypic alterations through its actions at PPARγ. Due to the two highly reactive electrophilic centers, 15d-PGJ_2 covalently binds to the PPARγ active site [194]. Accordingly, small but localized increases in 15d-PGJ_2 could have profound phenotypic effects. As such, IT LPS-RS induced production of 15d-PGJ_2 would be expected to provide sustained levels of this lipid. Taken together, these data suggest that 15d-PGJ_2 could have long-term beneficial effects by activating the PPARγ pathway.

Peripheral delivery of TLR4 antagonists reduce inflammation and cartilage destruction during inflammatory arthritis [85] and they attenuate neuropathic pain following chronic constriction injury [88] subsequent to spinal administration. Of note, this is the first report demonstrating that spinal injection of TLR4 antagonists attenuate inflammatory arthritis. We have demonstrated a link between TLR4 mediated nociception during the inflammation phase of K/BxN serum transfer arthritis and the establishment of a persistent pain state as well as the establishment of 15-deoxy-PGJ_2 levels fluctuating concurrently with arthritis initiation and TLR4 blockade

treatment. This data provides an exciting potential mechanism for future experimental work and therapeutic investigations regarding TLR4 actions during transitional phases of chronic inflammation.

3.5 Acknowledgments

Chapter 3, in part, has been submitted for publication to appear in *Pain* as "Role of toll-like receptor 4 in 15d-PGJ_2 mediated mechanical hypersensitivity following K/BxN serum transfer arthritis" by Christianson CA, Dumlao DS, Corr M, Stokes JA, Dennis E, Svensson CI, Yaksh TL. The dissertation author was the primary investigator and author of this material.

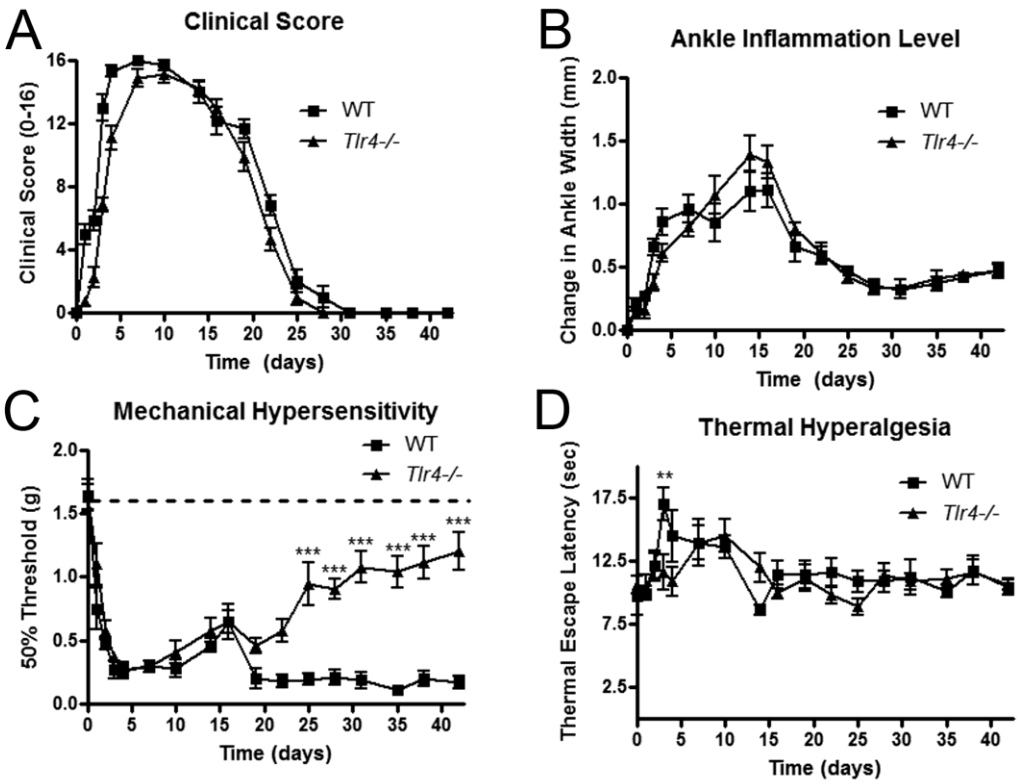

Figure 3.1 TLR4 is required to maintain mechanical hypersensitivity in the post inflammation stage of K/BxN serum transfer arthritis. Graphs displaying (A) ankle thickness as measured using calipers and (B) clinical scores indicate no significant differences between WT and *Tlr4-/-* during the progression of K/BxN serum transfer arthritis. (C) Tactile thresholds (g) indicate significant mechanical hypersensitivity day 2-21 for WT and *Tlr4-/-* mice compared to baseline levels, as marked by the dotted line at 1.55g on the graph. *Tlr4-/-* mice display significant improvements in mechanical hypersensitivity as compared to time matched WT mice days 24-42. (D) WT mice display significant thermal hyposensitivity compared to *Tlr4-/-* mice only on day 3. Each time point represents mean ± SEM (n=9 mice/group), ***= $p<0.001$ by Bonferroni post-test.

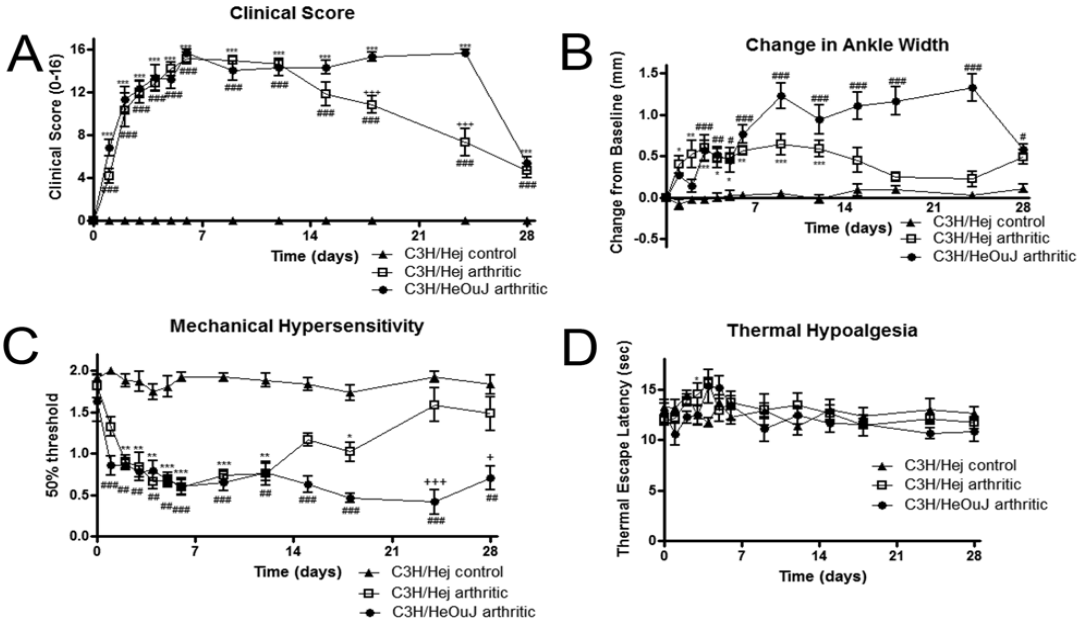

Figure 3.2 TLR4 is required to maintain persistent mechanical hypersensitivity. (A) Tactile thresholds (g) indicate significant mechanical hypersensitivity day 1-28 for C3H/HeOuJ and day 1-18 for C3H/Hej (TLR4 point mutant) arthritic mice as compared to naïve sera C3H/Hej mice. C3H/Hej (TLR4 point mutant) arthritic mice display significant improvements compared to C3H/HeOuJ mice day 24-28. (B) No significant thermal hypersensitivity is displayed by C3H/HeJ or C3H/HeOuJ arthritic mice compared to naïve sera controls. (C) Ankle thickness as measured using calipers is significantly reduced in C3H/Hej (TLR4 point mutants) as compared to C3H/H3OuJ day 18-24. (D) Clinical scores are reduced in C3H/Hej compared to C3H/HeOuJ day 9 and 15-24. Each time point represents mean ± SEM (n=6 mice/group),#: C3H/HeOuJ arthritic vs non-arthritic control; *: C3H/Hej arthritic vs non-arthritic control; +: C3H/Hej arthritic vs C3H/HeOuJ arthritic. *=$p<0.05$, **=$p<0.01$, ***= $p<0.001$ by Bonferroni post test.

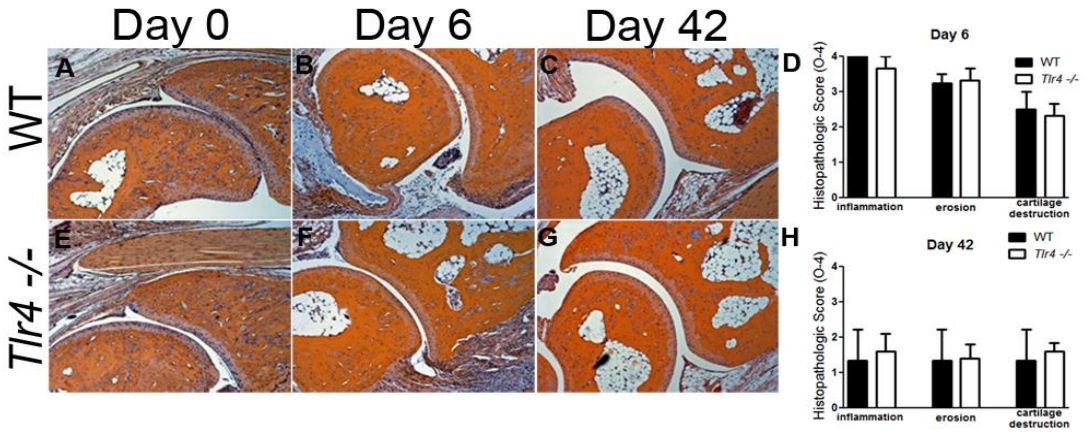

Figure 3.3 K/BxN serum transfer induced peripheral joint histopathology in WT and *Tlr4-/-* mice. (A) Mice were sacrificed 0, 6 and 42 days after arthritis induction and the ankle joints were removed, prepared for histology, sectioned and stained with Hematoxylin and Eosin. WT (B) and *Tlr4-/-* (C) arthritic mice have prominent inflammation, erosion, and cartilage destruction at day 6 and day 42 which are not statistically different between genotypes.

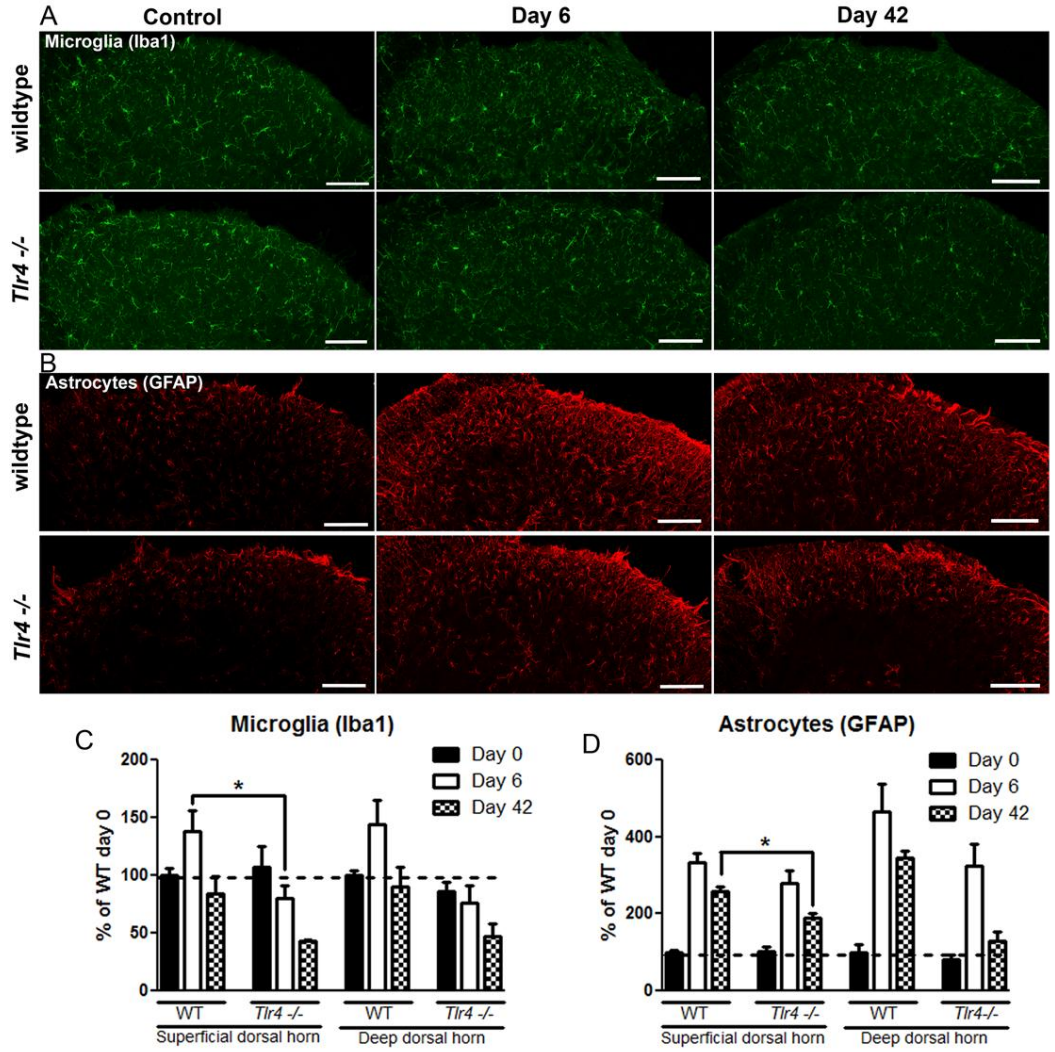

Figure 3.4 Spinal immunohistochemistry of microglia (Iba1) and astrocytes (GFAP) from the dorsal horn of WT and *Tlr4-/-* mice 0, 6, and 42 days after K/BxN serum transfer arthritis induction. (A) Dorsal horn Iba-1 staining is increased at day 6 in WT, but not *Tlr4-/-* mice. (B) Dorsal horn GFAP staining is increased in WT and *Tlr4-/-* mice at day 6 and day 42. Densitometry indicates that WT mice increase Iba-1 immunoreactivity (C) and GFAP immunoreactivity (D) to a greater degree following K/BxN serum transfer than do *Tlr4-/-* mice compared to naive.

Quantification of images is shown by densitometry (using integrated intensity). Scale bars: 50μm. *= $p<0.05$, ***=$p<0.001$ by Bonferroni post test. All experiments n= 3 mice, 3 sections per mouse. Representative sections shown.

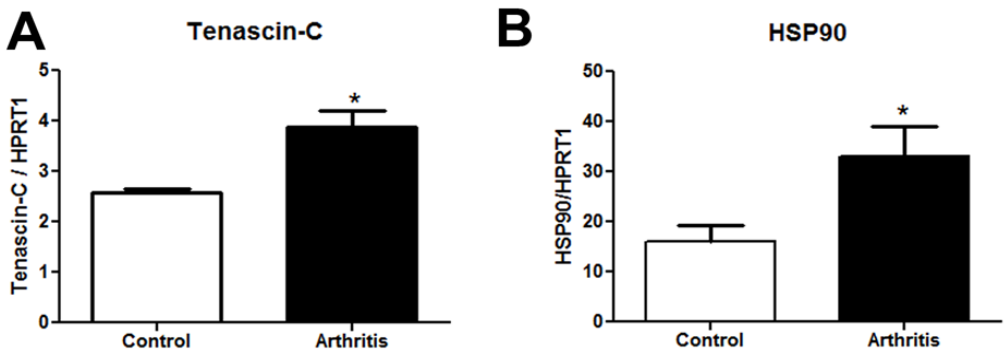

Figure 3.5 TLR4 ligands are elevated post-inflammation (d42) during progression of K/BxN serum transfer arthritis. mRNA relative expression unites normalized to HPRT1 levels of tenascin-C (A), and HSP90 (B) are elevated in the spinal cords of WT arthritic mice as compared to control serum treated animals. Each group represents mean ± SEM (n=5-6 mice/group), *=$p<0.05$, **= $p<0.01$, and ***=$p<0.001$ by student's t-test.

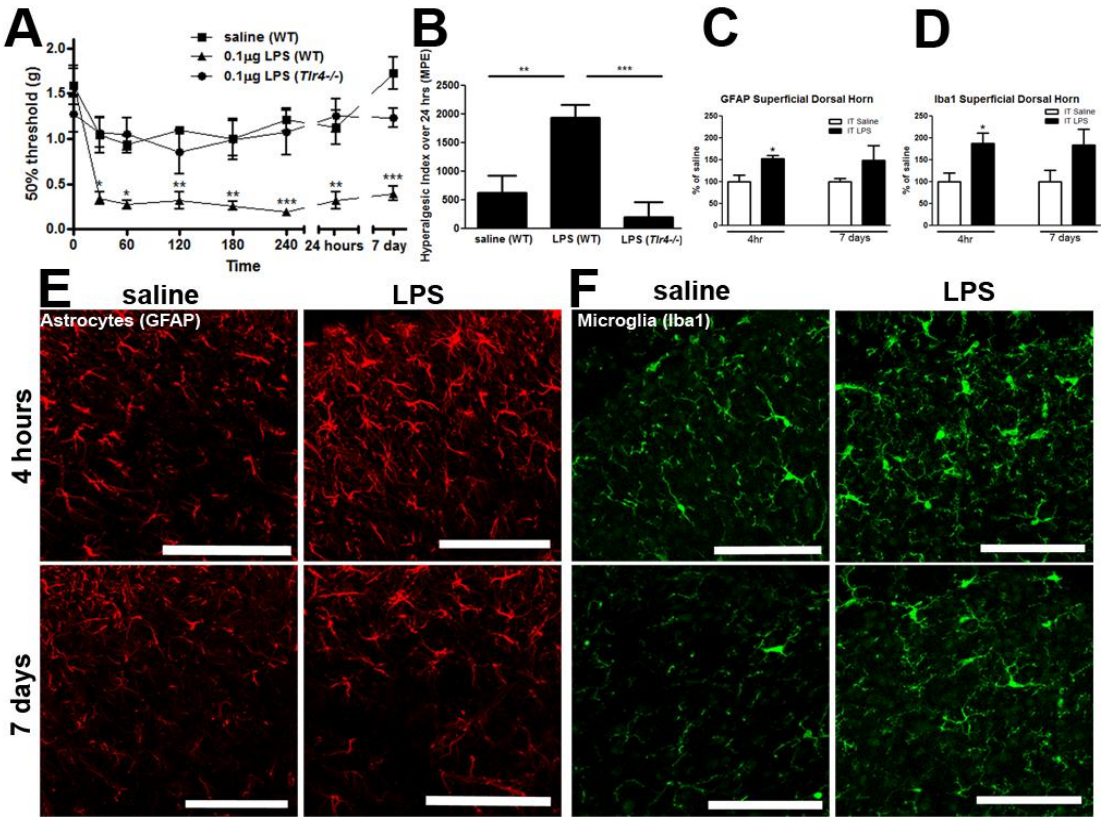

Figure 3.6 Intrathecal activation of TLR4 produced mechanical hypersensitivity. **(**A) IT LPS (0.1µg) produced mechanical hypersensitivity (30 minutes to 7 days) in WT, but not *Tlr4-/-* mice or in WT saline treated mice which is visualized in (B) by the hyperalgesic index. (C) Astrocyte staining (GFAP) is increased in the spinal dorsal horn 4hr after IT LPS which is visualized in (E). (D) Microglia staining (Iba1) is increased in the spinal dorsal horn 4 hr after IT LPS which is visualized in (F). Each time point represents mean ± SEM (n=6 mice/group), *= $p<0.05$, **= $p<0.01$, and ***= $p<0.001$ by Bonferroni post-test. Scale bars= 50µm.

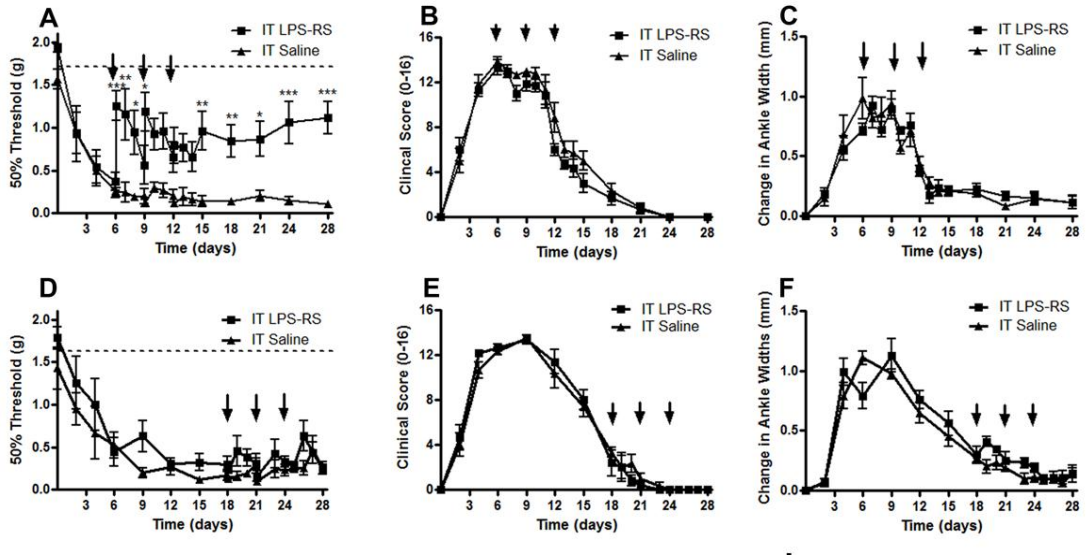

Figure 3.7 Intrathecal (IT) delivery of a TLR4 antagonist (LPS-RS) during the inflammation period but not during the post-inflammation period of WT mice will improve mechanical hypersensitivity without altering inflammation levels. IT delivery of LPS-RS (10µg) on days 6, 9, and 12 post K/BxN serum transfer in WT mice will (A) significantly improve mechanical hypersensitivity days 15, 18, 21, 24, and 28 (C) not significantly affect ankle width and (F) not significantly alter clinical scores as compared to arthritic animals treated IT with saline. IT delivery of LPS-RS (10µg) on days 18, 21, and 24 post-K/BxN serum transfer in WT mice does not significantly alter (B) mechanical hypersensitivity (D) ankle width or (F) clinical scores as compared to IT salineEach group represents mean ± SEM (n=4-6 mice/group), *=$p<0.05$, **= $p<0.01$, and ***=$p<0.001$ by Bonferroni post-test.

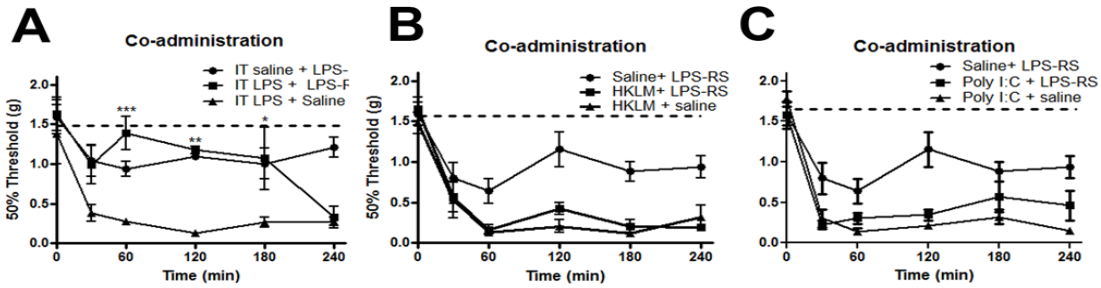

Figure 3.8 Co-administration of TLR4 antagonist LPS-RS delays mechanical hypersensitivity from TLR4, but not TLR2 (HKLM) or TLR3 (PolyI:C) agonist. (A) Intrathecal co-administration of LPS-RS (10µg) with LPS (0.1µg) significantly delayed LPS induced mechanical hypersensitivity for 180 minutes. (B) Intrathecal co-administration of LPS-RS (10µg) with HKLM (10^6 cells) did not significantly alter HKLM induced mechanical hypersensitivity. (C) Intrathecal co-administration of LPS-RS (10µg) with PolyI:C (0.5µg) did not significantly alter PolyI:C induced mechanical hypersensitivity. Dotted line indicates average initial threshold baseline of 1.51g, 1.57g, and 1.65g respectively. Each time point represents mean +/- SEM (n=6 mice/ group). *=p<0.05, **=p<0.01, ***= p<0.001 by Bonferroni post test.

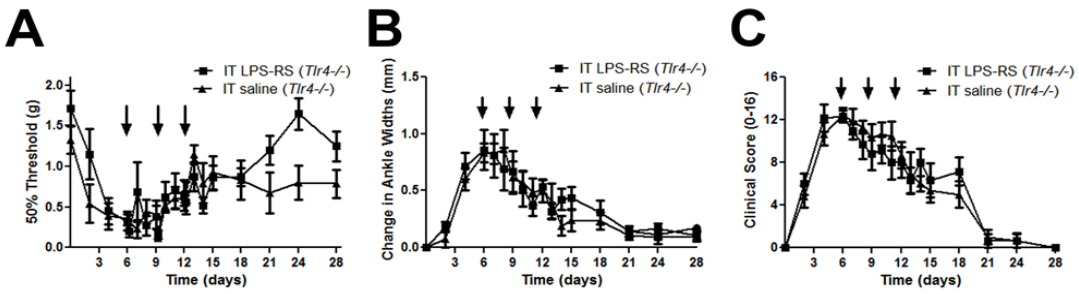

Figure 3.9 IT delivery of a TLR4 antagonist (LPS-RS) during the inflammation period to a *Tlr4-/-* mouse has no behavioral effect. IT delivery of LPS-RS(10µg) on days 6, 9, and 12 post K/BxN serum transfer to *Tlr4* -/- mice does significantly alter (A) mechanical hypersensitivity (B) ankle widths or (C) clinical scores as compared to *Tlr4-/-* mice treated with IT saline. Each time point represents mean +/- SEM (n=6 mice/ group).

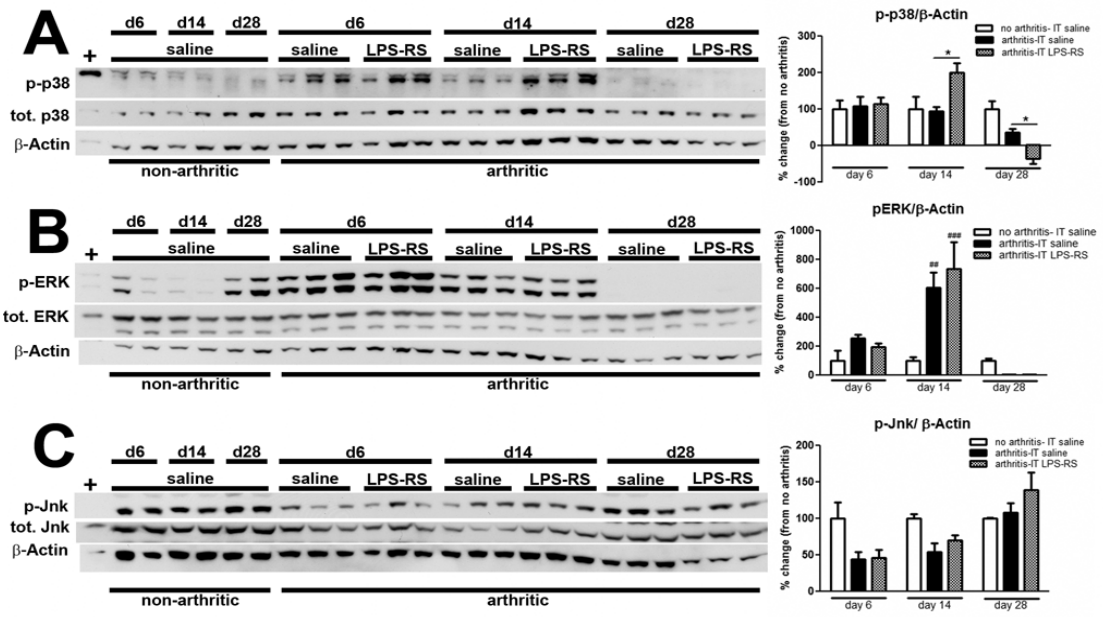

Figure 3.10 Western blot quantification of intrathecal administration of LPS-RS (10µg) on day 6, 9, and 12. Data indicates (A) significantly increased phosphorylated p38 in the spinal cord on day 14 and significantly decreased p-p38 it on day 28 relative to intrathecal saline in K/BxN serum transfer arthritic mice. Western blot quantification indicates (B) significantly increased phosphorylated ERK in the spinal cord on day 14 in arthritic mice compared to non-arthritic mice independent of drug treatment. Western blot quantification indicates (C) no significant effect upon phosphorylated JnK levels due to either K/BxN serum transfer arthritis or IT LPS-RS treatment. Each time point represents mean +/- SEM (n=3 mice/ group). *=p<0.05 IT LPS-RS vs IT saline; ##=p<0.01arthritis + IT saline vs non-arthritic; ###p<0.001 arthritis + IT LPS-RS vs non-arthritic by Bonferroni post-test.

Figure 3.11 Heat map displaying the relative fold-changes in the eicosanoid profile.

(A) The changes in the eicosanoid profile in day 6 K/BxN serum transfer arthritic mice with respect to non-arthritic control mice. (B) A direct comparison between the relative eicosanoid levels detected in day 6 arthritic mice (treated with IT LPS-RS) versus day 6 arthritic mice (treated with IT saline). This analysis was determined from non-arthritic control (n=8), arthritic + IT saline (n=7), and arthritic + IT LPS-RS (n=8) mice. ND (black) indicates that the eicosanoid was either not detected or below our level of detection.

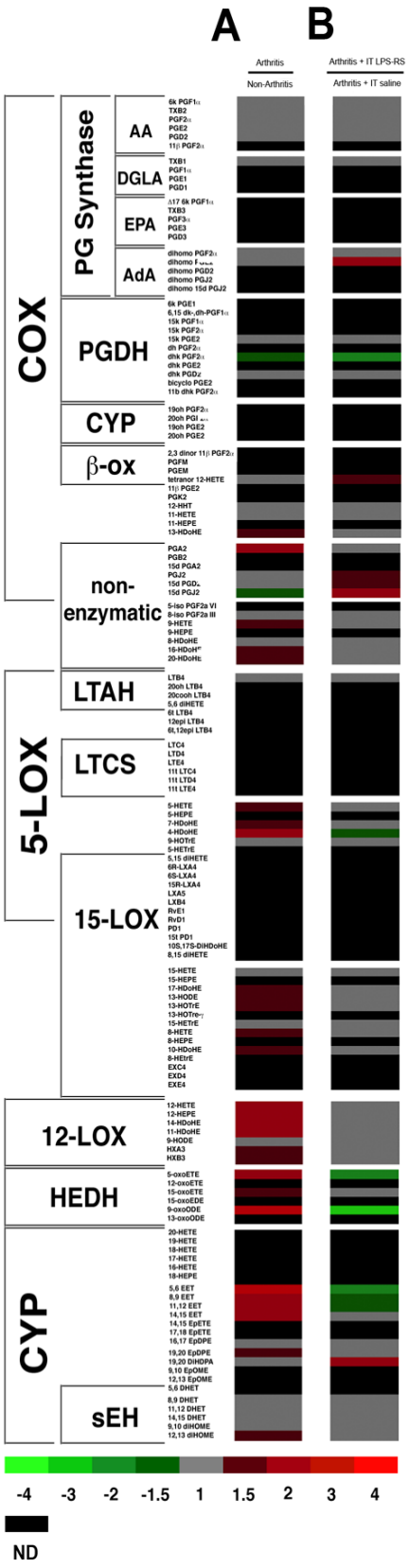
A
B
Arthritis
Non-Arthritis
Arthritis + IT LPS-RS
Arthritis + IT saline
COX
PG Synthase
AA
DGLA
EPA
AdA
PGDH
CYP
β-ox
non-enzymatic
5-LOX
LTAH
LTCS
15-LOX
12-LOX
HEDH
CYP
sEH
-4
-3
-2
-1.5
1
1.5
2
3
4
ND

Figure 3.12. Effects of arthritis and IT LPS-RS administration on PGE_2 and PGD_2 and their breakdown products of 15k-PGE_2 and 15d-PGJ_2 in the spinal cord on day 6, 2 hours after drug delivery. (A) PGE_2 is significantly increased 2 hours after IT LPS-RS treatment vs. IT saline in arthritic mice. (B) There are no significant changes in PGD_2 levels across treatment groups. (C) There no significant changes in 15-keto-PGE_2 (PGE_2 enzymatic breakdown product) levels across treatment groups. (D) 15-deoxy-PGJ_2 is significantly decreased on day 6 in arthritic vs. non-arthritic mice 2 hours after having both received IT saline injections. This decrease is significantly recovered in arthritic mice 2 hours after administration of IT LPS-RS (10μg). (E)Mechanical hypersensitivity is significantly improved 15minutes after IT delivery of 15d-PGJ_2 on day 6 K/BxN serum transfer arthritis which is graphed (F) according to the hyperalgesic index across the 2 hours post-delivery. Each group represents mean +/- S.E.M (n=8 mice/group: mass spectrometry; n=5 mice/group: behavior), *=$p<0.05$ by Bonferroni post-test.

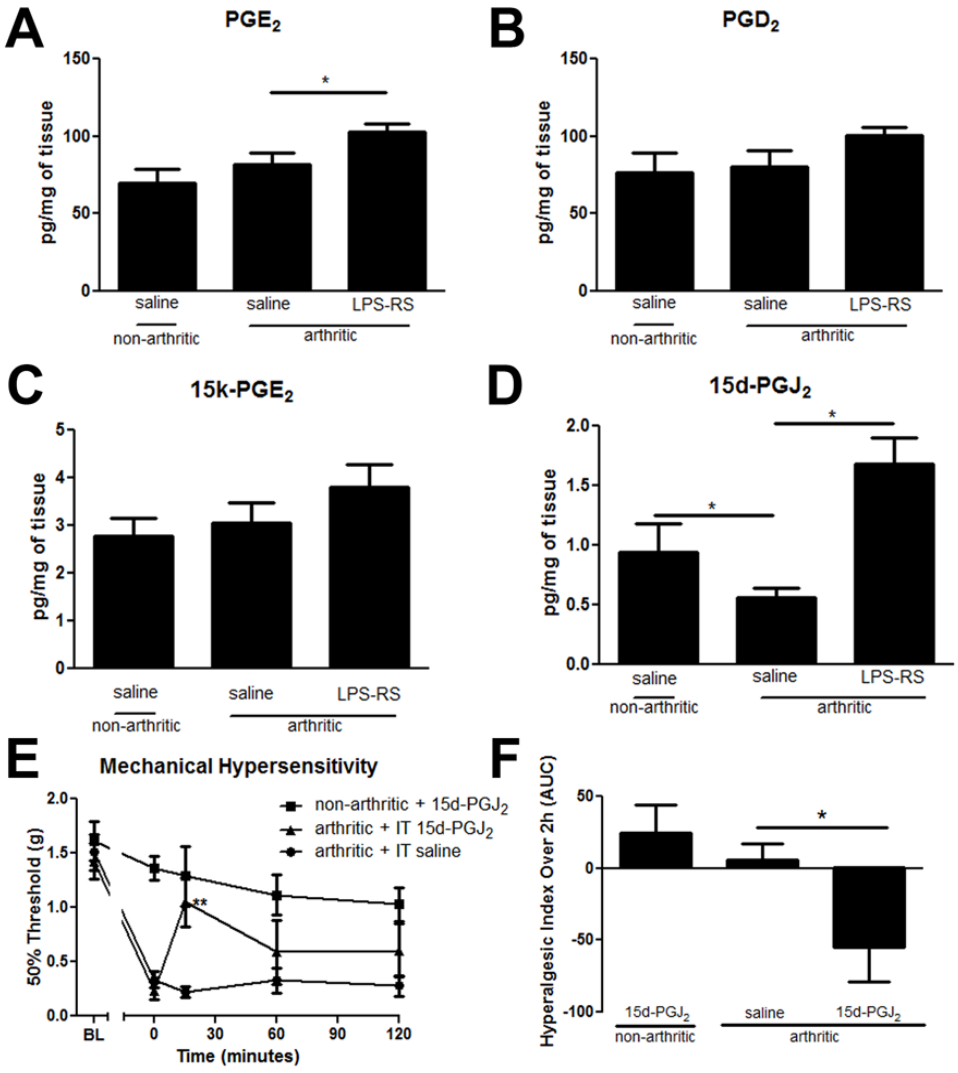
A
PGE2
pg/mg of tissue
150
100
50
0
*
saline
saline
LPS-RS
non-arthritic
arthritic
B
PGD2
pg/mg of tissue
150
100
50
0
saline
saline
LPS-RS
non-arthritic
arthritic
C
15k-PGE2
pg/mg of tissue
5
4
3
2
1
0
saline
saline
LPS-RS
non-arthritic
arthritic
D
15d-PGJ2
pg/mg of tissue
2.0
1.5
1.0
0.5
0.0
*
*
saline
saline
LPS-RS
non-arthritic
arthritic
E
Mechanical Hypersensitivity
50% Threshold (g)
2.0
1.5
1.0
0.5
0.0
non-arthritic + 15d-PGJ2
arthritic + IT 15d-PGJ2
arthritic + IT saline
**
BL
0
30
60
90
120
Time (minutes)
F
Hyperalgesic Index Over 2h (AUC)
50
0
-50
-100
*
15d-PGJ2
saline
15d-PGJ2
non-arthritic
arthritic

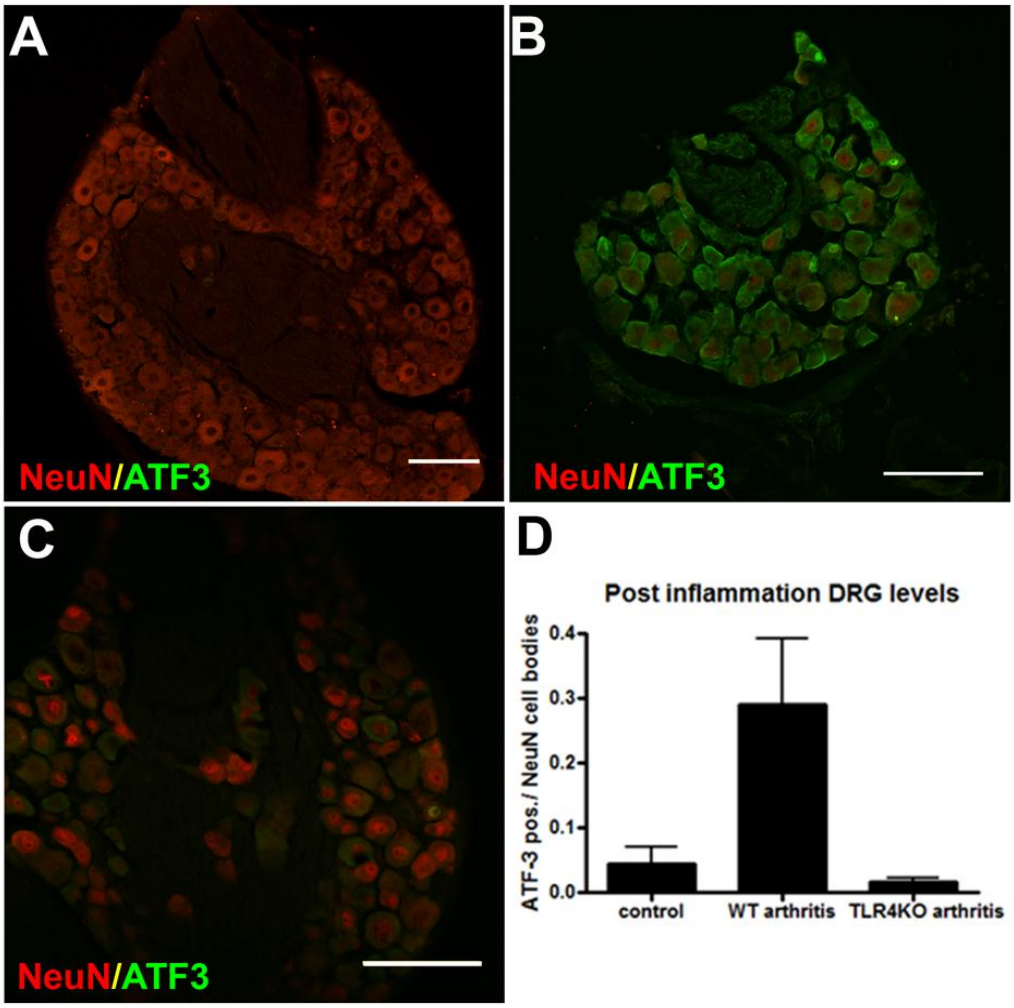

Figure 3.13. The increase in ATF3 positive cells in WT mice in the dorsal root ganglia following induction of K/BxN serum transfer arthritis is abrogated in *Tlr4-/-* mice. Representative images of (A) WT day 42 control mice with no ATF3 immunoreactivty, (B) WT day 42 arthritic mice with ATF3 immunoreactivity, and (C) *Tlr4-/-* day 42 arthritic mice with no ATF3 immunoreactivity are shown. (D) Graph showing the number of cells positive for ATF3 divided by the total number of NeuN positive nuclear cell bodies in the different groups. Each bar represents mean ± SEM (n=3-4/group, 3-5 sections per mouse) and *=$p<0.05$ by student's T-test. Scale bars represent 100μm.

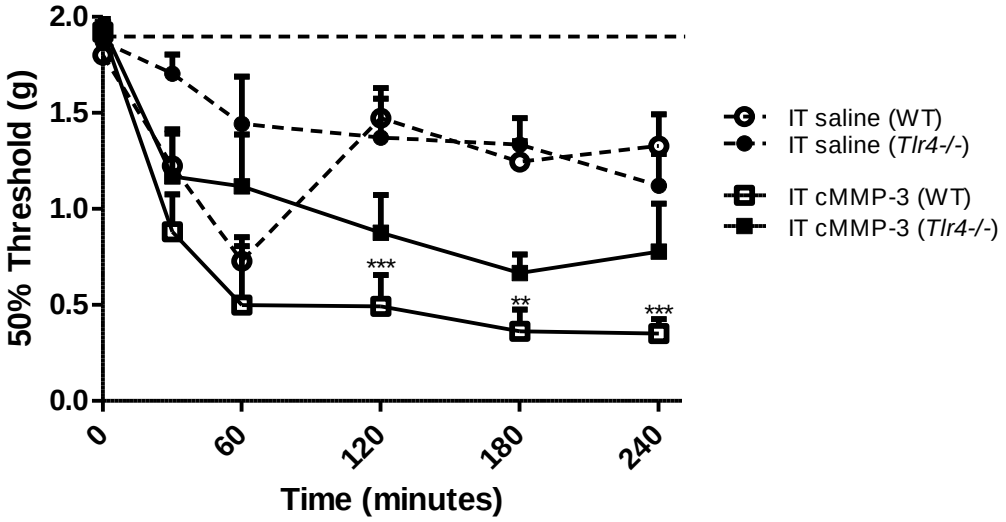

Figure 3.14 IT cMMP-3 induced mechanical hypersensitivity is TLR4 mediated. Intrathecal administration of cMMP-3 (1pmol) significantly induces mechanical hypersensitivity in WT but not *Tlr4-/-* mice as compared to IT saline injections at 120, 180, and 240 minutes after injection. Each group represents mean +/- SEM (n=6 mice/group), **=p<0.01, ***p<0.001 by Bonferroni post-test.

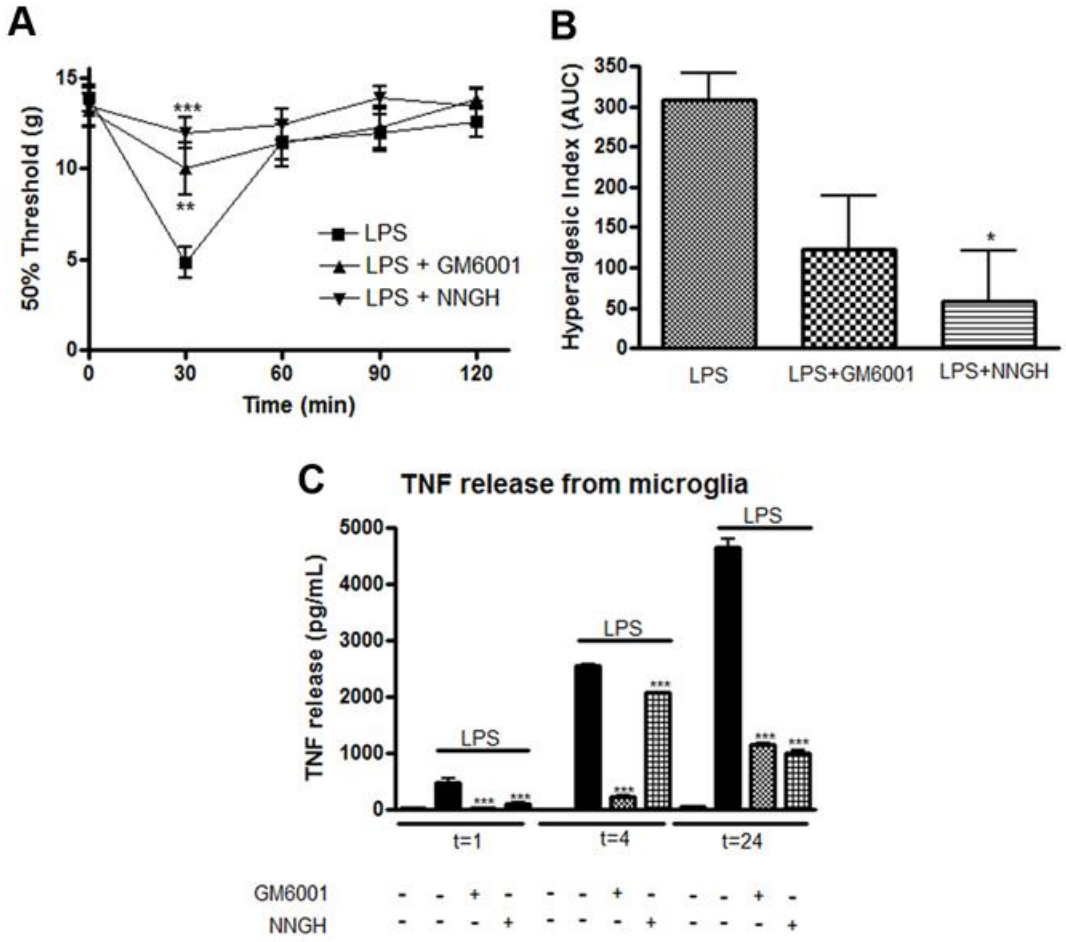

Figure 3.15 TLR4 mechanical hypersensitivity and TNF release is MMP-3 dependent. (A) IT pretreatment with GM6001 (1µg) or NNGH (7.5µg) significantly prevented LPS induced tactile allodynia in rats 30 minutes after LPS administration ($p<0.01$) which is graphed (B) according to the hyperalgesic index. (C) Primary spinal microglia were treated for 1, 4, and 24 hours with LPS (10ng/mL) in the presence and absence of GM6001 (1µg) and NNGH (7.5µg) 30 minute pretreatments. At all time points GM6001 and NNGH reduced the TNF release ($p<0.001$). (*=$p<0.05$, **=$p<0.01$, ***=$p<0.001$). n=6 rats per group.

Table 3.1. Eicosinoid profile of the lumbar spinal cord 6 days after K/BxN serum transfer arthritis induction. Non-arthritic mice (IT saline treated: n=8), arthritic (IT saline treated: n=7), and arthritic (IT LPS-RS; 10μg treated: n=8) mice were harvested 2 hours after drug treatment.

COMMON NAME	ABBREVIATION	non-arthritic- IT saline	arthritic + IT saline	arthritic + IT LPS-RS
6-keto-Prostaglandin F1a	6-keto PGF1a	[a]30.54 ± [b]3.35	31.45 ± 3.96	27.45 ± 3.28
Thromboxane B_2	TXB_2	28.63 ± 5.72	39.87 ± 5.68	26.25 ± 2.52
Prostaglandin F2a	PGF_{2a}	48.64 ± 7.03	51.20 ± 5.56	58.76 ± 3.18
Prostaglandin E_2	PGE_2	70.09 ± 8.59	81.66 ± 7.38	95.41 ± 12.72
Prostaglandin D_2	PGD_2	76.45 ± 13.09	80.54 ± 10.18	118.23 ± 1.06
15-keto-Prostaglandin E2	15-keto PGE_2	2.77 ± 0.37	3.05 ± 0.43	2.09 ± 0.34
13,14-dihydro-15-keto Prostaglandin F2a	dhk PGF_{2a}	1.15 ± 0.27	0.71 ± 0.34	0.30 ± 0.06
13,14-dihydro-15-keto Prostaglandin E2	dhk PGE_2	2.26 ± 0.39	2.45 ± 0.33	3.56 ± 0.08
13,14-dihydro-15-keto Prostaglandin D2	dhk PGD_2	0.13 ± 0.03	0.10 ± 0.01	0.09 ± 0.00
tetranor 12-hydroxy-eicosatetraenoic acid	tetranor 12-HETE	87.42 ± 12.37	105.21 ± 11.62	89.60 ± 5.85
12S-hydroxy-heptadecatrienoic acid	12-HHT	86.73 ± 12.46	103.62 ± 9.74	122.28 ± 6.01
11-hydroxy-eicosatetraenoic acid	11-HETE	4.27 ± 0.61	6.41 ± 0.97	6.89 ± 0.19
Prostaglandin J_2	PGJ_2	8.30 ± 1.44	7.66 ± 2.13	10.51 ± 0.91
15-deoxy-Δ12,14-PGD2	15-deoxy PGD_2	5.53 ± 0.83	3.95 ± 0.54	6.89 ± 0.72
15-deoxy-Δ12,14-PGJ2	15-deoxy PGJ_2	0.97 ± 0.23	0.56 ± 0.07	1.05 ± 0.11
Isoprostane F_{2a}-III	8-iso PGF_{2a} III	2.68 ± 0.38	3.32 ± 0.31	3.35 ± 0.22
9-hydroxy-eicosatetraenoic acid	9-HETE	1.54 ± 0.21	2.81 ± 0.29	2.24 ± 0.16
8-hydroxy-docosahexaenoic Acid	8-HDoHE	2.33 ± 0.25	3.15 ± 0.33	3.66 ± 0.25
16-hydroxy-docosahexaenoic Acid	16-HDoHE	1.54 ± 0.19	2.54 ± 0.43	2.69 ± 0.14
20-hydroxy-docosahexaenoic Acid	20-HDoHE	3.31 ± 0.40	5.25 ± 0.90	5.13 ± 0.22
Leukotriene B_4	LTB_4	0.17 ± 0.02	0.24 ± 0.05	0.30 ± 0.02
5-hydroxy-eicosapentaenoic acid	5-HETE	6.97 ± 0.84	11.57 ± 0.93	12.07 ± 0.49
5-hydroxy-eicosapentaenoic acid	5-HEPE	0.23 ± 0.03	0.50 ± 0.08	0.38 ± 0.02
7-hydroxy-docosahexaenoic Acid	7-HDoHE	0.61 ± 0.13	1.03 ± 0.14	1.41 ± 0.07
4-hydroxy-docosahexaenoic Acid	4-HDoHE	2.45 ± 0.39	6.15 ± 0.82	4.50 ± 0.17
9-hydroxy-octadecatrienoic acid	9-HOTrE	0.22 ± 0.04	0.28 ± 0.02	0.35 ± 0.15
15-hydroxy-eicosatetraenoic acid	15-HETE	24.19 ± 3.39	33.92 ± 3.73	30.23 ± 1.85
17-hydroxy Docosahexaenoic Acid	17-HDoHE	3.48 ± 0.44	6.92 ± 0.83	4.97 ± 0.17
13-hydroxy-octadecadienoic acid	13-HODE	5.49 ± 0.86	9.47 ± 1.22	7.20 ± 2.04
13-hydroxy-octadecatrienoic acid	13-HOTrE	0.40 ± 0.06	0.75 ± 0.11	0.85 ± 0.24
13-hydroxy-octadecatrienoic acid	13-HOTre-g	0.06 ± 0.01	0.01 ± 0.00	0.17 ± 0.14
15-hydroxy-eicosatrienoic acid	15-HETrE	0.74 ± 0.09	1.02 ± 0.16	1.02 ± 0.05
8-hydroxy-eicosatetraenoic acid	8-HETE	2.17 ± 0.30	3.96 ± 0.51	3.55 ± 0.15
10-hydroxy Docosahexaenoic Acid	10-HDoHE	1.33 ± 0.17	2.52 ± 0.31	2.31 ± 0.17
8-hydroxy-eicosatrienoic acid	8-HEtrE	0.08 ± 0.05	0.18 ± 0.11	0.14 ± 0.04
12-hydroxy-eicosatetraenoic acid	12-HETE	56.15 ± 12.54	133.40 ± 28.42	113.37 ± 9.42
12-hydroxy-eicosapentaenoic acid	12-HEPE	1.97 ± 0.47	4.43 ± 1.08	3.81 ± 0.37
14-hydroxy-docosahexaenoic Acid	14-HDoHE	10.28 ± 2.27	24.14 ± 5.75	15.85 ± 1.54
11-hydroxy-docosahexaenoic Acid	11-HDoHE	0.99 ± 0.13	2.03 ± 0.30	1.90 ± 0.13
9-hydroxy-octadecadienoic acid	9-HODE	5.99 ± 1.06	8.80 ± 1.08	6.88 ± 2.24
Hepoxilin A_3	HXA_3	4.26 ± 0.50	7.21 ± 0.90	5.68 ± 0.49
Hepoxilin B_3	HXB_3	11.68 ± 1.78	19.67 ± 3.63	11.12 ± 0.64
5-oxo-eicosatetraenoic acid	5-oxoETE	0.65 ± 0.14	1.86 ± 0.29	0.84 ± 0.05
15-oxo-eicosatetraenoic acid	15-oxoETE	2.95 ± 0.51	5.34 ± 0.79	3.92 ± 0.25
13-oxo-octadecadienoic acid	13-oxoODE	1.07 ± 0.34	3.27 ± 1.16	1.67 ± 1.05
18-hydroxy-eicosatetraenoic acid	18-HETE	0.27 ± 0.04	0.28 ± 0.05	0.30 ± 0.02
5(6)-epoxy-eicosatrienoic acid	5,6 EET	1.21 ± 0.18	4.30 ± 0.51	2.58 ± 0.20
8(9)-epoxy-eicosatrienoic acid	8,9 EET	0.80 ± 0.23	1.91 ± 0.41	1.47 ± 0.24
11(12)-epoxy-eicosatrienoic acid	11,12 EET	1.44 ± 0.22	3.20 ± 0.45	3.90 ± 0.34
14(15)-epoxy-eicosatrienoic acid	14,15 EET	1.65 ± 0.29	4.10 ± 0.61	5.07 ± 0.42
16,17-epoxy Docosapentaenoic Acid	16,17 EpDPE	2.88 ± 0.29	4.20 ± 0.60	6.60 ± 0.50
19,20-epoxy Docosapentaenoic Acid	19,20 EpDPE	1.39 ± 0.32	2.66 ± 0.44	5.32 ± 0.61
19,20-dihydroxy-docosapentaenoic acid	19,20 DiHDPA	1.77 ± 0.23	1.81 ± 0.19	2.98 ± 0.05
9(10)epoxy-octadecenoic acid	9,10 EpOME	- ± -	0.17 ± 0.14	2.31 ± 1.23
12(13)epoxy-octadecenoic acid	12,13 EpOME	- ± -	- ± -	1.70 ± 0.72
8,9-dihydroxy-eicosatrienoic acid	8,9 DHET	0.42 ± 0.08	0.56 ± 0.09	0.54 ± 0.06
11,12-dihydroxy-eicosatrienoic acid	11,12 DHET	0.78 ± 0.11	1.03 ± 0.10	1.19 ± 0.08
14,15-dihydroxy-eicosatrienoic acid	14,15 DHET	0.88 ± 0.12	1.20 ± 0.12	1.50 ± 0.08
9,10-dihydroxy-octadecenoic acid	9,10 diHOME	0.61 ± 0.07	0.91 ± 0.10	0.92 ± 0.10
12,13-dihydroxy-octadecenoic acid	12,13 diHOME	1.03 ± 0.11	1.57 ± 0.20	1.71 ± 0.07

[a]Values are reported as pg/mg of tissue

[b]Error values are reported as S.E.M.

Chapter 4

Spinal matrix metalloproteinase 3 mediates inflammatory hyperalgesia via a TNF dependent mechanism

4.1 Introduction:

Matrix metalloproteinases (MMPs) are zinc dependent endopeptidases that have been widely investigated regarding their dynamic role in the processing of extra cellular matrix (ECM) protein [195]. Activation of matrix metalloproteinases during inflammation and injury have been implicated [196] in a variety of neurologic diseases including multiple sclerosis [197], spinal cord injury [198], cerebral ischemia [199], and neuropathic pain [200]. Pain-like behavior and hypersensitivity result in part from the release of inflammatory mediators that activate and sensitize peripheral and central nociceptive components [42]. Here we demonstrate for the first time the role of MMP-3 in spinal nociceptive processing likely by dorsal horn non-neuronal cell communication via a TNF dependent pathway activated during peripheral inflammation and mediating the associated hyperalgesia.

Constitutive RNA expression of MMP-2, 3, 7, 9, and 13 have been demonstrated in the spinal cord [201]. The expression of MMPs and related regulatory enzymes such Tissue Inhibitors of Metalloproteinase (TIMPs) in microglia, astrocytes or neurons are differentially regulated during the initiation of neurological pathologies [92]. Such differential regulation correlates with enhanced spinal secretion of cytokines including TNF, IL-1β, and IL-10 which have been implicated in central sensitization [95]. MMP-3 is of particular interest as it lies upstream in the MMP

cascade, activating for example proMMP-9 [98], which in turn has been demonstrated to activate microglia and regulate onset of neuropathic pain in an IL-1β dependent manner [99, 202]. In addition, MMP-3 activates other key nociceptive linkages including nerve growth factor (NGF) and brain derived neurotrophic factor (BDNF) [203], osteopontin [204], and IL-1β [205] which regulate neuronal and non-neuronal cell excitability [206].

Recent work from our laboratory and that of others indicates that generation and maintenance of enhanced pain states after peripheral injury involves activation of spinal non-neuronal cells such as microglia and astrocytes [207]. Intrathecal minocycline pretreatment will attenuate glial activation and pain hypersensitivity arising from tissue injury [37] and reduce MMP activity [91, 208]. Given the enzymatic activation by MMP-3 of known pro-nociceptive mediators, the aim of this study was to investigate spinal MMP-3 activity via pharmacological blockade during peripheral inflammation induced hypersensitivity and explore MMP-3 regulation of TNF release during non-neuronal cell signaling.

4.2 Experimental Procedures:

4.2.1 Animals

All experiments were carried out according to protocols approved by the Institutional Animal Care and Use Committee of the University of California, San Diego**.** Male rats (250-350 g; Harlan, Holtzman) were housed in individual cages at

room temperature and maintained on a 12-h light/dark cycle. Testing was performed during the light cycle. Food and water were available *ad libitum*.

4.2.2 Intrathecal catheter implantation

For intrathecal (IT) bolus drug delivery, lumbar catheters were surgically implanted into the IT space using a modification of a previously described protocol [209]. Briefly, animals were anesthetized, secured in a stereotaxic head holder, the cisternal membrane exposed and an incision made through which a single lumen 8.5cm polyethylene catheter (PE-5) was inserted ending at the L3-L4 spinal segments. The other end of the catheter was fused to a piece of PE-10 tubing and externalized. Rats were allowed to recover for five to six days before experimentation.

4.2.3 Behavioral tests

To assess the thermally evoked paw withdrawal response, a Hargreaves-type testing device was used (UARDG, Department of Anesthesiology, La Jolla, CA). Rats are placed individually in plexiglass cubicles on a glass surface (maintained at 25 °C) and a thermal stimulus below the glass surface regulates a timer. Latency was defined as the time required for the paw briskly withdrawal as detected by motion sensors controlling the timer and terminating the stimulus [116].

Mechanical sensitivity was assessed using von Frey hairs with hair values ranging from 3.61g to 15g and the up–down method was applied as previously described [17].

The 50% withdrawal threshold (force of the von Frey hair to which an animal reacts to 50% of the presentations) was recorded.

Data were also presented as a hyperalgesic index, which represents the area under the time effect curve after stimulation. The formula is [(baseline latency − post-drug latency) × 100 (baseline latency)$^{-1}$] x min, where latency is expressed in seconds. Decreased values indicate analgesic efficacy. For post-treatments, hyperalgesic index values were calculated using the value at the time point before drug delivery as the baseline value.

4.2.4 Drugs and drug delivery

Local inflammation was induced with 100µl of 2% carrageenan in saline (lambda, Sigma-Aldrich) injected subcutaneously into the plantar surface of the hind paw. Intrathecally delivered drugs were prepared in a final volume of 10µL and followed by a 10µL saline flush. The following drugs and their doses were employed *in vivo*: GM6001, (N-[(2R)-2-(Hydroxamidocarbonylmethyl)-4-methylpentanoyl]-L-tryptophan Methylamide) (Calbiochem, 0.01µg, 0.1 µg or 1µg); NNGH (N-Isobutyl-N-(4-methoxyphenylsulfonyl)-glycylhydroxamic Acid), (Calbiochem, 2.5 µg or 7.5 µg); PY-2 (synthesized in the laboratory of S.M. Cohen, Dept of Chemistry and Biochemistry, UCSD [210] , 0.3µg, 1 µg, or 3µg); Etanercept (Amgen, 100 µg); cMMP-3 and proMMP-3 (EMD biosciences, 1pmol). GM6001, NNGH, and PY-2 were prepared in 3% DMSO, which was also used as the respective vehicle. Etanercept, cMMP-3, and proMMP-3 were prepared in saline, which was also used as

the vehicle. Etanercept was delivered as a 1 hour pretreatment. GM6001, NNGH, and PY-2 were delivered as 30 minute pretreatments in all experiments, except where delivered as a post-treatment at 105 min. *In vitro* the following drugs and their doses were employed: GM6001 (7.5μg/mL), NNGH (7. 5μg/mL), LPS (Sigma, 100ng/mL), cMMP-3 (400ng/mL). The experimenter was blinded to drug treatments during all behavioral testing.

4.2.5 Western blotting

Rats were anesthetized in 4% isoflurane, decapitated, and spinal cords hydroextruded. 1.5 cm of the spinal cord lumbar enlargement was collected in 3% SDS lysis buffer (50mM Tris, 150mM NaCl, 1 mM EDTA, 0.5% Triton X-100, 3% SDS pH 7.4) containing protease and phosphatase inhibitors and homogenized by sonication. 30μg of protein were loaded with 0.1M DTT and 1xLDS loading buffer (Invitrogen) and separated on a 4-12% Bis-Tris gel (Invitrogen). Proteins were transferred to a 0.45μm nitrocellulose membrane (Invitrogen), and blocked with 5% non-fat milk. Blots were incubated in anti-MMP-3 (Sigma; 1:500) or β-actin (Sigma; 1:100,000) followed by anti-rabbit/ anti-mouse secondary HRP conjugated antibody (Cell Signaling), for 1 hour at room temperature in 5% NFM. Blots were developed using femto (anti-MMP-3) or pico (anti-β-actin) sensitive enhanced chemiluminescent detection system (SuperSignal Pierce). Western blots were scanned and quantified by densitometry using ImageQuant (Molecular Dynamics).

4.2.6Tissue Preparation and Immunohistochemistry

Naïve rats were anesthetized with 0.5 mL Euthasol (Virbac), perfused intracardially with 0.9% NaCl followed by 4% paraformaldehyde (PFA) in 0.1 M sodium phosphate buffer (PBS), and.spinal cords post fixed in 4% PFA overnight and cryoprotected in sucrose.

Floating sections (30µm) were blocked (5% normal serum, 0.2% Triton X-100 in PBS) for 1 hour at room temperature before incubating with anti-MMP-3 (1:50; Sigma), and anti Iba-1 (1:500; Abcam), or anti GFAP (1:1000; Sigma), or anti NeuN (1:1000; Chemicon) for 72 hr at 4 °C. MMP-3 was amplified with a biotinylated anti-rabbit secondary (1:250; Vector) and an Alexa 488 avitin conjugate. All other primaries were visualized using the appropriate secondary linked to Alexa 555 (1: 5000; Molecular Probes). Sections were mounted and cover slipped (prolong gold antifade medium; Invitrogen).

Staining and visualization procedures were performed as described for floating sections. All images were captured with a Leica TCS SP5 confocal imaging system and processed using Adobe Photoshop CS2 software.

4.2.7 TNF ELISA

Rats were deeply anesthetized with 4% isoflurane, decapitated, and spinal cords hydroextruded. 1.5 cm of the spinal cord lumbar enlargement (approximately L2-L7) was collected in a modified RIPA buffer containing protease and phosphatase inhibitors and homogenized by sonication, and centrifuged for 12,000xg for 15

minutes at 4ºC. The supernatant was collected and total protein was established using the Bradford method. 1000µg of total protein in a volume of 100µl was added to each well and TNF levels were quantified according to manufacturer's instructions using an ELISA kit (BD Biosciences). TNF content in the spinal cord samples was expressed as pg/mL of spinal cord extract.

4.2.8 Cell culture

Purified cultures of rat spinal microglia and astrocytes were prepared using a method described previously with some modifications [37]. One- to three-day-old Sprague-Dawley rat pups were anaesthetized, the spinal cords ejected, mechanically triturated, centrifuged at 215 g for 5 min, re-suspended in DMEM containing 10% fetal bovine serum (FBS; Gibco), 1% penicillin/streptomycin (P/S; Gibco), plated in a flask previously coated with poly l-lysine (Sigma) and maintained at 37 ºC in a humidified 5% CO_2 incubator. On day 14, microglia were removed by shaking for 2 h at 37 °C, centrifuged at 215 g for 5 min and plated onto 96-well plates at 40,000 cells/well and allowed to adhere for 24 hours.

Mother cultures were shook a second time and cells were determined to be astrocytes, trypsanized, centrifuged at 215g for 5 minutes, re-suspended in DMEM with 10% FBS and 1% P/S, and plated until they reached 70-80% confluence.

4.2.9 Statistics

All the data are presented as mean ± SEM. Statistics were performed using Student's t-tests or one-way ANOVA with multiple *post hoc* comparison made using the Bonferroni tests (Prism Statistical Software, San Diego, CA, USA) except for TNF ELISAs which were evaluated by Dunnett's multiple comparison test using the vehicle as the control value. Critical values corresponding to $p < 0.05$ were deemed statistically significant.

.

4.3 Results:

4.3.1 Inhibition of spinal MMP-3 reduces inflammation-induced thermal and tactile hypersensitivity

Carregeenan thermal hyperalgesia and tactile allodynia.

Carrageenan injected into the ipsilateral hind paw of male Holtzman rats elicited a time-dependent increase in the thickness of the injected paw (not shown) and decrease in the thermal latency of the inflamed paw with no significant changes in the response latency of the non-injected contralateral paw. Thus, in animals receiving intrathecal (IT) injections of vehicle (3% DMSO), the baseline thermal escape latency of the ipsilateral paw decreased from 11.4 (± 0.7 sec) to 3.2 (± 0.6 sec) between baseline and 2 hours, ($p < 0.05$ vs baseline; Figure 4.1A, B, C).

In a separate group of animals, we showed that, in addition to decreased thermal latencies, intraplantar carrageenan also produced a time-dependent decrease in the tactile threshold of the inflamed paw. Thus, the tactile threshold of the ipsilateral

paw in IT 3% DMSO vehicle treated rats decreased from the baseline 15g to 2.1g (± 0.5g) at 2 hours ($p < 0.05$, Figure 4.2A).

IT MMP-3 inhibition and pretreatment.

To define the role of endogenous spinal MMP-3 during inflammation evoked thermal hyperalgesia, rats received an IT pretreatment (30 min in advance of the intraplantar carrageenan) of several agents known to inhibit MMP-3 enzymatic activity. Here, IT pretreatment delivery of GM6001, a broad spectrum MMP inhibitor (Figure 4.1A), NNGH, a semi-selective MMP-3 inhibitor (Figure 4.1B), or PY-2, a semi-selective MMP-3 inhibitor (Figure 4.1C) resulted in an attenuation of the intraplantar carrageenan evoked thermal hyperalgesia. When the data for the ipsilateral, inflamed paw, are presented according to the hyperalgesic index, a dose dependent anti-nociceptive effect as compared to a 3% DMSO vehicle is observed with: GM6001 (Figure 4.1D: 0.01μg; $p < 0.05$, 0.1μg; $p < 0.01$, 1μg; $p < 0.001$) and NNGH (Figure 4.1E: 2.5μg; not significant, 7.5μg; $p<0.001$). For PY-2 all doses display a significant reduction as compared to vehicle control (Figure 4.1F: 0.3μg; $p < 0.001$, 1μg; $p < 0.01$, 3μg; $p < 0.05$).

To define the role of endogenous spinal MMP-3 in the inflammation evoked tactile allodynia, the most efficacious doses of GM6001, NNGH, and PY-2, as determined during the dose response thermal hypersensitivity experiments were delivered as 30 minute IT pretreatments. These doses showed a comparable anti-allodynic action for GM6001 (1μg; $p < 0.001$), NNGH (7.5μg; $p < 0.001$) and PY-2

(1μg; $p < 0.01$) as compared to the 3% DMSO vehicle (Figure 4.2A and 4.2B). Importantly, none of the IT inhibitors or the vehicle at the doses employed in this pre-treatment series caused any sedation or signs of motor dysfunction (e.g. rats displayed normal spontaneous symmetrical ambulation, hind paw placing and stepping, pinnae and blink reflexes).

IT MMP-3 inhibition and post-treatment.

To determine if the MMP inhibition effects were observed when delivered following the initiation of the hyperalgesic state, we delivered intrathecally the efficacious doses of GM6001 (1μg), NNGH (7.5μg), and PY-2 (1μg) at 105 min after intraplantar carrageenan injection and recorded the changes in thermal thresholds from rats from 120-240min (Figure 4.3A). Delivery of NNGH and PY-2 indicate no significant increases in thermal thresholds following post-treatment delivery as compared to 3% DMSO vehicle. As indicated, IT GM6001 demonstrated a transient increase in thermal thresholds at 180min following carrageenan (Figure 4.3A; $p< 0.05$ vs 3% DMSO), however, calculation of the hyperalgesic index showed no significant anti-hyperalgesic effects in thermal thresholds as compared to 3% DMSO vehicle. To determine the effect of post-treatments upon the hyperalgesic index, baseline values were set according to 90min values and the area under the curve from 120-240 minutes was calculated.

4.3.2 Peripheral inflammation increases spinal MMP-3 protein expression

The behavioral data suggested that spinal MMP-3 activation was mediating the inflammation evoked hyperalgesia. To characterize spinal MMP-3 activation, protein levels were measured by western blotting for the pro form and the catalytically active forms of MMP-3 in the lumbar spinal cord (L4-L6) following intraplantar carrageenan (Figure 4.4A). There was indeed a significant increase in catalytic MMP-3, 2 and 4 hours post-injection ($p < 0.05$, Figure 4.4B) and in proMMP-3, 2 hours after the intraplantar carrageenan ($p < 0.05$; Figure 4.4C) as compared to naïve animals. This coincides with the time at which the carrageenan induced hyperaglesia and allodynia, attenuated by spinal MMP3 inhibition were observed.

4.3.3 MMP-3 is expressed in spinal astrocytes, microglia, and neurons

We next investigated the distribution and cellular location of MMP-3 in the rat spinal cord by immunohistochemistry. MMP-3 immunoreactivity was seen in all laminae in the dorsal and ventral horn. As shown in Figure 4.5, cells co-labeled with antibodies against MMP-3 and with antibodies against protein markers for each of the major cell types in the spinal cord, i.e., astrocytes (GFAP), microglia: (Iba1), and neurons: (NeuN); suggesting that MMP-3 is expressed by multiple cell types.

4.3.4 Spinal administration of catalytic MMP-3 (cMMP-3) causes thermal hyperalgesia and tactile allodynia

Given the effects of spinal MMP-3 inhibition and the appearance of increased spinal cMMP-3, we sought to determine if exogenous cMMP-3 or proMMP-3

delivered intrathecally would mimic the pro-algesic actions of the peripheral inflammation. Rats were injected IT with cMMP-3 (1 pmol), proMMP-3 (1 pmol) or saline and evaluated for changes in thermal and tactile thresholds. 30 minutes after IT injection of cMMP-3, the thermal escape latency dropped from baseline 10.8 ± 0.9 seconds to 6.6 ± 0.2 seconds ($p < 0.05$; Figure 4.6A) and remained significantly decreased for 90 minutes, whereas neither the pro form of MMP-3 (1 pmol) nor the saline control had any effect. Changes are presented according to the hyperalgesic index in Figure 4.6B, indicating a significant increase in pain-like behavior following catalytic but not proMMP-3 or saline intrathecal delivery ($p < 0.05$). Similarly, 30 minutes after IT cMMP-3 the tactile threshold dropped from baseline 14.5 (±0.5g) to 7.2 (±1.2g) ($p < 0.001$; Figure 4.6C) and remained decreased for 60 minutes, with no changes in tactile threshold following IT saline or proMMP-3. Changes presented according to the hyperalgesic index in Figure 4.6D show a significant increase in pain-like behavior following catalytic but not after IT proMMP-3 or saline ($p < 0.01$). An increase in nociceptive behavior by the spinal application of catalytic MMP-3 but not the unprocessed pro form indicates an enzymatic role for this protein in the spinal nociceptive processing.

The specificity of the IT cMMP-3 action was further defined by pretreatment with MMP and MMP-3 antagonists. Pretreatment (30 min) with IT GM6001 (1μg) or IT NNGH (7.5μg) abrogated the IT cMMP-3 induced thermal hypersensitivity (Figure 4.6E). At no time point was there a significant difference between baseline thresholds and thresholds 30 or 60 minutes after IT cMMP-3 when rats were pretreated with

GM6001 or NNGH. Changes presented according to the hyperalgesic index in Figure 4.6F show a significant increase in pain-like behavior in the four hours after IT cMMP-3 which is attenuated by NNGH or GM6001pre treatment ($p < 0.01$).

4.3.5 IT cMMP-3 but not pro-MMP-3 increases spinal TNF concentrations

MMP-3 application increases TNF levels *in vitro* in microglial cell cultures [96]. Given that TNF is a potent pro-inflammatory cytokine and produces enhanced nociception after IT delivery [211], [212], we investigated if MMP-3 could induce TNF levels *in vivo* in the spinal cord following intrathecal delivery. Following IT saline or IT proMMP-3, TNF levels were not different 30min after injection 295pg/mL +/- 7 vs 311pg.mL +/-35. In contrast, at 30min after injection, IT cMMP-3 significantly increased spinal cord TNF concentration 423pg/mL +/- 22 (Figure 4.7A; $p < 0.01$ vs saline, $p < 0.05$ vs proMMP-3). At later times, measured out to 4 hour, TNF levels were numerically greater than either the saline or proMMP-3 groups, but these differences did not reach statistical significance.

4.3.6 Thermal hyperalgesia and tactile allodynia evoked by IT cMMP-3 is mediated by TNF.

To functionally assess the role of TNF in cMMP-3 mediated nociception, we examined the spinal effect of etanercept, a TNF sequestering molecule, on IT cMMP-3 induced hyperalgesia. As before, IT cMMP-3 produced a significant reduction in thermal threshold at 30 minutes and the effect persisted for 90 minutes, which was

prevented by a 1hour pretreatment with IT etanercept (Figure 4.7B). This data is also presented according to the hyperalgesic index, indicating a pretreatment (1h) with IT etanercept effectively prevented an IT cMMP-3 induced thermal hyperalgesia ($p < 0.001$, Figure 4.7C). Rats pretreated with etanercept showed no difference from control (saline) animals ($p > 0.05$ at any time points).

4.3.7 Peripheral inflammation induces spinal TNF which is regulated by MMPs

To further establish the relationship between spinal MMP-3 activity and spinal TNF production we measured by TNF ELISA the concentrations of TNF in the lumbar spinal cord from groups of rats receiving IT pretreatments (30min in advance of the intraplantar carrageenan) with: IT 3% DMSO (vehicle control); IT 1μg GM6001, or IT 7.5μg NNGH. Animals were then randomly assigned to undergo tissue harvest at 30 minutes, 120 minutes, or 240 minutes after intraplantar carrageenan injection. Spinal TNF concentrations in control animals 512pg/mL+/- 127 were increased in a time dependent fashion after intraplantar carrageenan, reaching statistical significance, 1062pg/mL +/- 208 at 120 minutes after injection (Figure 4.8; $p < 0.05$) and continuing to rise through 240 minutes 2579pg/mL +/- 117 (Figure 4.8; $p < 0.001$). These plantar inflammation induced increases in spinal TNF concentrations were significantly reduced at the 120 min time point by pretreatment with IT GM6001 (316pg/mL +/- 61; $p<0.01$) and by IT NNGH (532pg/mL +/- 209; $p < 0.05$). By 4.5hrs after drug delivery, the inhibitory effects of IT GM6001 (2320pg/mL +/- 342) or NNGH (206 pg/mL +/- 241) were lost, with these spinal TNF concentrations not

differing from those observed in the vehicle control animals at this time (2579pg/mL +/- 117) **.** This attenuation of the time dependent increase in spinal TNF levels corresponds with the IT GM6001, NNGH, and PY-2 regulated behavioral attenuation of thermal and tactile hypersensitivity demonstrated in the intraplantar carrageenan treated animal.

4.3.8 cMMP-3 evoked TNF release from microglia, but not astrocytes.

Considerable work has demonstrated that stimulated astrocytes and microglia display increased extracellular concentrations of TNF [213]. Given the role of TNF in the spinal MMP-3 actions, we examined whether cMMP-3 would initiate TNF release from primary spinal microglia and astrocyte cultures. The addition of cMMP-3 to microglia cultures resulted in a prominent increase in TNF as compared to media controls 4.5pg/mL ±2.6 vs cMMP-3 application 296.5pg/mL ± 84.2 at four hours (Figure 4.9A; $p<0.01$). In contrast, application of cMMP-3 did not, at any time point, induce significant release of TNF from astrocytes as compared to media control values (Figure 4.9B; $p>0.05$). This lack of effect in astrocytes stands in contrast to the effect of the TLR4 agonist, LPS (100ng/mL), which induced a significant increase in TNF released from microglia ($p < 0.01$) and from astrocytes ($p < 0.05$) at all time points (Figure 4.9A and 4.9B). Importantly, this increase in TNF release from microglia is blocked by pretreatment with GM6001 (31.6pg/mL ±12.4, $p > 0.05$ vs. media control) or with NNGH (40.3 pg/mL ±2.8, $p > 0.05$ vs. media control).

4.4 Discussion

Matrix metalloproteinases are a diverse class of zinc-dependent enzymes which are recognized to play an important regulatory role in the organization of extracellular matrix proteins**.** The present studies emphasize a novel role for catalytically active MMP-3, showing it to be a key component in a novel spinal cascade initiated by peripheral inflammation resulting in a robust behaviorally defined thermal hyperalgesia and tactile allodynia. We hypothesize that the peripheral inflammatory stimulus leads to an increase in spinal cMMP-3 resulting in a spinal release of TNF, likely from non-neuronal cells to evoke a facilitated state of dorsal horn processing. Convergent data supporting this hypothesis will be considered below.

The facilitated state is initiated by the catalytically active form of MMP-3.

In the present study, intrathecally delivered MMP-3 was found to result in a potent and reversible tactile allodynia and thermal hyperalgesia. The effects of the exogenously delivered MMP were observed to occur only with the catalytically active monomer. Thus, i) intrathecal delivery of exogenous cMMP-3, but not proMMP-3 initiated a short latencied and reversible thermal hyperalgesia and tactile allodynia; ii) the cMMP-3, but not proMMP-3 resulted in increased spinal TNF *in vivo* and iii) the effects of the cMMP-3 on TNF concentrations were blocked by MMP and MMP-3 antagonists GM6001 and NNGH, respectively.

Peripheral inflammation leads to a significant elevation of spinal cMMP-3.

In agreement with other reports, western blotting and imunohistochemistry indicate that MMP-3 is constitutively expressed in spinal cord [95, 214, 215] and differentially regulated during inflammatory CNS diseases including multiple sclerosis, stroke, and neuropathic pain (reviewed in [196]. In the present work there was a significant increase in spinal cord MMP-3 protein expression at 2 hrs following peripheral inflammation. This is consistent with previous work which demonstrated that MMP-3 is subject to up-regulation by signaling pathways including MAPK and PI3K/AKT [216]. Thus, inhibition of these pathways has been reported to diminish expression of MMPs [217], [218] in addition to attenuation of post-inflammation hyperalgesia [219], [220]. Conversion of proMMP-3 to its active form (cMMP-3) can occur through cleavage by a variety of extracellular serine protease systems including that for plasmin/plasminogen [221]. Tissue type plasminogen is induced *in vivo* in spinal astrocytes after injury and blockade is associated with a loss of hyperalgesia [222]. Future investigation of the upstream regulatory mechanisms for MMP-3 cleavage during acute peripheral inflammation would be of great scientific and pharmacologic development interest.

Endogenous spinal cMMP-3 mediates inflammation evoked hyperalgesia.

Intrathecal delivery of a broad spectrum and two MMP-3 preferring inhibitors resulted in a robust attenuation in the onset of the tactile and thermal hypersensitivity otherwise observed following peripheral inflammation. While reports indicate that

GM6001 has off target effects including inactivation of TACE [223], which would itself lead to decreased TNF, the parallel results associated with NNGH and PY-2, structurally diverse antagonists provides strong evidence for MMP-3 selectivity in this series of experiments. Previous work has shown that NNGH shows little inhibition of TACE but does have modest inhibitory effects against MMP-12 [224] and MMP-10 [225]. PY-2 is a semi-selective inhibitor that also inhibits MMP-8 and -12, but has little efficacy against MMP-1, 2, 7, 9, and 13 [210]. *In vitro* PY-2 has greater specificity against MMP-3 (0.13μM NNGH vs. 0.077μM PY-2 Ki) [210] with no inhibitory effects against TACE. The block of the thermal and tactile hyperalgesia afforded by an IT pretreatment with both MMP-3 inhibitors corroborates that the change in hypersensitivity is specific to MMP-3 inhibition. As these agents are believed to exert their actions by binding at the active enzymatic site [226-228], their actions thus provides further confirmation that it is the catalytically active form which is responsible for the observed effects of both endogenous and exogenous MMP-3.

Extracellular cMMP-3 in the dorsal horn initiates a facilitatory state though the release of TNF.

In the spinal cord, the IT delivery of cMMP-3 resulted in a prominent increase in spinal TNF concentrations, the time course of which paralleled the temporal profile of the pain-like behavior observed with the same doses of IT cMMP-3. The functional significance of this increase is evidenced by the block of the IT cMMP-3 evoked hyperalgesia by the spinal pretreatment of etanercept (a TNF sequestering protein).

These observations are consistent with previous reports that intrathecal TNF evokes a significant hyperalgesic state mediated by TNF receptor 1 (TNFR1) [229], [230], [231]. Activation of these spinal TNF receptors will activate kinases which, though phosphorylation of voltage sensitive channels [232], NMDA ionophores [233] and AMPA trafficking to the neuronal membrane [234] will lead to an enhanced excitability of dorsal horn neurons believed to underlie the hyperalgesic and allodynic states [235]. These results emphasize the likely role of downstream TNF release in mediating the cascade initiated by both exogenous and endogenous spinal cMMP-3. Moreover, these early effects upon spinal TNF concentrations were inhibited by MMP-3 antagonists at spinal doses which were shown to prevent the ITcMMP-3 induced hyperalgesia.

Non-Neuronal Cells

Spinal immunohistochemistry demonstrates the presence of MMP-3 immunoreactivity in both astrocytes and microglia in accordance with previous reports [95, 214, 215]. Manipulation of spinal microglial and astrocyte function will influence development and maintenance of acute and chronic pain conditions [236], [153], [237]. To further consider this mechanism, we undertook work with primary spinal cell cultures to determine the effects of cMMP-3 on these subpopulations. The primary spinal cell culture work provided two unexpected observations. The first was that cMMP-3 served to release TNF from microglia, but not astrocytes. Consistent with the *in vivo* work, this release was produced by the catalytic form and was blocked by

cMMP-3 inhibitors previously shown to be active *in vivo*. Secondly, the cMMP-3 effects in microglia were evident only after four hours, a finding in contrast to the robust and early onset in increased spinal TNF observed after IT cMMP-3 *in vivo*. These two results stand in contrast to the parallel observations that the TLR4 agonist LPS resulted in an immediate increase in TNF release from both astrocytes and microglia indicating that these actions of the cMMP-3 were peculiar to this exogenous agent and not the culture system. Our unexpected results show that cMMP-3 has a distinct effect upon microglia vs astrocytes and suggests that, while both astrocytes and microglia express MMP-3 and both are capable of releasing TNF, the two cell types have a distinct response to exogenous cMMP-3. These results raise the speculative hypothesis that cMMP-3 exerts its actions in a cell specific regulated manner. It further suggests that the net effects of the exogenous agent are not the result of a simple cleavage of TNF from the cell membrane, in accordance with previous biochemical data [238]. The observed delay in release within the cell culture system further reflects upon the distinction between understanding drug action where there is a homogenous cell type vs the intact organ system where complex interactions invariably occur.

Concluding Overview

These results indicate the constitutive presence of MMP-3 and a functional role of exogenous cMMP-3 and endogenous cMMP-3 in initiating a facilitated state of nociceptive processing in the spinal cord. Our novel observations regarding cMMP-3-

induced TNF release in the spinal lumbar region, prompts the hypothesis that cMMP-3 could be released and serve in a paracrine capacity in the activation of non-neuronal cells and may function in a capacity to initiate and sustain a facilitated pain state similar to other enzyme agonists including secretory PLA2 [239] or proteases acting though the proteinase activated receptors (PARs) [240], [241] to regulate at the spinal level the response following tissue injury and inflammation. Alternatively, cMMP-3 may directly cleave TNF in a manner similar to TACE, though this mechanism would suggest that cMMP-3 would have an effect in all TNF-expressing cell systems which is not supported by the astrocyte cell culture data. While the specific target for the enzymatic activity of cMMP-3 remains to be elucidated, this novel role for cMMP-3 as a factor in the initiation of pro-inflammatory cytokine release and in the facilitatory cascades in the dorsal horn relevant to spinal pain processing are clearly delineated by these present studies.

4.5 Acknowledgements

Chapter 4, in full, has been submitted for publication to appear in *Neuroscience* as " Spinal matrix metalloproteinase 3 mediates inflammatory hyperalgesia via a TNF dependent mechanism" by by Christianson CA, Fitzsimmons BF, Shim JH, Agrawal A, Cohen S, Hua XY, Yaksh TL. The dissertation author was the primary investigator and author of this material.

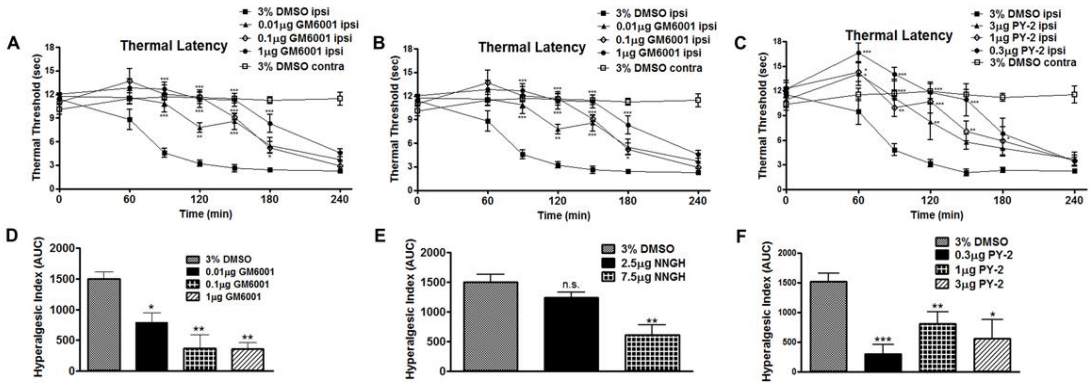

Figure 4.1 Spinal MMP inhibition delays onset of thermal hyperalgesia following peripheral inflammation in a dose dependent manner. A 30 minute IT pretreatment delayed thermal hyperalgesia onset compared to a 3% DMSO vehicle treatment for (A) 3 hours with GM6001 (1µg; $p<0.05$), which are graphed (D) according to the hyperalgesic index; for (B) 2.5 hours with NNGH (7.5µg; $p<0.05$) which are graphed (E) according to the hyperalgesic index; and for (C) 2 hours with PY-2 (1µg; $p<0.05$) which are graphed (F) according to the hyperalgesic index. n=6 rats for all groups. (*= $p<0.05$, **= $p<0.01$, ***= $p<0.001$)

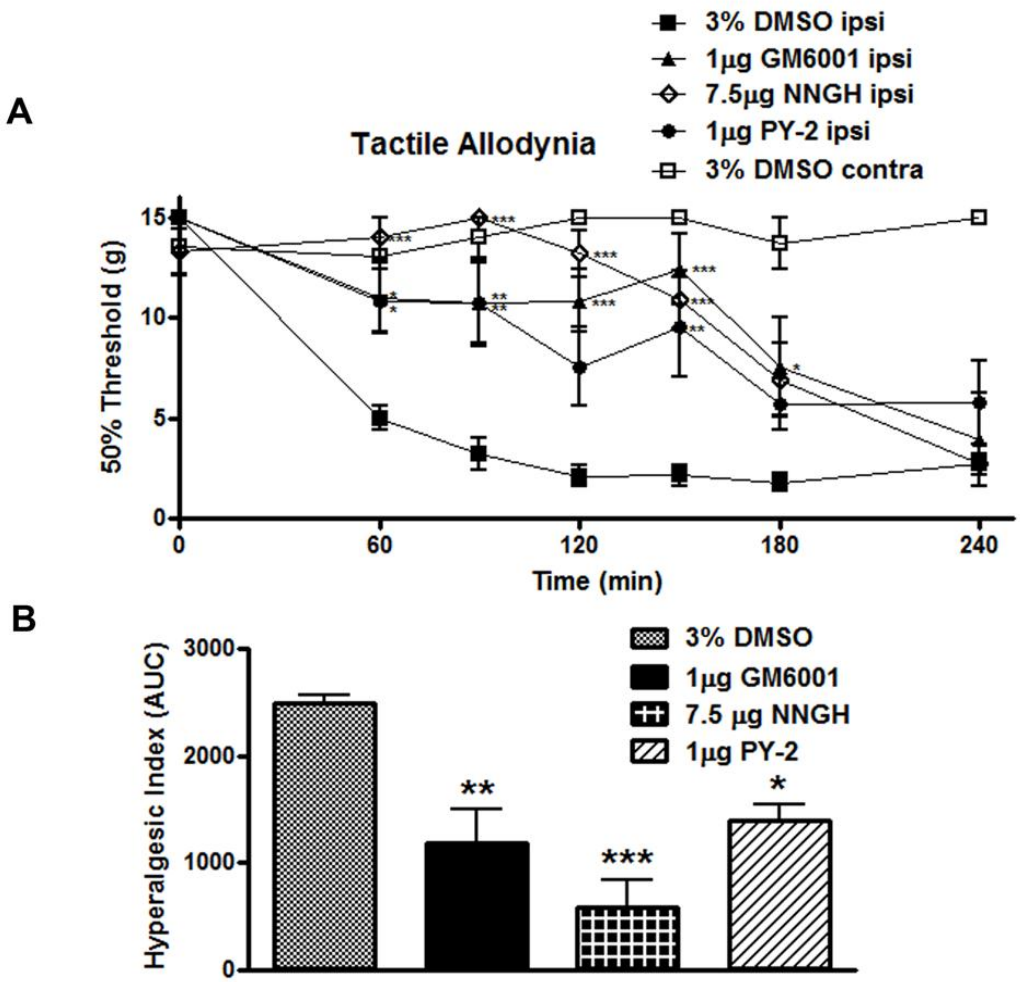

Figure 4.2 Spinal MMP inhibition delays onset of tactile allodynia following peripheral inflammation. (A) A 30 minute IT pretreatment with GM6001 (1µg), NNGH (7.5 µg), or PY-2 (1µg) significantly delayed the onset of tactile allodynia through 150 minutes ($p<0.05$) vs. 3% DMSO vehicle which is graphed (B) according to the hyperalgesic index. n=6 rats for all groups. (*= $p<0.05$, **= $p<0.01$, ***= $p<0.001$)

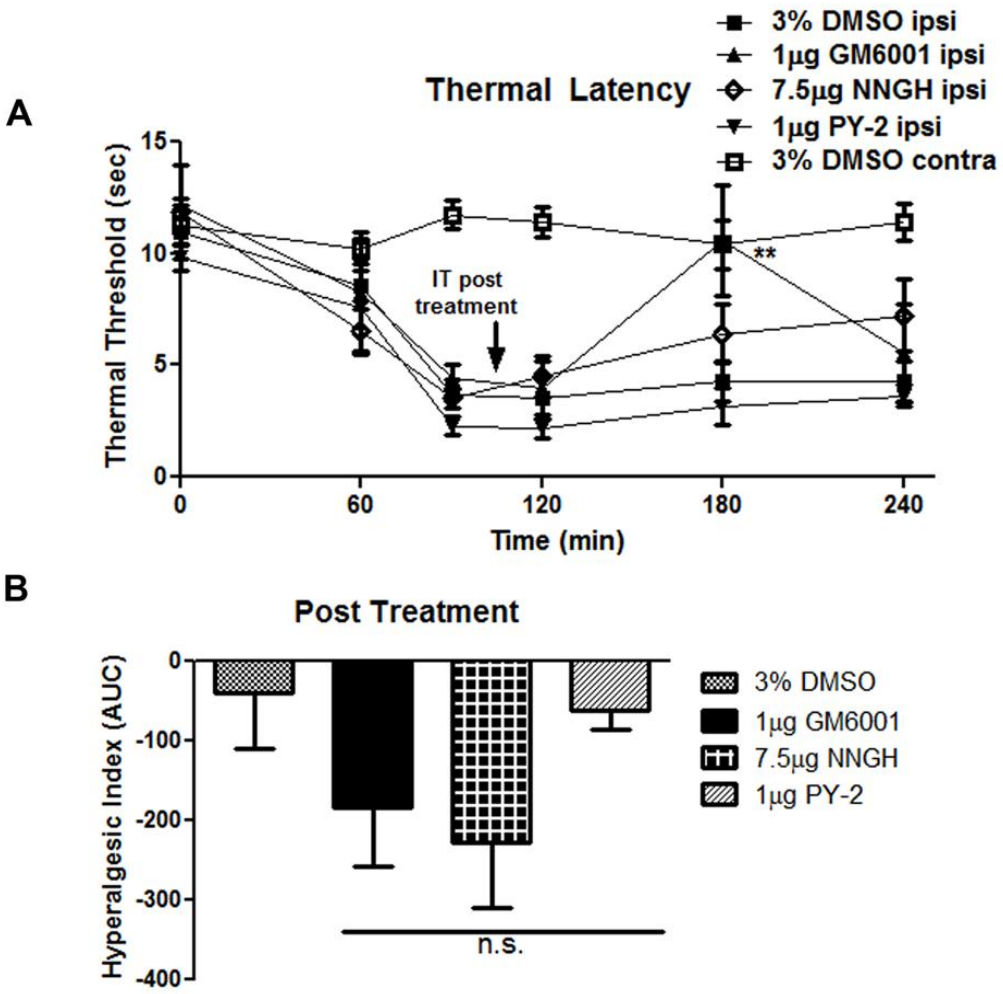

Figure 4.3 A post treatment with NNGH (7.5µg) or PY-2 (1µg) at 105min after carreengan administration had no significant effect upon thermal hyperalgesia. (A) A post treatment with GM6001 (1µg) increased thermal thresholds 180min after carrageenan injection ($p<0.01$). Graphed (B) according to the hyperalgesic index IT post-treatment of GM6001, NNGH, and PY-2 had no significant effect upon the hyperalgesic index on the inflamed paw. n=5-7 rats for all groups. (*= $p<0.05$, **= $p<0.01$).

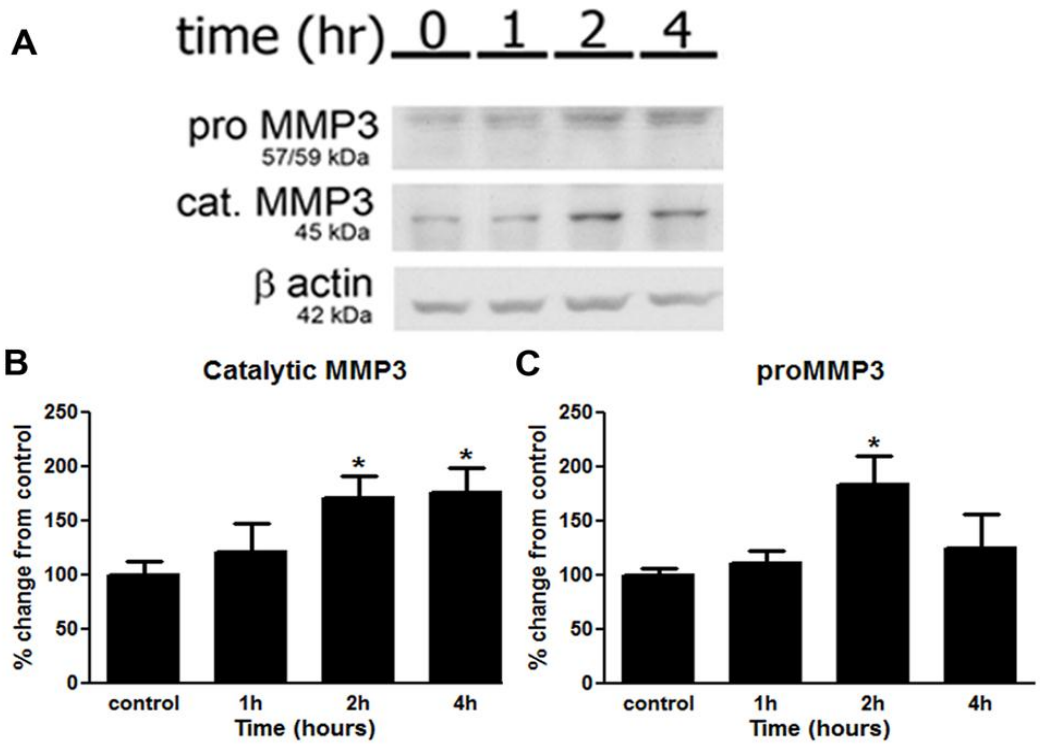

Figure 4.4 cMMP-3 increased in the lumbar spinal cord following peripheral inflammation. (A) The L4-L6 region of the spinal cord was blotted against MMP-3 following peripheral inflammation (B) cMMP-3 increased significantly in the spinal cord of rats 2 and 4 hours and (C) proMMP-3 increased significantly in the spinal cord of rats 2 hours following induction of peripheral inflammation as determined by densitometry ($p<0.05$) and normalized to β-actin. Densitometric results shown are the average of three independent experiments. *= $p<0.05$.

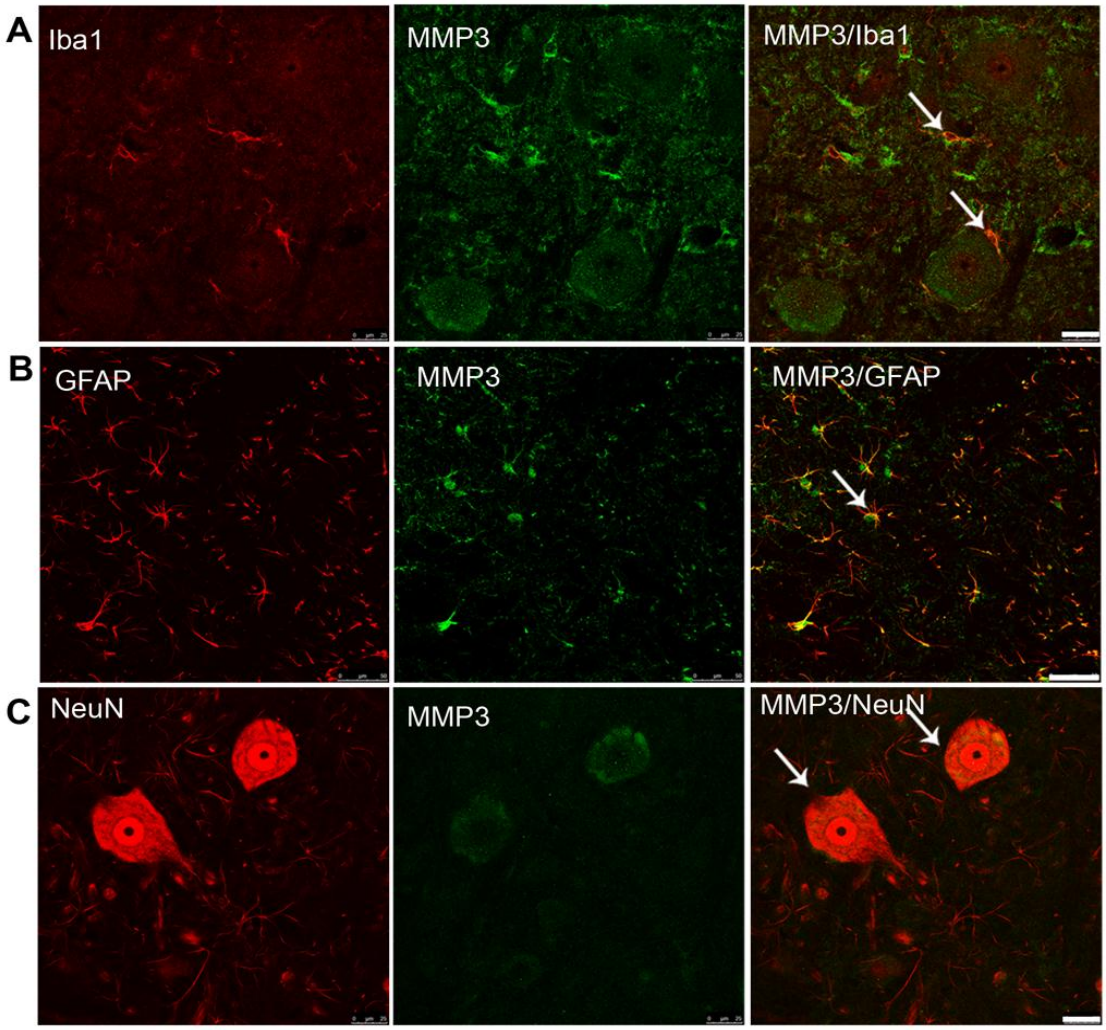

Figure 4.5 MMP-3 co-labeled with the markers for astrocytes, microglia, and neurons in the spinal cord. MMP-3 (green) co-stained in (A) with the astrocyte marker GFAP (red) and in (B) with the microglia marker Iba-1 (red) and in (C) with the neuronal marker NeuN (red) as shown in the merged images. All slides are representative slices from the L4-L6 lumbar section of the superficial dorsal horn in naïve rats. Scale bars are 25, 50 and 25 µm respectively.

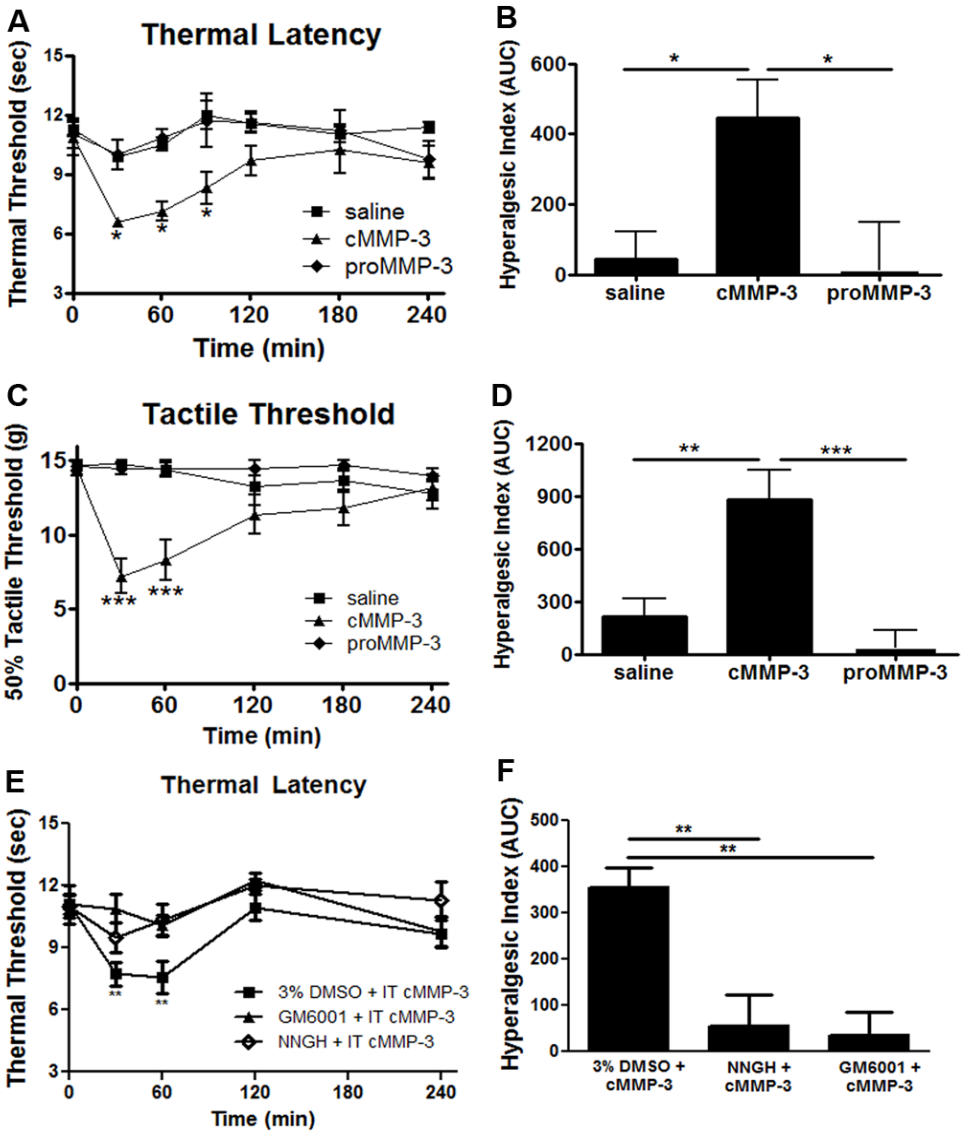

Figure 4.6 IT cMMP-3 reduced thermal and tactile thresholds. (A) IT cMMP-3 (1 pmol), but not proMMP-3 (1 pmol) induced thermal hyperalgesia 30, 60, and 90 minutes after delivery ($p<0.05$) vs. saline vehicle, which is graphed (B) according to the hyperalgesic index. (C) IT cMMP-3 (1 pmol), but not proMMP-3 (1 pmol) induced tactile allodynia 30 and 60 minutes after delivery ($p<0.05$) vs. saline vehicle which is graphed (D) according to the hyperalgesic index. (E) IT cMMP-3 induced thermal hyperalgesia is attenuated by IT GM6001 or NNGH pretreatment, which is graphed (F) according to the hyperalgesic index. n=4-8 rats. *= $p<0.05$, **= $p<0.01$, ***= $p<0.001$

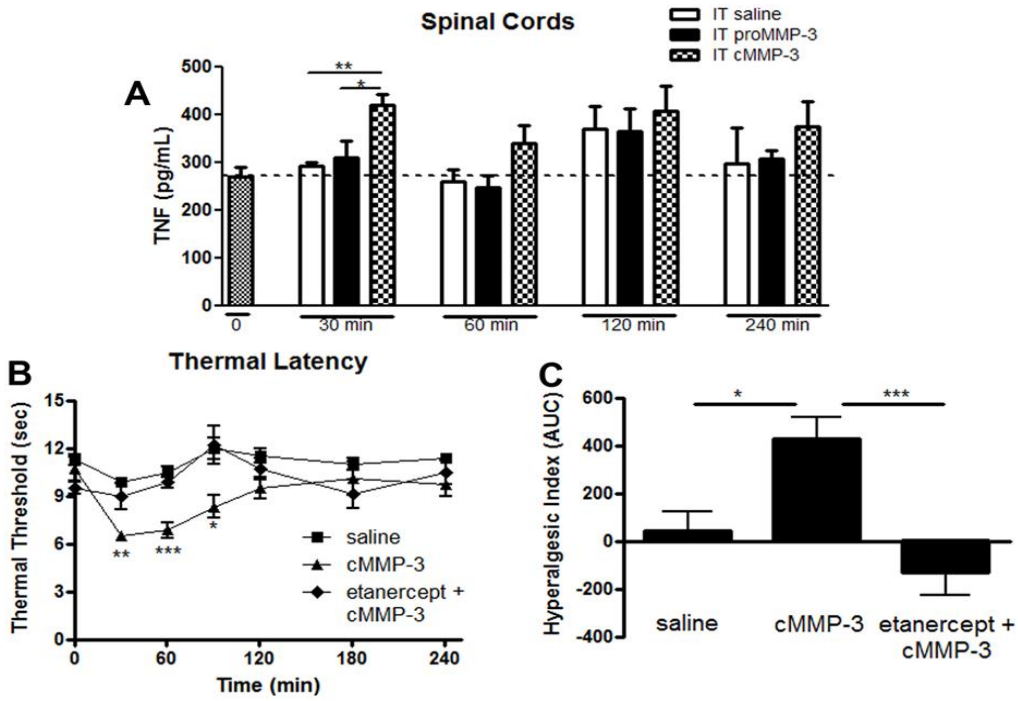

Figure 4.7 IT cMMP-3 reduced thermal and tactile thresholds is TNF dependent. (A) IT cMMP3 will significantly increase spinal TNF levels as compared to saline and proMMP-3 injections 30min but not 60min, 120min, or 240min after delivery. (B) A 60 minute IT pretreatment with a Etanercept (100μg) prevented IT cMMP-3 induced thermal hyperalgesia at 30, 60, and 90 minutes vs. control which is graphed (C) according to the hyperalgesic index. n=6 rats for all behavior groups. n=4 rats for TNF ELISA groups. *= $p<0.05$, **= $p<0.01$, ***= $p<0.001$

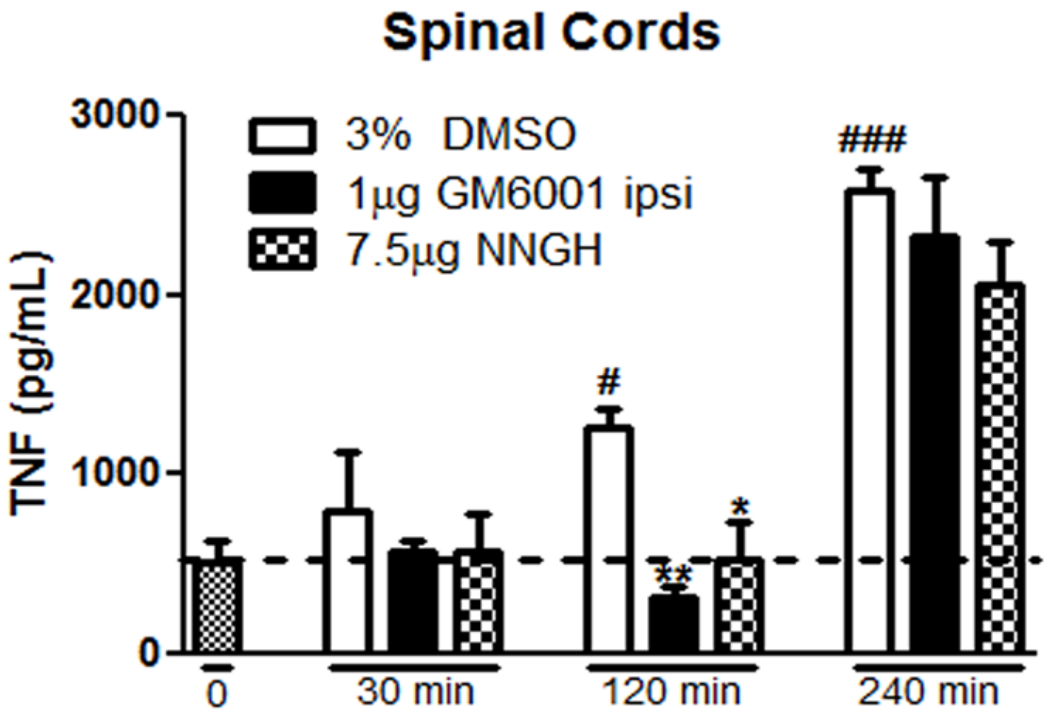

Figure 4.8 Peripheral inflammation increases spinal TNF levels which are reduced by 30 minute pre-treatment with MMP inhibitors. Carrageenan injection significantly increases TNF in the spinal cord 120 and 240 minutes after injection ($p<0.05$ vs t=0). This increase in TNF is blocked by IT pre-treatment with GM6001 (1µg; $p<0.01$) or NNGH (7.5µg; $p<0.05$) at 120 minutes but not 240 minutes after carrageenan. N=4 rats; *=$p<0.05$ vs 3% DMSO, **=$p<0.01$ vs 3%DMSO, #=$p<0.05$ vs t=0, ###=$p<0.001$ vs t=0.

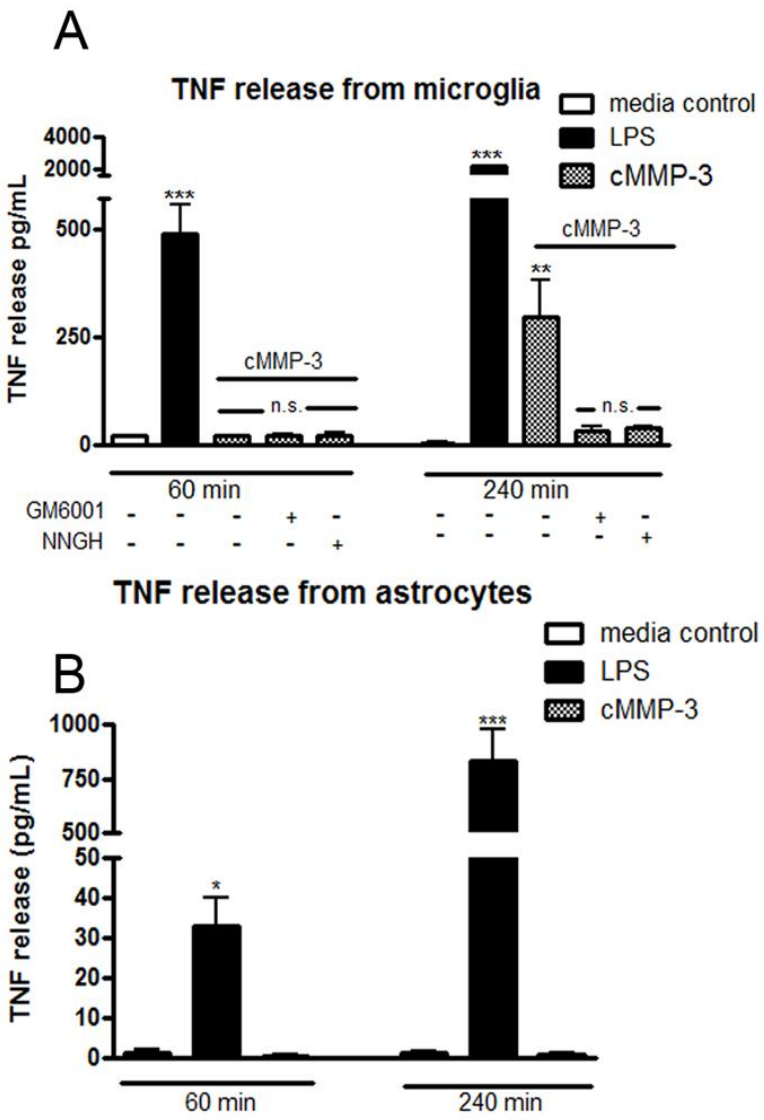

Figure 4.9 cMMP-3 induced TNF release from microglia but not astrocytes. (A) Primary spinal microglia were treated for 1 or 4 hours with cMMP-3 (400ng/mL) in both the presence and absence of either GM6001 (7.5µg/mL) or NNGH (7.5µg/mL). cMMP-3 induced significant TNF release at 4 hours ($p<0.01$) vs. media and was prevented by pretreatment with GM001 and NNGH. (B) Treatment of primary spinal astrocytes with cMMP-3 did not induce an increase in TNF release ($p>0.05$) at any time. LPS (10ng/mL), induced TNF released in microglia and astrocytes at all time points ($p<0.05$) vs. media control. Results are the average of 3-4 independent experiments.

Chapter 5

Concluding Overview

The contents of this thesis suggest two major concepts in understanding the transitions present during chronic inflammatory induced pain. One, a reduction in peripheral inflammation is not sufficient in this model of rheumatoid arthritis to reduce the persistent pain phenotype. Two, there is a complex interplay that is not fully elucidated nor realized between components of the innate immune system and elements of nociceptive processing.

We have characterized and demonstrated the utility in a new inflammatory pain model, which exhibits a persistent pain-like state despite the resolution of the obvious clinical signs of inflammation. This work is critical in shaping the basis for future experiments as it suggests there may be a disconnection between the peripheral inflammation and the pain state of the patient or animal. Further data supporting this concept includes the correlation between ATF-3 activation in K/BxN serum transfer arthritic mice during the post-inflammation (persistent pain) stage and the lack of ATF-3 activation in *Tlr4-/-* mice during the same time period. This suggests that the persistent pain stage contains elements characteristic of a neuropathic pain. Future work establishing the integrity of the peripheral nerves at the ankle joints during K/BxN serum transfer arthritis would be of great interest and could illuminate the consequences of a long-term(weeks vs hours/days) model of inflammation. A disruption in nerve integrity would indicate that diseases resulting in persistent inflammation should be considered for potential nerve damaging consequences. This

could better inform decisions about pharmacological development and chronic pain treatment during persistent pain resulting from chronic inflammation. If no disruption in nerve integrity were identified, it would be of equal interest as it would suggest the need to consider alternative mechanisms for the ATF-3 activation seen during K/BxN serum transfer arthritis. For example, high osteoclast activity during the formation of boney erosions could be releasing high acid levels and therefore sensitizing peripheral nerves without resulting damage.

The distinct ATF-3 activation in the DRG during the persistent pain state suggests the need to further investigate DRG specific mechanisms of persistent pain-like behavior in this model system. DRGs were collected in addition to spinal cords on day 6 and day 28 following K/BxN serum transfer arthritis and will be analyzed for changes in lipid mediators.

The utilization of the activation and resolution phases of the innate immune system during acute inflammation is well established. Here it is intriguing to speculate that chronic inflammation and persistent pain-like behavior may represent a dysregulation of this system. Future experiments focusing upon understanding contributions of other TLRs, downstream TLR mediators, the temporal profile of end product formation, and the regulation of neutrophil and macrophage chemotaxis would be of immense relevance. It is interesting to speculate if this TLR4 regulation of acute to chronic pain transitions is specific to particular TLRs, to MyD88 or TRIF mediated signaling, and if it is conserved between multiple animal models. This thesis suggests the presence of endogenous TLR mediators formed in the spinal cord during

peripheral inflammation which could be of great significance during disease progression.

In addition, the relevance of investigating a temporal profile when considering both the initiation and resolution of the peripheral clinical signs as well as the mechanism underlying the initiation and maintenance of a pain-like state is demonstrated in this thesis. To this end, we have begun to investigate some of these temporal TLR pathway questions utilizing WT, *Tlr4-/-*, *Tlr2-/-*, and *Tlr2/4-/-* mice. It would be interesting to correlate any significant changes identified between these pain-like phenotypically different genotypes and the eicosanoid and gene array products according to the cell types that produce them and assay both cords and DRGs for their influx. Given the apparent interplay between the innate immune cells and the generation of inflammation and the required clearance to avoid a persistent pain-like state this is likely to inform future pharmacological targets.

REFERENCES

1. Kehlet, H., T.S. Jensen, and C.J. Woolf, *Persistent postsurgical pain: risk factors and prevention.* Lancet, 2006. **367**(9522): p. 1618-25.

2. Katz, J. and Z. Seltzer, *Transition from acute to chronic postsurgical pain: risk factors and protective factors.* Expert Rev Neurother, 2009. **9**(5): p. 723-44.

3. Burke, S. and G.D. Shorten, *When pain after surgery doesn't go away.* Biochem Soc Trans, 2009. **37**(Pt 1): p. 318-22.

4. Voscopoulos, C. and M. Lema, *When does acute pain become chronic?* Br J Anaesth. **105 Suppl 1**: p. i69-85.

5. Sokka, T., et al., *QUEST-RA: quantitative clinical assessment of patients with rheumatoid arthritis seen in standard rheumatology care in 15 countries.* Ann Rheum Dis, 2007. **66**(11): p. 1491-6.

6. Strand, V. and D. Khanna, *The impact of rheumatoid arthritis and treatment on patients' lives.* Clin Exp Rheumatol. **28**(3 Suppl 59): p. S32-40.

7. Schaible, H.G., et al., *The role of proinflammatory cytokines in the generation and maintenance of joint pain.* Ann N Y Acad Sci. **1193**: p. 60-9.

8. Taylor, P.C., *The importance of the patients' experience of RA compared with clinical measures of disease activity.* Clin Exp Rheumatol. **28**(3 Suppl 59): p. S28-31.

9. Williams, R.O., *Models of rheumatoid arthritis.* Ernst Schering Res Found Workshop, 2005(50): p. 89-117.

10. Inglis, J.J., et al., *Collagen-induced arthritis as a model of hyperalgesia: functional and cellular analysis of the analgesic actions of tumor necrosis factor blockade.* Arthritis Rheum, 2007. **56**(12): p. 4015-23.

11. Inglis, J.J., et al., *Protocol for the induction of arthritis in C57BL/6 mice.* Nat Protoc, 2008. **3**(4): p. 612-8.

12. Courtenay, J.S., et al., *Immunisation against heterologous type II collagen induces arthritis in mice.* Nature, 1980. **283**(5748): p. 666-8.

13. Allen, J.W. and T.L. Yaksh, *Tissue injury models of persistent nociception in rats.* Methods Mol Med, 2004. **99**: p. 25-34.

14. Kouskoff, V., et al., *Organ-specific disease provoked by systemic autoimmunity.* Cell, 1996. **87**(5): p. 811-22.

15. Matsumoto, I., et al., *Arthritis provoked by linked T and B cell recognition of a glycolytic enzyme.* Science, 1999. **286**(5445): p. 1732-5.

16. Dirig, D.M. and T.L. Yaksh, *Differential right shifts in the dose-response curve for intrathecal morphine and sufentanil as a function of stimulus intensity.* Pain, 1995. **62**(3): p. 321-8.

17. Chaplan, S.R., et al., *Quantitative assessment of tactile allodynia in the rat paw.* J Neurosci Methods, 1994. **53**(1): p. 55-63.

18. Scholz, J. and C.J. Woolf, *Can we conquer pain?* Nat Neurosci, 2002. **5 Suppl**: p. 1062-7.

19. Torebjork, E., *Nociceptor activation and pain.* Philos Trans R Soc Lond B Biol Sci, 1985. **308**(1136): p. 227-34.

20. Gracely, R.H., *Pain measurement.* Acta Anaesthesiol Scand, 1999. **43**(9): p. 897-908.

21. LaMotte, R.H., et al., *Neurogenic hyperalgesia: psychophysical studies of underlying mechanisms.* J Neurophysiol, 1991. **66**(1): p. 190-211.

22. Matsumoto, M., et al., *Pharmacological switch in Abeta-fiber stimulation-induced spinal transmission in mice with partial sciatic nerve injury.* Mol Pain, 2008. **4**: p. 25.

23. Sandkuhler, J., *Understanding LTP in pain pathways.* Mol Pain, 2007. **3**: p. 9.

24. Herrero, J.F., J.M. Laird, and J.A. Lopez-Garcia, *Wind-up of spinal cord neurones and pain sensation: much ado about something?* Prog Neurobiol, 2000. **61**(2): p. 169-203.

25. Cervero, F., *Spinal cord hyperexcitability and its role in pain and hyperalgesia.* Exp Brain Res, 2009. **196**(1): p. 129-37.

26. Latremoliere, A. and C.J. Woolf, *Central sensitization: a generator of pain hypersensitivity by central neural plasticity.* J Pain, 2009. **10**(9): p. 895-926.

27. Villanueva, L., D. Chitour, and D. Le Bars, *Involvement of the dorsolateral funiculus in the descending spinal projections responsible for diffuse noxious inhibitory controls in the rat.* J Neurophysiol, 1986. **56**(4): p. 1185-95.

28. McMahon, S.B. and M. Malcangio, *Current challenges in glia-pain biology.* Neuron, 2009. **64**(1): p. 46-54.

29. Tsuda, M., et al., *P2X4 receptors induced in spinal microglia gate tactile allodynia after nerve injury.* Nature, 2003. **424**(6950): p. 778-83.

30. Sweitzer, S.M., et al., *Acute peripheral inflammation induces moderate glial activation and spinal IL-1beta expression that correlates with pain behavior in the rat.* Brain Res, 1999. **829**(1-2): p. 209-21.

31. Schwei, M.J., et al., *Neurochemical and cellular reorganization of the spinal cord in a murine model of bone cancer pain.* J Neurosci, 1999. **19**(24): p. 10886-97.

32. Milligan, E.D., et al., *Systemic administration of CNI-1493, a p38 mitogen-activated protein kinase inhibitor, blocks intrathecal human immunodeficiency virus-1 gp120-induced enhanced pain states in rats.* J Pain, 2001. **2**(6): p. 326-33.

33. Coyle, D.E., *Partial peripheral nerve injury leads to activation of astroglia and microglia which parallels the development of allodynic behavior.* Glia, 1998. **23**(1): p. 75-83.

34. Garrison, C.J., et al., *Staining of glial fibrillary acidic protein (GFAP) in lumbar spinal cord increases following a sciatic nerve constriction injury.* Brain Res, 1991. **565**(1): p. 1-7.

35. Svensson, C.I. and E. Brodin, *Spinal astrocytes in pain processing: non-neuronal cells as therapeutic targets.* Mol Interv. **10**(1): p. 25-38.

36. Inoue, K. and M. Tsuda, *Microglia and neuropathic pain.* Glia, 2009. **57**(14): p. 1469-79.

37. Hua, X.Y., et al., *Intrathecal minocycline attenuates peripheral inflammation-induced hyperalgesia by inhibiting p38 MAPK in spinal microglia.* Eur J Neurosci, 2005. **22**(10): p. 2431-40.

38. Raghavendra, V., F. Tanga, and J.A. DeLeo, *Inhibition of microglial activation attenuates the development but not existing hypersensitivity in a rat model of neuropathy.* J Pharmacol Exp Ther, 2003. **306**(2): p. 624-30.

39. Guo, W., et al., *Glial-cytokine-neuronal interactions underlying the mechanisms of persistent pain.* J Neurosci, 2007. **27**(22): p. 6006-18.

40. Sweitzer, S.M., P. Schubert, and J.A. DeLeo, *Propentofylline, a glial modulating agent, exhibits antiallodynic properties in a rat model of neuropathic pain.* J Pharmacol Exp Ther, 2001. **297**(3): p. 1210-7.

41. Scholz, J. and C.J. Woolf, *The neuropathic pain triad: neurons, immune cells and glia.* Nat Neurosci, 2007. **10**(11): p. 1361-8.

42. McMahon, S.B., W.B. Cafferty, and F. Marchand, *Immune and glial cell factors as pain mediators and modulators.* Exp Neurol, 2005. **192**(2): p. 444-62.

43. Lucas, S.M., N.J. Rothwell, and R.M. Gibson, *The role of inflammation in CNS injury and disease.* Br J Pharmacol, 2006. **147 Suppl 1**: p. S232-40.

44. Twining, C.M., et al., *Activation of the spinal cord complement cascade might contribute to mechanical allodynia induced by three animal models of spinal sensitization.* J Pain, 2005. **6**(3): p. 174-83.

45. Ji, H., et al., *Genetic influences on the end-stage effector phase of arthritis.* J Exp Med, 2001. **194**(3): p. 321-30.

46. Nathan, C., *Points of control in inflammation.* Nature, 2002. **420**(6917): p. 846-52.

47. Lee, D.M., et al., *Mast cells: a cellular link between autoantibodies and inflammatory arthritis.* Science, 2002. **297**(5587): p. 1689-92.

48. Clatworthy, A.L., et al., *Role of peri-axonal inflammation in the development of thermal hyperalgesia and guarding behavior in a rat model of neuropathic pain.* Neurosci Lett, 1995. **184**(1): p. 5-8.

49. Kim, N.D., et al., *A unique requirement for the leukotriene B4 receptor BLT1 for neutrophil recruitment in inflammatory arthritis.* J Exp Med, 2006. **203**(4): p. 829-35.

50. Johnston, B., et al., *Chronic inflammation upregulates chemokine receptors and induces neutrophil migration to monocyte chemoattractant protein-1.* J Clin Invest, 1999. **103**(9): p. 1269-76.

51. Babior, B.M., J.T. Curnutte, and B.J. McMurrich, *The particulate superoxide-forming system from human neutrophils. Properties of the system and further evidence supporting its participation in the respiratory burst.* J Clin Invest, 1976. **58**(4): p. 989-96.

52. Segal, A.W., *How neutrophils kill microbes.* Annu Rev Immunol, 2005. **23**: p. 197-223.

53. Schafers, M., et al., *Increased sensitivity of injured and adjacent uninjured rat primary sensory neurons to exogenous tumor necrosis factor-alpha after spinal nerve ligation.* J Neurosci, 2003. **23**(7): p. 3028-38.

54. Inoue, A., et al., *Interleukin-1beta induces substance P release from primary afferent neurons through the cyclooxygenase-2 system.* J Neurochem, 1999. **73**(5): p. 2206-13.

55. Min, K.J., I. Jou, and E. Joe, *Plasminogen-induced IL-1beta and TNF-alpha production in microglia is regulated by reactive oxygen species.* Biochem Biophys Res Commun, 2003. **312**(4): p. 969-74.

56. Boumsell, L. and M.S. Meltzer, *Mouse mononuclear cell chemotaxis. I. Differential response of monocytes and macrophages.* J Immunol, 1975. **115**(6): p. 1746-8.

57. Austin, P.J. and G. Moalem-Taylor, *The neuro-immune balance in neuropathic pain: involvement of inflammatory immune cells, immune-like glial cells and cytokines.* J Neuroimmunol. **229**(1-2): p. 26-50.

58. Zhang, X. and D.M. Mosser, *Macrophage activation by endogenous danger signals.* J Pathol, 2008. **214**(2): p. 161-78.

59. Laskin, D.L., et al., *Macrophages and tissue injury: agents of defense or destruction?* Annu Rev Pharmacol Toxicol. **51**: p. 267-88.

60. Glaros, T., M. Larsen, and L. Li, *Macrophages and fibroblasts during inflammation, tissue damage and organ injury.* Front Biosci, 2009. **14**: p. 3988-93.

61. Porcheray, F., et al., *Macrophage activation switching: an asset for the resolution of inflammation.* Clin Exp Immunol, 2005. **142**(3): p. 481-9.

62. Stout, R.D. and J. Suttles, *Functional plasticity of macrophages: reversible adaptation to changing microenvironments.* J Leukoc Biol, 2004. **76**(3): p. 509-13.

63. Pfeffer, K., et al., *Mice deficient for the 55 kd tumor necrosis factor receptor are resistant to endotoxic shock, yet succumb to L. monocytogenes infection.* Cell, 1993. **73**(3): p. 457-67.

64. Serhan, C.N., *Lipoxins and aspirin-triggered 15-epi-lipoxin biosynthesis: an update and role in anti-inflammation and pro-resolution.* Prostaglandins Other Lipid Mediat, 2002. **68-69**: p. 433-55.

65. Cartmell, T., et al., *Endogenous interleukin-10 is required for the defervescence of fever evoked by local lipopolysaccharide-induced and Staphylococcus aureus-induced inflammation in rats.* J Physiol, 2003. **549**(Pt 2): p. 653-64.

66. Tracey, K.J., *The inflammatory reflex.* Nature, 2002. **420**(6917): p. 853-9.

67. Borovikova, L.V., et al., *Vagus nerve stimulation attenuates the systemic inflammatory response to endotoxin.* Nature, 2000. **405**(6785): p. 458-62.

68. Woiciechowsky, C., et al., *Sympathetic activation triggers systemic interleukin-10 release in immunodepression induced by brain injury.* Nat Med, 1998. **4**(7): p. 808-13.

69. Arita, M., et al., *Resolvin E1, an endogenous lipid mediator derived from omega-3 eicosapentaenoic acid, protects against 2,4,6-trinitrobenzene sulfonic acid-induced colitis.* Proc Natl Acad Sci U S A, 2005. **102**(21): p. 7671-6.

70. Hong, S., et al., *Novel docosatrienes and 17S-resolvins generated from docosahexaenoic acid in murine brain, human blood, and glial cells. Autacoids in anti-inflammation.* J Biol Chem, 2003. **278**(17): p. 14677-87.

71. Lima-Garcia, J., et al., *The precursor of resolvin D series and aspirin-triggered resolvin D1 display anti-hyperalgesic properties in adjuvant-induced arthritis in rats.* Br J Pharmacol.

72. Xu, Z.Z., et al., *Resolvins RvE1 and RvD1 attenuate inflammatory pain via central and peripheral actions.* Nat Med. **16**(5): p. 592-7, 1p following 597.

73. Mosmann, T.R. and S. Sad, *The expanding universe of T-cell subsets: Th1, Th2 and more.* Immunol Today, 1996. **17**(3): p. 138-46.

74. Carty, M. and A.G. Bowie, *Evaluating the role of Toll-like receptors in diseases of the central nervous system.* Biochem Pharmacol. **81**(7): p. 825-37.

75. Means, T.K., D.T. Golenbock, and M.J. Fenton, *Structure and function of Toll-like receptor proteins.* Life Sci, 2000. **68**(3): p. 241-58.

76. Kawai, T. and S. Akira, *The role of pattern-recognition receptors in innate immunity: update on Toll-like receptors.* Nat Immunol. **11**(5): p. 373-84.

77. O'Neill, L.A. and A.G. Bowie, *The family of five: TIR-domain-containing adaptors in Toll-like receptor signalling.* Nat Rev Immunol, 2007. **7**(5): p. 353-64.

78. Palsson-McDermott, E.M. and L.A. O'Neill, *Signal transduction by the lipopolysaccharide receptor, Toll-like receptor-4.* Immunology, 2004. **113**(2): p. 153-62.

79. Banerjee, A., et al., *Diverse Toll-like receptors utilize Tpl2 to activate extracellular signal-regulated kinase (ERK) in hemopoietic cells.* Proc Natl Acad Sci U S A, 2006. **103**(9): p. 3274-9.

80. Olson, J.K. and S.D. Miller, *Microglia initiate central nervous system innate and adaptive immune responses through multiple TLRs.* J Immunol, 2004. **173**(6): p. 3916-24.

81. Bowman, C.C., et al., *Cultured astrocytes express toll-like receptors for bacterial products.* Glia, 2003. **43**(3): p. 281-91.

82. Carpentier, P.A., et al., *Differential activation of astrocytes by innate and adaptive immune stimuli.* Glia, 2005. **49**(3): p. 360-74.

83. Tang, S.C., et al., *Pivotal role for neuronal Toll-like receptors in ischemic brain injury and functional deficits.* Proc Natl Acad Sci U S A, 2007. **104**(34): p. 13798-803.

84. Abdollahi-Roodsaz, S., et al., *Stimulation of TLR2 and TLR4 differentially skews the balance of T cells in a mouse model of arthritis.* J Clin Invest, 2008. **118**(1): p. 205-16.

85. Abdollahi-Roodsaz, S., et al., *Inhibition of Toll-like receptor 4 breaks the inflammatory loop in autoimmune destructive arthritis.* Arthritis Rheum, 2007. **56**(9): p. 2957-67.

86. Abdollahi-Roodsaz, S., et al., *Shift from toll-like receptor 2 (TLR-2) toward TLR-4 dependency in the erosive stage of chronic streptococcal cell wall arthritis coincident with TLR-4-mediated interleukin-17 production.* Arthritis Rheum, 2008. **58**(12): p. 3753-64.

87. Tanga, F.Y., N. Nutile-McMenemy, and J.A. DeLeo, *The CNS role of Toll-like receptor 4 in innate neuroimmunity and painful neuropathy.* Proc Natl Acad Sci U S A, 2005. **102**(16): p. 5856-61.

88. Hutchinson, M.R., et al., *Non-stereoselective reversal of neuropathic pain by naloxone and naltrexone: involvement of toll-like receptor 4 (TLR4).* Eur J Neurosci, 2008. **28**(1): p. 20-9.

89. Saito, O., et al., *Spinal glial TLR4-mediated nociception and production of prostaglandin E(2) and TNF.* Br J Pharmacol. **160**(7): p. 1754-64.

90. Lin, C.S., et al., *Chronic intrathecal infusion of minocycline prevents the development of spinal-nerve ligation-induced pain in rats.* Reg Anesth Pain Med, 2007. **32**(3): p. 209-16.

91. Vidal, A., et al., *Synthesis and in vitro evaluation of targeted tetracycline derivatives: effects on inhibition of matrix metalloproteinases.* Bioorg Med Chem, 2007. **15**(6): p. 2368-74.

92. Yong, V.W., et al., *Metalloproteinases in biology and pathology of the nervous system.* Nat Rev Neurosci, 2001. **2**(7): p. 502-11.

93. Fu, X., W.C. Parks, and J.W. Heinecke, *Activation and silencing of matrix metalloproteinases.* Semin Cell Dev Biol, 2008. **19**(1): p. 2-13.

94. Ogbureke, K.U. and L.W. Fisher, *Renal expression of SIBLING proteins and their partner matrix metalloproteinases (MMPs).* Kidney Int, 2005. **68**(1): p. 155-66.

95. Nuttall, R.K., et al., *Metalloproteinases are enriched in microglia compared with leukocytes and they regulate cytokine levels in activated microglia.* Glia, 2007. **55**(5): p. 516-26.

96. Kim, Y.S., et al., *Matrix metalloproteinase-3: a novel signaling proteinase from apoptotic neuronal cells that activates microglia.* J Neurosci, 2005. **25**(14): p. 3701-11.

97. Vempati, P., E.D. Karagiannis, and A.S. Popel, *A biochemical model of matrix metalloproteinase 9 activation and inhibition.* J Biol Chem, 2007. **282**(52): p. 37585-96.

98. Ogata, Y., J.J. Enghild, and H. Nagase, *Matrix metalloproteinase 3 (stromelysin) activates the precursor for the human matrix metalloproteinase 9.* J Biol Chem, 1992. **267**(6): p. 3581-4.

99. Kawasaki, Y., et al., *Distinct roles of matrix metalloproteases in the early- and late-phase development of neuropathic pain.* Nat Med, 2008. **14**(3): p. 331-6.

100. Overall, C.M., *Molecular determinants of metalloproteinase substrate specificity: matrix metalloproteinase substrate binding domains, modules, and exosites.* Mol Biotechnol, 2002. **22**(1): p. 51-86.

101. Pezet, S., M. Malcangio, and S.B. McMahon, *BDNF: a neuromodulator in nociceptive pathways?* Brain Res Brain Res Rev, 2002. **40**(1-3): p. 240-9.

102. Monach, P.A., D. Mathis, and C. Benoist, *The K/BxN arthritis model.* Curr Protoc Immunol, 2008. **Chapter 15**: p. Unit 15 22.

103. Schaible, H.G., et al., *Joint pain.* Exp Brain Res, 2009. **196**(1): p. 153-62.

104. Leffler, A.S., et al., *Somatosensory perception and function of diffuse noxious inhibitory controls (DNIC) in patients suffering from rheumatoid arthritis.* Eur J Pain, 2002. **6**(2): p. 161-76.

105. Kidd, B.L., A. Photiou, and J.J. Inglis, *The role of inflammatory mediators on nociception and pain in arthritis.* Novartis Found Symp, 2004. **260**: p. 122-33; discussion 133-8, 277-9.

106. Tsujino, H., et al., *Activating transcription factor 3 (ATF3) induction by axotomy in sensory and motoneurons: A novel neuronal marker of nerve injury.* Mol Cell Neurosci, 2000. **15**(2): p. 170-82.

107. Calza, L., et al., *Long-lasting regulation of galanin, opioid, and other peptides in dorsal root ganglia and spinal cord during experimental polyarthritis.* Exp Neurol, 2000. **164**(2): p. 333-43.

108. Jones, E., et al., *Neuropathic changes in equine laminitis pain.* Pain, 2007. **132**(3): p. 321-31.

109. Raghavendra, V., F.Y. Tanga, and J.A. DeLeo, *Complete Freunds adjuvant-induced peripheral inflammation evokes glial activation and proinflammatory cytokine expression in the CNS.* Eur J Neurosci, 2004. **20**(2): p. 467-73.

110. Watkins, L.R., et al., *Evidence for the involvement of spinal cord glia in subcutaneous formalin induced hyperalgesia in the rat.* Pain, 1997. **71**(3): p. 225-35.

111. Cao, H. and Y.Q. Zhang, *Spinal glial activation contributes to pathological pain states.* Neurosci Biobehav Rev, 2008. **32**(5): p. 972-83.

112. Choe, J.Y., et al., *Interleukin 1 receptor dependence of serum transferred arthritis can be circumvented by toll-like receptor 4 signaling.* J Exp Med, 2003. **197**(4): p. 537-42.

113. Tanabe, M., et al., *Gabapentin and pregabalin ameliorate mechanical hypersensitivity after spinal cord injury in mice.* Eur J Pharmacol, 2009. **609**(1-3): p. 65-8.

114. Eroglu, C., et al., *Gabapentin receptor alpha2delta-1 is a neuronal thrombospondin receptor responsible for excitatory CNS synaptogenesis.* Cell, 2009. **139**(2): p. 380-92.

115. Domer, F., *Characterization of the analgesic activity of ketorolac in mice.* Eur J Pharmacol, 1990. **177**(3): p. 127-35.

116. Dirig, D.M., et al., *Characterization of variables defining hindpaw withdrawal latency evoked by radiant thermal stimuli.* J Neurosci Methods, 1997. **76**(2): p. 183-91.

117. Pfaffl, M.W., *A new mathematical model for relative quantification in real-time RT-PCR.* Nucleic Acids Res, 2001. **29**(9): p. e45.

118. Zimmermann, M., *Pathobiology of neuropathic pain.* Eur J Pharmacol, 2001. **429**(1-3): p. 23-37.

119. Butler, S.H., et al., *A limited arthritic model for chronic pain studies in the rat.* Pain, 1992. **48**(1): p. 73-81.

120. Knight, B., et al., *Induction of adjuvant arthritis in mice.* Clin Exp Immunol, 1992. **90**(3): p. 459-65.

121. Gerecz-Simon, E.M., et al., *Measurement of pain threshold in patients with rheumatoid arthritis, osteoarthritis, ankylosing spondylitis, and healthy controls.* Clin Rheumatol, 1989. **8**(4): p. 467-74.

122. Dhondt, W., et al., *Pain threshold in patients with rheumatoid arthritis and effect of manual oscillations.* Scand J Rheumatol, 1999. **28**(2): p. 88-93.

123. Edwards, R.R., et al., *Enhanced reactivity to pain in patients with rheumatoid arthritis.* Arthritis Res Ther, 2009. **11**(3): p. R61.

124. Geranton, S.M., et al., *A rapamycin-sensitive signaling pathway is essential for the full expression of persistent pain states.* J Neurosci, 2009. **29**(47): p. 15017-27.

125. Li, M.M., et al., *Extracellular signal-regulated kinases mediate melittin-induced hypersensitivity of spinal neurons to chemical and thermal but not mechanical stimuli.* Brain Res Bull, 2008.

126. Nozaki-Taguchi, N. and T.L. Yaksh, *A novel model of primary and secondary hyperalgesia after mild thermal injury in the rat.* Neurosci Lett, 1998. **254**(1): p. 25-8.

127. Thompson, S.W., A. Dray, and L. Urban, *Leukemia inhibitory factor induces mechanical allodynia but not thermal hyperalgesia in the juvenile rat.* Neuroscience, 1996. **71**(4): p. 1091-4.

128. Takasu, K., et al., *Spinal alpha(2)-adrenergic and muscarinic receptors and the NO release cascade mediate supraspinally produced effectiveness of gabapentin at decreasing mechanical hypersensitivity in mice after partial nerve injury.* Br J Pharmacol, 2006. **148**(2): p. 233-44.

129. Malfait, A.M., et al., *ADAMTS-5 deficient mice do not develop mechanical allodynia associated with osteoarthritis following medial meniscal destabilization.* Osteoarthritis Cartilage. **18**(4): p. 572-80.

130. Hai, T., et al., *ATF3 and stress responses.* Gene Expr, 1999. **7**(4-6): p. 321-35.

131. Hamann, W., et al., *Pulsed radiofrequency applied to dorsal root ganglia causes a selective increase in ATF3 in small neurons.* Eur J Pain, 2006. **10**(2): p. 171-6.

132. Tsuzuki, K., et al., *Differential regulation of P2X(3) mRNA expression by peripheral nerve injury in intact and injured neurons in the rat sensory ganglia.* Pain, 2001. **91**(3): p. 351-60.

133. Ivanavicius, S.P., et al., *Structural pathology in a rodent model of osteoarthritis is associated with neuropathic pain: increased expression of ATF-3 and pharmacological characterisation.* Pain, 2007. **128**(3): p. 272-82.

134. Romero-Sandoval, A., et al., *A comparison of spinal Iba1 and GFAP expression in rodent models of acute and chronic pain.* Brain Res, 2008. **1219**: p. 116-26.

135. Wipke, B.T., et al., *Dynamic visualization of a joint-specific autoimmune response through positron emission tomography.* Nat Immunol, 2002. **3**(4): p. 366-72.

136. Chen, M., et al., *Predominance of cyclooxygenase 1 over cyclooxygenase 2 in the generation of proinflammatory prostaglandins in autoantibody-driven K/BxN serum-transfer arthritis.* Arthritis Rheum, 2008. **58**(5): p. 1354-65.

137. Ji, H., et al., *Critical roles for interleukin 1 and tumor necrosis factor alpha in antibody-induced arthritis.* J Exp Med, 2002. **196**(1): p. 77-85.

138. Rosner, H., L. Rubin, and A. Kestenbaum, *Gabapentin adjunctive therapy in neuropathic pain states.* Clin J Pain, 1996. **12**(1): p. 56-8.

139. Segal, A.Z. and G. Rordorf, *Gabapentin as a novel treatment for postherpetic neuralgia.* Neurology, 1996. **46**(4): p. 1175-6.

140. Fehrenbacher, J.C., C.P. Taylor, and M.R. Vasko, *Pregabalin and gabapentin reduce release of substance P and CGRP from rat spinal tissues only after inflammation or activation of protein kinase C.* Pain, 2003. **105**(1-2): p. 133-41.

141. Maneuf, Y.P., J. Hughes, and A.T. McKnight, *Gabapentin inhibits the substance P-facilitated K(+)-evoked release of [(3)H]glutamate from rat caudial trigeminal nucleus slices.* Pain, 2001. **93**(2): p. 191-6.

142. Lu, Y. and K.N. Westlund, *Gabapentin attenuates nociceptive behaviors in an acute arthritis model in rats.* J Pharmacol Exp Ther, 1999. **290**(1): p. 214-9.

143. Jin, X. and R.W.t. Gereau, *Acute p38-mediated modulation of tetrodotoxin-resistant sodium channels in mouse sensory neurons by tumor necrosis factor-alpha.* J Neurosci, 2006. **26**(1): p. 246-55.

144. Opree, A. and M. Kress, *Involvement of the proinflammatory cytokines tumor necrosis factor-alpha, IL-1 beta, and IL-6 but not IL-8 in the development of heat hyperalgesia: effects on heat-evoked calcitonin gene-related peptide release from rat skin.* J Neurosci, 2000. **20**(16): p. 6289-93.

145. Boettger, M.K., et al., *Antinociceptive effects of tumor necrosis factor alpha neutralization in a rat model of antigen-induced arthritis: evidence of a neuronal target.* Arthritis Rheum, 2008. **58**(8): p. 2368-78.

146. Radstake, T.R., et al., *Expression of toll-like receptors 2 and 4 in rheumatoid synovial tissue and regulation by proinflammatory cytokines interleukin-12 and interleukin-18 via interferon-gamma.* Arthritis Rheum, 2004. **50**(12): p. 3856-65.

147. Ospelt, C., et al., *Overexpression of toll-like receptors 3 and 4 in synovial tissue from patients with early rheumatoid arthritis: toll-like receptor expression in early and longstanding arthritis.* Arthritis Rheum, 2008. **58**(12): p. 3684-92.

148. Midwood, K., et al., *Tenascin-C is an endogenous activator of Toll-like receptor 4 that is essential for maintaining inflammation in arthritic joint disease.* Nat Med, 2009. **15**(7): p. 774-80.

149. Miyake, K., *Innate immune sensing of pathogens and danger signals by cell surface Toll-like receptors.* Semin Immunol, 2007. **19**(1): p. 3-10.

150. Laflamme, N. and S. Rivest, *Toll-like receptor 4: the missing link of the cerebral innate immune response triggered by circulating gram-negative bacterial cell wall components.* FASEB J, 2001. **15**(1): p. 155-163.

151. Wadachi, R. and K.M. Hargreaves, *Trigeminal nociceptors express TLR-4 and CD14: a mechanism for pain due to infection.* J Dent Res, 2006. **85**(1): p. 49-53.

152. Hansson, E. and L. Ronnback, *Glial neuronal signaling in the central nervous system.* FASEB J, 2003. **17**(3): p. 341-8.

153. Tsuda, M., K. Inoue, and M.W. Salter, *Neuropathic pain and spinal microglia: a big problem from molecules in "small" glia.* Trends Neurosci, 2005. **28**(2): p. 101-7.

154. Wu, H.E., et al., *dextro-Naloxone or levo-naloxone reverses the attenuation of morphine antinociception induced by lipopolysaccharide in the mouse spinal cord via a non-opioid mechanism.* Eur J Neurosci, 2006. **24**(9): p. 2575-80.

155. Materazzi, S., et al., *Cox-dependent fatty acid metabolites cause pain through activation of the irritant receptor TRPA1.* Proc Natl Acad Sci U S A, 2008. **105**(33): p. 12045-50.

156. Buczynski, M.W., et al., *Inflammatory hyperalgesia induces essential bioactive lipid production in the spinal cord.* J Neurochem. **114**(4): p. 981-93.

157. Hall, L.M. and R.C. Murphy, *Electrospray mass spectrometric analysis of 5-hydroperoxy and 5-hydroxyeicosatetraenoic acids generated by lipid peroxidation of red blood cell ghost phospholipids.* J Am Soc Mass Spectrom, 1998. **9**(5): p. 527-32.

158. Christianson, C.A., et al., *Characterization of the acute and persistent pain state present in K/BxN serum transfer arthritis.* Pain. **151**(2): p. 394-403.

159. DeLeo, J.A. and R.P. Yezierski, *The role of neuroinflammation and neuroimmune activation in persistent pain.* Pain, 2001. **90**(1-2): p. 1-6.

160. Poltorak, A., et al., *Defective LPS signaling in C3H/HeJ and C57BL/10ScCr mice: mutations in Tlr4 gene.* Science, 1998. **282**(5396): p. 2085-8.

161. Hutchinson, M.R., et al., *Evidence for a role of heat shock protein-90 in toll like receptor 4 mediated pain enhancement in rats.* Neuroscience, 2009. **164**(4): p. 1821-32.

162. Ji, R.R., et al., *Protein kinases as potential targets for the treatment of pathological pain.* Handb Exp Pharmacol, 2007(177): p. 359-89.

163. Ji, R.R., et al., *MAP kinase and pain.* Brain Res Rev, 2009. **60**(1): p. 135-48.

164. Cahill, C.M., A. Dray, and T.J. Coderre, *Enhanced thermal antinociceptive potency and anti-allodynic effects of morphine following spinal administration of endotoxin.* Brain Res, 2003. **960**(1-2): p. 209-18.

165. Jack, C.S., et al., *TLR signaling tailors innate immune responses in human microglia and astrocytes.* J Immunol, 2005. **175**(7): p. 4320-30.

166. Bsibsi, M., et al., *Broad expression of Toll-like receptors in the human central nervous system.* J Neuropathol Exp Neurol, 2002. **61**(11): p. 1013-21.

167. Rossignol, D.P. and M. Lynn, *TLR4 antagonists for endotoxemia and beyond.* Curr Opin Investig Drugs, 2005. **6**(5): p. 496-502.

168. Cristofaro, P. and S.M. Opal, *Role of Toll-like receptors in infection and immunity: clinical implications.* Drugs, 2006. **66**(1): p. 15-29.

169. Mollen, K.P., et al., *Emerging paradigm: toll-like receptor 4-sentinel for the detection of tissue damage.* Shock, 2006. **26**(5): p. 430-7.

170. Zhang, Y.P., et al., *Glial NF-kappa B inhibition alters neuropeptide expression after sciatic nerve injury in mice.* Brain Res. **1385**: p. 38-46.

171. Luo, P., et al., *Anti-inflammatory and analgesic effect of plumbagin through inhibition of nuclear factor-kappaB activation.* J Pharmacol Exp Ther. **335**(3): p. 735-42.

172. Fu, E.S., et al., *Transgenic inhibition of glial NF-kappa B reduces pain behavior and inflammation after peripheral nerve injury.* Pain. **148**(3): p. 509-18.

173. Ohashi, K., et al., *Cutting edge: heat shock protein 60 is a putative endogenous ligand of the toll-like receptor-4 complex.* J Immunol, 2000. **164**(2): p. 558-61.

174. Wang, Y., et al., *Stimulation of Th1-polarizing cytokines, C-C chemokines, maturation of dendritic cells, and adjuvant function by the peptide binding fragment of heat shock protein 70.* J Immunol, 2002. **169**(5): p. 2422-9.

175. Peetermans, W.E., et al., *Mycobacterial heat-shock protein 65 induces proinflammatory cytokines but does not activate human mononuclear phagocytes.* Scand J Immunol, 1994. **39**(6): p. 613-7.

176. Smiley, S.T., J.A. King, and W.W. Hancock, *Fibrinogen stimulates macrophage chemokine secretion through toll-like receptor 4.* J Immunol, 2001. **167**(5): p. 2887-94.

177. Saito, S., et al., *The fibronectin extra domain A activates matrix metalloproteinase gene expression by an interleukin-1-dependent mechanism.* J Biol Chem, 1999. **274**(43): p. 30756-63.

178. Okamura, Y., et al., *The extra domain A of fibronectin activates Toll-like receptor 4.* J Biol Chem, 2001. **276**(13): p. 10229-33.

179. Termeer, C., et al., *Oligosaccharides of Hyaluronan activate dendritic cells via toll-like receptor 4.* J Exp Med, 2002. **195**(1): p. 99-111.

180. Park, J.S., et al., *Involvement of toll-like receptors 2 and 4 in cellular activation by high mobility group box 1 protein.* J Biol Chem, 2004. **279**(9): p. 7370-7.

181. Yang, L.C., M. Marsala, and T.L. Yaksh, *Characterization of time course of spinal amino acids, citrulline and PGE2 release after carrageenan/kaolin-induced knee joint inflammation: a chronic microdialysis study.* Pain, 1996. **67**(2-3): p. 345-54.

182. Shi, L., et al., *Peripheral inflammation modifies the effect of intrathecal IL-1beta on spinal PGE2 production mainly through cyclooxygenase-2 activity. A spinal microdialysis study in freely moving rats.* Pain, 2006. **120**(3): p. 307-14.

183. Svensson, C.I., et al., *Spinal p38 MAP kinase is necessary for NMDA-induced spinal PGE(2) release and thermal hyperalgesia.* Neuroreport, 2003. **14**(8): p. 1153-7.

184. Blaho, V.A., et al., *Lipidomic analysis of dynamic eicosanoid responses during the induction and resolution of Lyme arthritis.* J Biol Chem, 2009. **284**(32): p. 21599-612.

185. Churi, S.B., et al., *Intrathecal rosiglitazone acts at peroxisome proliferator-activated receptor-gamma to rapidly inhibit neuropathic pain in rats.* J Pain, 2008. **9**(7): p. 639-49.

186. Forman, B.M., et al., *15-Deoxy-delta 12, 14-prostaglandin J2 is a ligand for the adipocyte determination factor PPAR gamma.* Cell, 1995. **83**(5): p. 803-12.

187. Kliewer, S.A., et al., *A prostaglandin J2 metabolite binds peroxisome proliferator-activated receptor gamma and promotes adipocyte differentiation.* Cell, 1995. **83**(5): p. 813-9.

188. Moreno, S., S. Farioli-Vecchioli, and M.P. Ceru, *Immunolocalization of peroxisome proliferator-activated receptors and retinoid X receptors in the adult rat CNS.* Neuroscience, 2004. **123**(1): p. 131-45.

189. Kawahito, Y., et al., *15-deoxy-delta(12,14)-PGJ(2) induces synoviocyte apoptosis and suppresses adjuvant-induced arthritis in rats.* J Clin Invest, 2000. **106**(2): p. 189-97.

190. Shiojiri, T., et al., *PPAR gamma ligands inhibit nitrotyrosine formation and inflammatory mediator expressions in adjuvant-induced rheumatoid arthritis mice.* Eur J Pharmacol, 2002. **448**(2-3): p. 231-8.

191. Ricote, M., et al., *The peroxisome proliferator-activated receptor(PPARgamma) as a regulator of monocyte/macrophage function.* J Leukoc Biol, 1999. **66**(5): p. 733-9.

192. Jiang, C., A.T. Ting, and B. Seed, *PPAR-gamma agonists inhibit production of monocyte inflammatory cytokines.* Nature, 1998. **391**(6662): p. 82-6.

193. Lawrence, T., D.A. Willoughby, and D.W. Gilroy, *Anti-inflammatory lipid mediators and insights into the resolution of inflammation.* Nat Rev Immunol, 2002. **2**(10): p. 787-95.

194. Soares, A.F., et al., *Covalent binding of 15-deoxy-delta12,14-prostaglandin J2 to PPARgamma.* Biochem Biophys Res Commun, 2005. **337**(2): p. 521-5.

195. Ganea, E., et al., *Matrix metalloproteinases: useful and deleterious.* Biochem Soc Trans, 2007. **35**(Pt 4): p. 689-91.

196. Agrawal, S.M., L. Lau, and V.W. Yong, *MMPs in the central nervous system: where the good guys go bad.* Semin Cell Dev Biol, 2008. **19**(1): p. 42-51.

197. Gijbels, K., et al., *Gelatinase B is present in the cerebrospinal fluid during experimental autoimmune encephalomyelitis and cleaves myelin basic protein.* J Neurosci Res, 1993. **36**(4): p. 432-40.

198. Noble, L.J., et al., *Matrix metalloproteinases limit functional recovery after spinal cord injury by modulation of early vascular events.* J Neurosci, 2002. **22**(17): p. 7526-35.

199. Rosenberg, G.A., et al., *Proteolytic cascade enzymes increase in focal cerebral ischemia in rat.* J Cereb Blood Flow Metab, 1996. **16**(3): p. 360-6.

200. Shubayev, V.I. and R.R. Myers, *Upregulation and interaction of TNFalpha and gelatinases A and B in painful peripheral nerve injury.* Brain Res, 2000. **855**(1): p. 83-9.

201. Clements, J.M., et al., *Matrix metalloproteinase expression during experimental autoimmune encephalomyelitis and effects of a combined matrix metalloproteinase and tumour necrosis factor-alpha inhibitor.* J Neuroimmunol, 1997. **74**(1-2): p. 85-94.

202. Shubayev, V.I. and R.R. Myers, *Matrix metalloproteinase-9 promotes nerve growth factor-induced neurite elongation but not new sprout formation in vitro.* J Neurosci Res, 2004. **77**(2): p. 229-39.

203. Lee, R., et al., *Regulation of cell survival by secreted proneurotrophins.* Science, 2001. **294**(5548): p. 1945-8.

204. Agnihotri, R., et al., *Osteopontin, a novel substrate for matrix metalloproteinase-3 (stromelysin-1) and matrix metalloproteinase-7 (matrilysin).* J Biol Chem, 2001. **276**(30): p. 28261-7.

205. Schonbeck, U., F. Mach, and P. Libby, *Generation of biologically active IL-1 beta by matrix metalloproteinases: a novel caspase-1-independent pathway of IL-1 beta processing.* J Immunol, 1998. **161**(7): p. 3340-6.

206. Cauwe, B., P.E. Van den Steen, and G. Opdenakker, *The biochemical, biological, and pathological kaleidoscope of cell surface substrates processed by matrix metalloproteinases.* Crit Rev Biochem Mol Biol, 2007. **42**(3): p. 113-85.

207. Milligan, E.D. and L.R. Watkins, *Pathological and protective roles of glia in chronic pain.* Nat Rev Neurosci, 2009. **10**(1): p. 23-36.

208. Duivenvoorden, W.C., H.W. Hirte, and G. Singh, *Use of tetracycline as an inhibitor of matrix metalloproteinase activity secreted by human bone-metastasizing cancer cells.* Invasion Metastasis, 1997. **17**(6): p. 312-22.

209. Malkmus, S.A. and T.L. Yaksh, *Intrathecal catheterization and drug delivery in the rat.* Methods Mol Med, 2004. **99**: p. 109-21.

210. Agrawal, A., et al., *Zinc-binding groups modulate selective inhibition of MMPs.* ChemMedChem, 2008. **3**(5): p. 812-20.

211. Junger, H. and L.S. Sorkin, *Nociceptive and inflammatory effects of subcutaneous TNFalpha.* Pain, 2000. **85**(1-2): p. 145-51.

212. Svensson, C.I., et al., *Spinal blockade of TNF blocks spinal nerve ligation-induced increases in spinal P-p38.* Neurosci Lett, 2005. **379**(3): p. 209-13.

213. Sawada, M., et al., *Production of tumor necrosis factor-alpha by microglia and astrocytes in culture.* Brain Res, 1989. **491**(2): p. 394-7.

214. Gawlak, M., et al., *High resolution in situ zymography reveals matrix metalloproteinase activity at glutamatergic synapses.* Neuroscience, 2009. **158**(1): p. 167-76.

215. Pagenstecher, A., et al., *Differential expression of matrix metalloproteinase and tissue inhibitor of matrix metalloproteinase genes in the mouse central nervous system in normal and inflammatory states.* Am J Pathol, 1998. **152**(3): p. 729-41.

216. Ito, S., et al., *Induction of matrix metalloproteinases (MMP3, MMP12 and MMP13) expression in the microglia by amyloid-beta stimulation via the PI3K/Akt pathway.* Exp Gerontol, 2007. **42**(6): p. 532-7.

217. Prast, J., et al., *Human chorionic gonadotropin stimulates trophoblast invasion through extracellularly regulated kinase and AKT signaling.* Endocrinology, 2008. **149**(3): p. 979-87.

218. Qiu, Q., et al., *EGF-induced trophoblast secretion of MMP-9 and TIMP-1 involves activation of both PI3K and MAPK signalling pathways.* Reproduction, 2004. **128**(3): p. 355-63.

219. Choi, J.I., et al., *Peripheral inflammation induces tumor necrosis factor dependent AMPA receptor trafficking and Akt phosphorylation in spinal cord in addition to pain behavior.* Pain. **149**(2): p. 243-53.

220. Svensson, C.I., et al., *Activation of p38 mitogen-activated protein kinase in spinal microglia is a critical link in inflammation-induced spinal pain processing.* J Neurochem, 2003. **86**(6): p. 1534-44.

221. Chakraborti, S., et al., *Regulation of matrix metalloproteinases: an overview.* Mol Cell Biochem, 2003. **253**(1-2): p. 269-85.

222. Kozai, T., et al., *Tissue type plasminogen activator induced in rat dorsal horn astrocytes contributes to mechanical hypersensitivity following dorsal root injury.* Glia, 2007. **55**(6): p. 595-603.

223. Jacobsen, F.E., et al., *A macrophage cell model for selective metalloproteinase inhibitor design.* Chembiochem, 2008. **9**(13): p. 2087-95.

224. Bertini, I., et al., *Conformational variability of matrix metalloproteinases: beyond a single 3D structure.* Proc Natl Acad Sci U S A, 2005. **102**(15): p. 5334-9.

225. Bertini, I., et al., *Crystal structure of the catalytic domain of human matrix metalloproteinase 10.* J Mol Biol, 2004. **336**(3): p. 707-16.

226. Grobelny, D., L. Poncz, and R.E. Galardy, *Inhibition of human skin fibroblast collagenase, thermolysin, and Pseudomonas aeruginosa elastase by peptide hydroxamic acids.* Biochemistry, 1992. **31**(31): p. 7152-4.

227. MacPherson, L.J., et al., *Discovery of CGS 27023A, a non-peptidic, potent, and orally active stromelysin inhibitor that blocks cartilage degradation in rabbits.* J Med Chem, 1997. **40**(16): p. 2525-32.

228. Romero-Perez, D., et al., *Effects of novel semiselective matrix metalloproteinase inhibitors on ex vivo cardiac structure-function.* J Cardiovasc Pharmacol, 2009. **53**(6): p. 452-61.

229. Youn, D.H., H. Wang, and S.J. Jeong, *Exogenous tumor necrosis factor-alpha rapidly alters synaptic and sensory transmission in the adult rat spinal cord dorsal horn.* J Neurosci Res, 2008. **86**(13): p. 2867-75.

230. Schafers, M., et al., *Cyclooxygenase inhibition in nerve-injury- and TNF-induced hyperalgesia in the rat.* Exp Neurol, 2004. **185**(1): p. 160-8.

231. Reeve, A.J., et al., *Intrathecally administered endotoxin or cytokines produce allodynia, hyperalgesia and changes in spinal cord neuronal responses to nociceptive stimuli in the rat.* Eur J Pain, 2000. **4**(3): p. 247-57.

232. Czeschik, J.C., et al., *TNF-alpha differentially modulates ion channels of nociceptive neurons.* Neurosci Lett, 2008. **434**(3): p. 293-8.

233. Chao, C.C., et al., *Interleukin-1 and tumor necrosis factor-alpha synergistically mediate neurotoxicity: involvement of nitric oxide and of N-methyl-D-aspartate receptors.* Brain Behav Immun, 1995. **9**(4): p. 355-65.

234. Stellwagen, D., et al., *Differential regulation of AMPA receptor and GABA receptor trafficking by tumor necrosis factor-alpha.* J Neurosci, 2005. **25**(12): p. 3219-28.

235. Zhang, H., H. Nei, and P.M. Dougherty, *A p38 mitogen-activated protein kinase-dependent mechanism of disinhibition in spinal synaptic transmission induced by tumor necrosis factor-alpha.* J Neurosci. **30**(38): p. 12844-55.

236. Watkins, L.R. and S.F. Maier, *Glia: a novel drug discovery target for clinical pain.* Nat Rev Drug Discov, 2003. **2**(12): p. 973-85.

237. Marchand, F., M. Perretti, and S.B. McMahon, *Role of the immune system in chronic pain.* Nat Rev Neurosci, 2005. **6**(7): p. 521-32.

238. Mohan, M.J., et al., *The tumor necrosis factor-alpha converting enzyme (TACE): a unique metalloproteinase with highly defined substrate selectivity.* Biochemistry, 2002. **41**(30): p. 9462-9.

239. Farooqui, A.A. and L.A. Horrocks, *Brain phospholipases A2: a perspective on the history.* Prostaglandins Leukot Essent Fatty Acids, 2004. **71**(3): p. 161-9.

240. Vergnolle, N., et al., *Proteinase-activated receptor-2 and hyperalgesia: A novel pain pathway.* Nat Med, 2001. **7**(7): p. 821-6.

241. Bunnett, N.W., *Protease-activated receptors: how proteases signal to cells to cause inflammation and pain.* Semin Thromb Hemost, 2006. **32 Suppl 1**: p. 39-48.